International Journal of Theoretical Physics, Group Theory and Nonlinear Optics
Volume 10, number 3 (2003) 285-369

PHASE CONJUGATION IN A LAYER OF NONLINEAR MATERIAL

Henk F. Arnoldus
Department of Physics & Astronomy, Mississippi State University,
P. O. Drawer 5167, Mississippi State, MS 39762-5167, USA
arnoldus@ra.msstate.edu

Thomas F. George
Office of the Chancellor
Departments of Chemistry & Biochemistry and Physics & Astronomy,
University of Missouri-St. Louis, St. Louis, MO 63121-4499, USA
tfgeorge@umsl.edu

ABSTRACT

We have studied theoretically optical phase conjugation through four-wave mixing in a slab of nonlinear material. When two strong counterpropagating laser beams irradiate a nonlinear crystal, the third-order susceptibility is activated, and can couple to an external weak probe field. A four-wave mixing process then generates a phase-conjugated or time-reversed replica of this incident probe field. We have investigated the mechanism of the production of phase-conjugated radiation in such a configuration by solving the nonlinear Maxwell equations for the electric field. The electric field in the material satisfies a set of two coupled wave equations, which couple positive and negative frequency components of the electric field. It is shown that the polarization of the pumps and the tensorial nature of the interaction can be accounted for by a simple polarization operator in the wave equations. Maxwell's equations for the field in the layer admit plane-wave solutions, although the dispersion relations are very different from the usual linear relation between the frequency and the wave number. The coupling between the two waves exhibits a strong resonance near the frequency of the pump beams. These plane-wave modes can be matched across the boundaries to the probe field and the reflected and transmitted waves, which we will assume to be plane traveling or evanescent waves. The response of the material can then be expressed in terms of Fresnel reflection and transmission coefficients for both *s*- and *p*-polarization. We have derived simple matrix equations for the set of Fresnel coefficients, which can be solved numerically, and we have also obtained closed-form analytical solutions for the various Fresnel coefficients. It is indicated that our solutions reduce to earlier results in the appropriate limits.

1. INTRODUCTION

When an electromagnetic wave travels through a medium, like the atmosphere, an optical fiber, or an amplifier, it builds up distortions during the propagation due to, for instance, inhomogeneities in the index of refraction of the material. Since Maxwell's equations for wave propagation are time-reversal invariant, it should be possible, in principle, to erase these distortions by sending the wave back through the medium and forcing it to evolve according the time-reversed Maxwell equations. This procedure would require, however, that the distorted wave which is incident on the medium for the second time is the time-reversed replica of the distorted wave, rather than the distorted wave itself. For this reason it is of great practical importance to develop techniques for the time reversal of wavefronts.

Devices which generate a time reversed wave for a certain input wave are collectively called 'phase conjugators', for the following reason. Let the electric field vector of a plane-wave component of a propagating electromagnetic wavefront be of the form

$$\boldsymbol{E}(\boldsymbol{r},t)_{inc} = E_o \,\mathrm{Re}\, \boldsymbol{\varepsilon}\, e^{i(\boldsymbol{k}\cdot\boldsymbol{r}-\omega t)} \ , \tag{1.1}$$

where the amplitude E_o, the wave vector $\boldsymbol{k}$, and the angular frequency ω are real. The polarization vector $\boldsymbol{\varepsilon}$ can be complex, and the notation *inc* indicates the incident wave. The corresponding time reversed image is then

$$\boldsymbol{E}(\boldsymbol{r},t)_{pc} = \boldsymbol{E}(\boldsymbol{r},-t)_{inc} = E_o \,\mathrm{Re}\, \boldsymbol{\varepsilon}\, e^{i(\boldsymbol{k}\cdot\boldsymbol{r}+\omega t)} \ , \tag{1.2}$$

which is the same as

$$\boldsymbol{E}(\boldsymbol{r},t)_{pc} = E_o \,\mathrm{Re}\, \boldsymbol{\varepsilon}^*\, e^{i(-\boldsymbol{k}\cdot\boldsymbol{r}-\omega t)} \ , \tag{1.3}$$

and this is again

$$\boldsymbol{E}(\boldsymbol{r},t)_{pc} = E_o \,\mathrm{Re}\left(\boldsymbol{\varepsilon}\, e^{i\boldsymbol{k}\cdot\boldsymbol{r}}\right)^* e^{-i\omega t} \ . \tag{1.4}$$

It is seen that replacing t by $-t$ is equivalent to taking the complex conjugate of the spatial part (the phase) of the wave, and hence the name 'phase conjugation'. For an arbitrary wave this can be done for each plane-wave component of the spatial Fourier spectrum. It follows from Eq. (1.3), when compared to Eq. (1.1), that the phase conjugated (*pc*) wave has $-\boldsymbol{k}$ as its wave vector, and therefore this *pc* wave travels in the direction opposite to the *inc* wave, as could be expected from a time-reversed replica. Another important observation that follows from Eq. (1.4) is that the polarization vector $\boldsymbol{\varepsilon}$ also has to be conjugated in order to obtain the correct time-reversed behavior.

The first experimental demonstration of wavefront-distortion correction after phase conjugation was given by Zel'dovich and co-workers in 1972 [1]. They distorted the

wavefront of a laser beam by letting it pass through an etched glass plate. Subsequently, the beam was sent into a cell with methane gas, which produced backscattered light via stimulated Brillouin scattering. This backscattered light was then sent through the glass plate in the opposite direction, and it appeared that the distortions had disappeared. They concluded that the cell operated as a phase conjugator.

After this experimental milestone, the field of optical phase conjugation developed rapidly. Phase conjugation in liquid CS_2 by Brillouin scattering [2] and Raman scattering [3] was demonstrated experimentally, and in 1977 Hellwarth [4] and Yariv and Pepper [5] proposed to construct a phase conjugator based on four-wave mixing in liquids or crystals. The great advantages of that scheme, as compared to Brillouin scattering, are that the response time of the medium is negligible, the frequency shift with the acoustic frequency of the medium is absent, and the required laser power is much less. Compared to three-wave mixing, four-wave mixing has the advantage that there are no phase-matching conditions for the various waves. Less than a year later, wavefront reversal by four-wave mixing in liquid CS_2 [6,7] and a lithium formate crystal [8] was realized experimentally.

A variety of other techniques for constructing a phase conjugator have been proposed. If an intense laser irradiates a thin metal film on a substrate, then the reflectivity changes by an amount which is proportional to the local intensity. In this fashion, the intensity pattern of the beam can be written on the film, and it can be shown that one of the reflected waves is the time-reversed replica of the original wave [9,10]. Another method of phase conjugation in thin films is described in [11,12]. A metal surface is coated with a thin layer of a nonlinear transparent material. Through multiple reflections in the layer, the incident beam can excite a surface plasmon wave on the metal, which in turn generates a conjugated wave. A disadvantage of this method is that the reflection coefficient is relatively low. Besides four-wave mixing in liquids and crystals, other bulk media have been proposed and analyzed. Heer and Griffen [13] observed a forward propagating phase-conjugated signal in sodium vapor, and Ducloy and Bloch [14,15] have studied the theoretical aspects of this configuration in detail. Less common media for four-wave mixing are organic dye molecules in a solid matrix [16] and microparticles suspended in a liquid [17]. Manneberg [18] has suggested to utilize the fifth-order nonlinear susceptibility of a bulk material to produce phase-conjugated radiation. The most extensively studied method for optical phase conjugation is four-wave mixing in photorefractive crystals like $BaTiO_3$, SBN and $LiNbO_3$ [19-29]. Here, the incident light liberates electrons or holes in the crystal, which move to the dark regions and form a local space-charge distribution. This results in local changes of the stress in the medium, which in turn alters the refractive index locally (Pockels effect). Scattering from this light-induced diffraction grating can then produce a phase-conjugated signal. Although these phase conjugators are usually operated in the four-wave mixing configuration, in principle there is no need for external pumps. A self-pumped phase conjugator was first observed experimentally by Feinberg [30] with a $BaTiO_3$ crystal. Although photorefractive self-pumped phase conjugators, based on internal reflection, can be constructed easily, it is not exactly clear how this mechanism works, as illustrated by the interesting measurements of Gower and Hribek [31]. A disadvantage of these phase conjugators is the very slow response time, although it can be as short as several picoseconds [32].

Phase conjugators are mainly designed for the purpose of wavefront-distortion correction. The physical mechanism of this process is intuitively easy to understand due to the analogy between phase conjugation and time reversal, but the theoretical justification for a realistic system is fairly complex [33-37]. If the incident field is a pulse, rather than a stationary wave, the situation is even more complicated [38-43], and can lead to instabilities [44], bistability [45], and deterministic chaos [46]. Also, resonators where one or more of the ordinary mirrors are replaced by phase-conjugating mirrors have been studied [47-51]. A remarkable effect was predicted [52-54] and confirmed experimentally [55,56]. If light is incident upon an ordinary mirror (dielectric), and a phase conjugator is placed behind the mirror, then the usual specularly-reflected wave disappears completely if the reflectivity of the phase conjugator equals unity.

These days, phase conjugators are readily available commercially, and they have become a standard device in optical experiments. For the numerous applications of optical phase conjugation and the many ways of constructing phase conjugators we refer to the existing reviews on this topic [57-61]. The subject has also found its way into the modern literature on nonlinear optics [62-64]. Another application of phase conjugation, and of a more speculative nature, is phase conjugation of atomic or molecular radiation [65,66]. When an exited atom decays to the ground state, it emits a photon. If this atom is placed near a phase conjugator, this photon can reflect at the phase conjugator. Based on the argument of time reversal, this photon will focus back on the atom, and it can be re-absorbed. It has been predicted that this would effectively increase the lifetime of the excited state, a phenomenon which could be potentially interesting for enhancement of chemical reactions. It turned out, at least in theory, that this intuitive prediction is incorrect, and that in effect lifetimes become shorter [67-70], although this conclusion has met some controversy [71-73]. The reason for this lies in the fact that near a phase conjugator also the vacuum field acquires a phase-conjugated image, containing real photons. This phase-conjugated vacuum, sometimes referred to as quantum noise [74], induces a more rapid decay from the excited state to the ground state, thereby reducing the lifetime. On the other hand, it also induces upward transitions, which leads to a permanent population of the excited state of the atom, simply because the atom is located near a phase conjugator. We have proposed [75] an experimental scheme to measure this spontaneous excitation of atoms through a measurement of the probe absorption profile. There must be a second line in the profile, which appears at a different frequency than the natural absorption line when the pump beams of the four-wave mixer are slightly off resonance with the atomic transition. Any observation of this second line in the profile would confirm a spontaneous population of the excited state in a phase-conjugating environment (it should be noted that it is essential that the phase conjugator is of the four-wave mixing type, as described below). When an atom is pumped continuously by a laser, it emits steady-state resonance fluorescence with a three-line spectral distribution, known as the Mollow triplet [76]. We have shown [77] that the phase-conjugated image is again a triplet, although the lines in the image are shifted with respect to their original locations.

2. DESCRIPTION OF THE PHASE CONJUGATOR

When a phase conjugator is needed for a specific system, like a light amplifier, then a self-pumped photorefractive crystal or a four-wave-mixing Brillouin mirror [78] are probably among the best choices. In other situations, such devices might not operate adequately. For instance, if the phase conjugator is applied as one of the mirrors in a resonator, then photons can be incident on the phase conjugator under any angle of incidence, and the field to be conjugated can be very weak. In this case, the above-mentioned choices don't work, due to the requirements on the angle of incidence and the high threshold for the input power. In this paper we investigate in very detail the properties of a realistic phase conjugator, operating in the four-wave mixing configuration. We put no restrictions on the angle of incidence, like in a paraxial approximation, or on the polarization, and we allow the field to have evanescent components. These evanescent waves have attracted much attention recently due to the rapid developments in near-field optics, where the evanescent part of the radiation field plays a crucial role. It has become necessary to study the phase conjugation of evanescent waves, in addition to the more common situation of pure traveling waves [79-81, 35]. We shall consider both types of input waves within a single theory. Furthermore, a dielectric constant other than unity is included, and the full tensorial nature of the interaction is accounted for (with some slight approximations). Also, the common slowly-varying amplitude approximation has been avoided.

The situation under consideration and the choice of coordinate system is illustrated in Fig. 1. Two strong monochromatic counterpropagating laser beams (the pumps) illuminate the sides of a nonlinear transparent medium. The slab has a thickness Δ in the z-direction, extending from $z = 0$ to $z = -\Delta$, a width L along the propagation direction of the beams, which we shall take as the y-direction with the medium occupying the region $-L/2 < y < L/2$, and is infinite in extend perpendicular to the page of the figure. A weak field is incident on the layer from the positive z-direction, and the four-wave mixing process inside the medium is expected to generate the phase-conjugated image of this field. Since the coupling of the various waves through the nonlinear interaction is tensorial, the operation of the phase conjugator will depend on the polarization of the pumps. In order to retain the symmetry for rotation about the z-axis, we take the pumps to be linearly polarized in the z-direction.

To be specific, for the electric components of the two incident counterpropagating pump fields we take

$$\boldsymbol{E}(\boldsymbol{r},t)_1 = \boldsymbol{e}_z \,\mathrm{Re}\, E_1\, e^{-i(\bar{k}y+\bar{\omega}t)} \ , \tag{2.1}$$

$$\boldsymbol{E}(\boldsymbol{r},t)_2 = \boldsymbol{e}_z \,\mathrm{Re}\, E_2\, e^{i(\bar{k}y-\bar{\omega}t)} \ , \tag{2.2}$$

so that field 1 (2) with complex amplitude E_1 (E_2) propagates in the $-y$ (y) -direction. Both waves have a wave number $\bar{k}$ and corresponding angular frequency $\bar{\omega} = c\bar{k} > 0$. It is assumed that the pumps illuminate the two sides $y = L/2$ and $y = -L/2$ evenly, and that the fields are zero in the regions $z > 0$ and $z < -\Delta$. The nonlinear material (to be specified below),

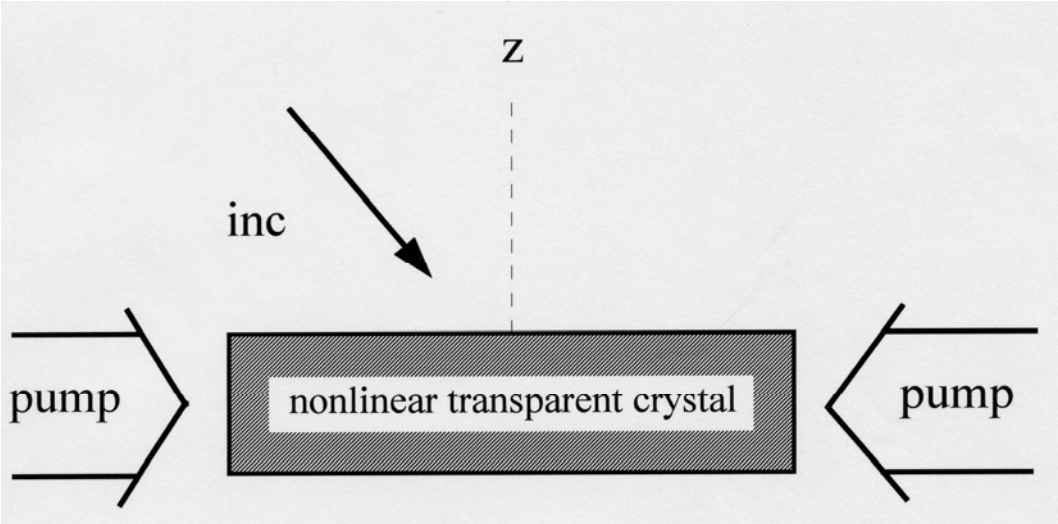

Figure 1: Schematic setup of a phase conjugator based on four-wave mixing in a nonlinear crystal. Shown are the two pump beams (labeled 1 for the beam coming from the right, and labeled 2 for the beam incident from the left) and the weak incident light.

together with the two pumps, forms the phase conjugator.

3. MAXWELL'S EQUATIONS

Radiation inside and outside the medium is represented by its electric and magnetic field components, $\boldsymbol{E}(\boldsymbol{r},t)$ and $\boldsymbol{B}(\boldsymbol{r},t)$, respectively, and charges and currents in the medium are described by a polarization field $\boldsymbol{P}(\boldsymbol{r},t)$. It will turn out to be convenient to work with the time-Fourier-transformed fields, defined as

$$\hat{\boldsymbol{E}}(\boldsymbol{r},\omega)=\int_{-\infty}^{\infty}dt\,e^{i\omega t}\,\boldsymbol{E}(\boldsymbol{r},t)\quad , \tag{3.1}$$

with inverse

$$\boldsymbol{E}(\boldsymbol{r},t)=\frac{1}{2\pi}\int_{-\infty}^{\infty}d\omega\,e^{-i\omega t}\,\hat{\boldsymbol{E}}(\boldsymbol{r},\omega)\quad . \tag{3.2}$$

Since the electric field is real

$$\boldsymbol{E}(\boldsymbol{r},t)^{*}=\boldsymbol{E}(\boldsymbol{r},t)\ , \tag{3.3}$$

we have in the Fourier domain

$$\hat{\boldsymbol{E}}(\boldsymbol{r},\omega)^{*} = \hat{\boldsymbol{E}}(\boldsymbol{r},-\omega) \ . \tag{3.4}$$

On occasion we will need the positive frequency part of $\boldsymbol{E}(\boldsymbol{r},t)$, which is defined as

$$\boldsymbol{E}(\boldsymbol{r},t)^{(+)} = \frac{1}{2\pi}\int_{0}^{\infty} d\omega\, e^{-i\omega t}\ \hat{\boldsymbol{E}}(\boldsymbol{r},\omega) \quad , \tag{3.5}$$

and the negative frequency part, which is the same integral but over the range $-\infty < \omega < 0$. From (3.4) we then have

$$\boldsymbol{E}(\boldsymbol{r},t)^{(-)} = \left(\ \boldsymbol{E}(\boldsymbol{r},t)^{(+)}\right)^{*} \ , \tag{3.6}$$

and therefore the total field is

$$\boldsymbol{E}(\boldsymbol{r},t) = \boldsymbol{E}(\boldsymbol{r},t)^{(+)} + \boldsymbol{E}(\boldsymbol{r},t)^{(-)} \ , \tag{3.7}$$

which can also be represented as

$$\boldsymbol{E}(\boldsymbol{r},t) = \frac{1}{\pi}\mathrm{Re}\int_{0}^{\infty} d\omega\, e^{-i\omega t}\ \hat{\boldsymbol{E}}(\boldsymbol{r},\omega) \quad . \tag{3.8}$$

In this last form it is most obvious that we need the field for positive frequencies only, although we shall see later that it is convenient for the present problem to use both positive and negative frequencies. The magnetic field and the polarization will be transformed similarly.

The three fields are related by Maxwell's equations, which read in the Fourier domain

$$\nabla\times(\nabla\times\hat{\boldsymbol{E}}(\boldsymbol{r},\omega)) - \frac{\omega^2}{c^2}\hat{\boldsymbol{E}}(\boldsymbol{r},\omega) = \frac{\omega^2}{c^2\varepsilon_o}\hat{\boldsymbol{P}}(\boldsymbol{r},\omega) \ , \tag{3.9}$$

$$\hat{\boldsymbol{B}}(\boldsymbol{r},\omega) = -\frac{i}{\omega}\nabla\times\hat{\boldsymbol{E}}(\boldsymbol{r},\omega) \ . \tag{3.10}$$

This set of two equations is equivalent to the more commonly encountered set of four equations [82]. Equations (3.9) and (3.10) have to hold simultaneously, and for all $\boldsymbol{r}$ and ω. The expression for $\hat{\boldsymbol{P}}(\boldsymbol{r},\omega)$ inside the medium will be derived below, and outside (vacuum) we set $\hat{\boldsymbol{P}}(\boldsymbol{r},\omega) = 0$. At the boundaries $z = 0$, $z = -\Delta$, $y = -L/2$ and $y = -L/2$, Maxwell's equations imply that $(\hat{\boldsymbol{E}} + \hat{\boldsymbol{P}}/\varepsilon_o)_{\perp}$, $\hat{\boldsymbol{E}}_{||}$ and $\hat{\boldsymbol{B}}$ must be continuous across the boundary. In

addition, we have the requirement that without the medium the solution must reduce to the sum of the two pump fields plus the weak incident field.

4. POLARIZATION

Polarization of a medium is caused by the presence of an electric field, which induces dipole moments in the atoms or molecules. Therefore, it should be possible to express $\boldsymbol{P}(\boldsymbol{r},t)$ in terms of $\boldsymbol{E}(\boldsymbol{r},t)$, and the most general (local and causal) relation in the Fourier domain is [83,84]

$$\hat{\boldsymbol{P}}(\boldsymbol{r},\omega)=\varepsilon_o\sum_{n=1}^{\infty}\frac{1}{(2\pi)^{n-1}}\int_{-\infty}^{\infty}d\omega_1\ldots\int_{-\infty}^{\infty}d\omega_n\,\delta(\omega-\omega_1\ldots-\omega_n)$$

$$\times\,\hat{\chi}^{(n)}(\omega_1,\ldots,\omega_n):\hat{\boldsymbol{E}}(\boldsymbol{r},\omega_1)\ldots\hat{\boldsymbol{E}}(\boldsymbol{r},\omega_n)\ . \tag{4.1}$$

Here, $\hat{\chi}^{(n)}(\omega_1,\ldots,\omega_n)$ is the n-fold Fourier transform of the n-th order susceptibility function, which is a Cartesian tensor of rank n+1, and the colon in Eq. (4.1) indicates the tensor product with the n electric field vectors at the different indicated frequencies. It is assumed that the medium is homogeneous, so that $\hat{\chi}^{(n)}(\omega_1,\ldots,\omega_n)$ is independent of $\boldsymbol{r}$.

As a first simplification, we assume that the medium is inversion invariant. Then it follows immediately that all even susceptibilities $\hat{\chi}^{(2)}$, $\hat{\chi}^{(4)}$,... are identically zero [83,84]. Furthermore, we know that the values of $\hat{\chi}^{(n)}$ decrease very rapidly with increasing n, so it is perfectly justified to retain only the n = 1 and n = 3 terms in Eq. (4.1). We write

$$\hat{\boldsymbol{P}}(\boldsymbol{r},\omega)=\hat{\boldsymbol{P}}(\boldsymbol{r},\omega)^{(1)}+\hat{\boldsymbol{P}}(\boldsymbol{r},\omega)^{(3)}\ , \tag{4.2}$$

in obvious notation.

The two remaining tensors $\hat{\chi}^{(1)}$ and $\hat{\chi}^{(3)}$ have 3^2 = 9 and 3^4 = 81 Cartesian components, respectively, which are all different functions of one and three frequencies, respectively. As a second assumption we take the medium to be isotropic, e.g., invariant for inversion in a plane and for rotation about an axis. Then it can be shown [83, 84] that $\hat{\chi}^{(1)}$ has only three non-zero Cartesian components, which are all equal, and that $\hat{\chi}^{(3)}$ has 21 non-zero components. Among these 21 components there are only three different ones, which are not even independent. With the relations listed in [83, 84], it is relatively easy to derive that the two tensor products reduce to

$$\hat{\chi}^{(1)}(\omega_1):\boldsymbol{a}=\hat{\chi}^{(1)}_{xx}(\omega_1)\boldsymbol{a}\ , \tag{4.3}$$

$$\hat{\chi}^{(3)}(\omega_1,\omega_2,\omega_3):\boldsymbol{a}\,\boldsymbol{b}\,\boldsymbol{c}=\hat{\chi}^{(3)}_{xxyy}(\omega_1,\omega_2,\omega_3)(\boldsymbol{b}\cdot\boldsymbol{c})\boldsymbol{a}+\hat{\chi}^{(3)}_{xyxy}(\omega_1,\omega_2,\omega_3)(\boldsymbol{a}\cdot\boldsymbol{c})\boldsymbol{b}$$

$$+ \hat{\chi}^{(3)}_{xyyx}(\omega_1,\omega_2,\omega_3)(\boldsymbol{a}\cdot\boldsymbol{b})\boldsymbol{c} \ , \tag{4.4}$$

for arbitrary vectors $\boldsymbol{a}$, $\boldsymbol{b}$ and $\boldsymbol{c}$. These two expressions are then substituted into Eq. (4.1). We can use the intrinsic permutation symmetry of the tensor components, like $\hat{\chi}^{(3)}_{xyyx}(\omega_1,\omega_2,\omega_3) = \hat{\chi}^{(3)}_{xyxy}(\omega_1,\omega_3,\omega_2)$, which holds in any medium, to change integration variables. Then we obtain for the two contributions to the polarization

$$\hat{\boldsymbol{P}}(\boldsymbol{r},\omega)^{(1)} = \varepsilon_o \, \hat{\chi}^{(1)}_{xx}(\omega)\boldsymbol{E}(\boldsymbol{r},\omega) \ , \tag{4.5}$$

$$\hat{\boldsymbol{P}}(\boldsymbol{r},\omega)^{(3)} = \frac{3\varepsilon_o}{4\pi^2} \int_{-\infty}^{\infty} d\omega_1 \int_{-\infty}^{\infty} d\omega_2 \int_{-\infty}^{\infty} d\omega_3 \, \delta(\omega-\omega_1-\omega_2-\omega_3)$$

$$\times \hat{\chi}^{(3)}_{xxyy}(\omega_1,\omega_2,\omega_3)\boldsymbol{E}(\boldsymbol{r},\omega_1)[\boldsymbol{E}(\boldsymbol{r},\omega_2)\cdot\boldsymbol{E}(\boldsymbol{r},\omega_3)] \ , \tag{4.6}$$

and we notice that only the tensor components $\hat{\chi}^{(1)}_{xx}(\omega)$ and $\hat{\chi}^{(3)}_{xxyy}(\omega_1,\omega_2,\omega_3)$ appear in these expressions. This great simplification followed from symmetry only.

From relation (3.4) for $\hat{\boldsymbol{E}}(\boldsymbol{r},\omega)$ we find that the tensor components have the property

$$\hat{\chi}^{(1)}_{xx}(\omega)^* = \hat{\chi}^{(1)}_{xx}(-\omega) \ , \tag{4.7}$$

$$\hat{\chi}^{(3)}_{xxyy}(\omega_1,\omega_2,\omega_3)^* = \hat{\chi}^{(3)}_{xxyy}(-\omega_1,-\omega_2,-\omega_3) \ . \tag{4.8}$$

It is convenient to introduce the dielectric constant of the medium

$$\varepsilon(\omega) = 1 + \hat{\chi}^{(1)}_{xx}(\omega) \ , \tag{4.9}$$

which obeys

$$\varepsilon(\omega)^* = \varepsilon(-\omega) \ . \tag{4.10}$$

If we substitute the above relations into Maxwell's equation (3.9), then we obtain the equation for the electric field

$$\nabla\times(\nabla\times\hat{\boldsymbol{E}}(\boldsymbol{r},\omega)) - \varepsilon(\omega)\frac{\omega^2}{c^2}\hat{\boldsymbol{E}}(\boldsymbol{r},\omega) = \frac{\omega^2}{c^2\varepsilon_o}\hat{\boldsymbol{P}}(\boldsymbol{r},\omega)^{(3)} \ , \tag{4.11}$$

whereas (3.10) for the magnetic field remains unchanged. For $\hat{\boldsymbol{P}}(\boldsymbol{r},\omega)^{(3)}$ on the right-hand side we have to substitute the right-hand side of Eq. (4.6). The boundary conditions are now that $(\varepsilon(\omega)\hat{\boldsymbol{E}}(\boldsymbol{r},\omega)+\hat{\boldsymbol{P}}(\boldsymbol{r},\omega)^{(3)}/\varepsilon_o)_\perp$, $\hat{\boldsymbol{E}}(\boldsymbol{r},\omega)_{||}$ and $\hat{\boldsymbol{B}}(\boldsymbol{r},\omega)$ must be continuous. The

appearance of $\varepsilon(\omega)$ in Eq. (4.11) is the standard linear contribution to the polarization. The nonlinear part is $\hat{\boldsymbol{P}}(\boldsymbol{r},\omega)^{(3)}$, as given by Eq. (4.6). The integrand in Eq. (4.6) has three factors $\hat{\boldsymbol{E}}(\boldsymbol{r},\omega)$, each at a different frequency, and these frequencies are integrated over. Hence Eq. (4.11) is not a single equation for $\hat{\boldsymbol{E}}(\boldsymbol{r},\omega)$ at a fixed ω, but a continuous set which couples every Fourier spectral component $\hat{\boldsymbol{E}}(\boldsymbol{r},\omega)$ with every other one.

5. WEAK INCIDENT FIELD

A major complication with expression (4.6) for $\hat{\boldsymbol{P}}(\boldsymbol{r},\omega)^{(3)}$ is that $\hat{\boldsymbol{E}}(\boldsymbol{r},\omega)$ represents the total electric field at position $\boldsymbol{r}$ inside the medium. It contains contributions from (i) the external pump fields which propagate through the medium, (ii) multiple reflections of these fields at the boundaries $y = \pm L/2$ when $\varepsilon \neq 1$, (iii) the field incident from the region $z > 0$, and (iv) any radiation which is generated by the linear and nonlinear interactions. In the Fourier domain, the pump fields (2.1) and (2.2) attain the form

$$\hat{\boldsymbol{E}}(\boldsymbol{r},\omega)_1 = \pi \boldsymbol{e}_z \{\delta(\omega-\overline{\omega})\, E_1\, e^{-i\bar{k}y} + \delta(\omega+\overline{\omega})\, E_1^*\, e^{i\bar{k}y}\}\ , \tag{5.1}$$

$$\hat{\boldsymbol{E}}(\boldsymbol{r},\omega)_2 = \pi \boldsymbol{e}_z \{\delta(\omega-\overline{\omega})\, E_2\, e^{i\bar{k}y} + \delta(\omega+\overline{\omega})\, E_2^*\, e^{-i\bar{k}y}\}\ . \tag{5.2}$$

These fields are incident from the right and the left, respectively, on the medium. Without the nonlinear interaction we could apply the superposition principle, and solve for the reflection and transmission of the pumps and of the incident field separately. In the linear case, where $\hat{\boldsymbol{P}}(\boldsymbol{r},\omega)^{(3)} = 0$, there is no coupling in Maxwell's equations between Fourier components $\hat{\boldsymbol{E}}(\boldsymbol{r},\omega)$ with different frequencies ω, and consequently the field inside the medium due to the external pumps would have the form $\hat{\boldsymbol{E}}(\boldsymbol{r},\omega) = \boldsymbol{e}(\boldsymbol{r})\delta(\omega-\overline{\omega}) + \boldsymbol{e}(\boldsymbol{r})^*\delta(\omega+\overline{\omega})$, with $\boldsymbol{e}(\boldsymbol{r})$ to be determined by matching the boundary conditions at $y = \pm L/2$. Therefore, for the present situation we assume that the electric field can be written as

$$\hat{\boldsymbol{E}}(\boldsymbol{r},\omega) = \hat{\boldsymbol{E}}(\boldsymbol{r},\omega)' + \boldsymbol{e}(\boldsymbol{r})\delta(\omega-\overline{\omega}) + \boldsymbol{e}(\boldsymbol{r})^*\delta(\omega+\overline{\omega})\ , \tag{5.3}$$

with $\boldsymbol{e}(\boldsymbol{r})$ representing the strong part due to the pumps, and still to be determined, and $\hat{\boldsymbol{E}}(\boldsymbol{r},\omega)'$ the remaining weak part, also still to be determined. It should be noted that the form of $\boldsymbol{e}(\boldsymbol{r})$ could be affected by the nonlinear interaction.

Next we substitute the right-hand side of Eq. (5.3) into the integrand of Eq. (4.6) three times (for $\omega = \omega_1$, ω_2 and ω_3), and carry out the triple integration over the three frequencies. This yields a host of terms which, symbolically, are of the forms $(E')^3$, $(E')^2 e$, $E'e^2$ and e^3. Under the assumption of a weak incident field, we can neglect the terms of the form $(E')^3$ and $(E')^2 e$, compared to the contributions from $E'e^2$ and e^3. With this approximation, the third-order polarization takes on the following form

$$\hat{\boldsymbol{P}}(\boldsymbol{r},\omega)^{(3)} = \boldsymbol{p}(\boldsymbol{r})\delta(\omega-\overline{\omega}) + \boldsymbol{p}(\boldsymbol{r})^*\delta(\omega+\overline{\omega}) + \boldsymbol{q}(\boldsymbol{r})\delta(\omega-3\overline{\omega}) + \boldsymbol{q}(\boldsymbol{r})^*\delta(\omega+3\overline{\omega})$$

$$+\frac{3\varepsilon_o}{4\pi^2}\Big[\,\hat{\chi}^{(3)}_{xxyy}(\omega-2\overline{\omega},\overline{\omega},\overline{\omega})\{\boldsymbol{e}(\boldsymbol{r})\cdot\boldsymbol{e}(\boldsymbol{r})\}\hat{\boldsymbol{E}}(\boldsymbol{r},\omega-2\overline{\omega})'$$

$$+\hat{\chi}^{(3)}_{xxyy}(\omega+2\overline{\omega},-\overline{\omega},-\overline{\omega})\{\boldsymbol{e}(\boldsymbol{r})^*\cdot\boldsymbol{e}(\boldsymbol{r})^*\}\hat{\boldsymbol{E}}(\boldsymbol{r},\omega+2\overline{\omega})'$$

$$+\{\hat{\chi}^{(3)}_{xxyy}(\omega,\overline{\omega},-\overline{\omega})+\hat{\chi}^{(3)}_{xxyy}(\omega,-\overline{\omega},\overline{\omega})\}\{\boldsymbol{e}(\boldsymbol{r})\cdot\boldsymbol{e}(\boldsymbol{r})^*\}\hat{\boldsymbol{E}}(\boldsymbol{r},\omega)'$$

$$+\{\hat{\chi}^{(3)}_{xxyy}(\overline{\omega},\omega-2\overline{\omega},\overline{\omega})+\hat{\chi}^{(3)}_{xxyy}(\overline{\omega},\overline{\omega},\omega-2\overline{\omega})\}\{\boldsymbol{e}(\boldsymbol{r})\cdot\hat{\boldsymbol{E}}(\boldsymbol{r},\omega-2\overline{\omega})'\}\boldsymbol{e}(\boldsymbol{r})$$

$$+\{\hat{\chi}^{(3)}_{xxyy}(\overline{\omega},\omega,-\overline{\omega})+\hat{\chi}^{(3)}_{xxyy}(\overline{\omega},-\overline{\omega},\omega)\}\{\boldsymbol{e}(\boldsymbol{r})^*\cdot\hat{\boldsymbol{E}}(\boldsymbol{r},\omega)'\}\boldsymbol{e}(\boldsymbol{r})$$

$$+\{\hat{\chi}^{(3)}_{xxyy}(-\overline{\omega},\omega,\overline{\omega})+\hat{\chi}^{(3)}_{xxyy}(-\overline{\omega},\overline{\omega},\omega)\}\{\boldsymbol{e}(\boldsymbol{r})\cdot\hat{\boldsymbol{E}}(\boldsymbol{r},\omega)'\}\boldsymbol{e}(\boldsymbol{r})^*$$

$$+\{\hat{\chi}^{(3)}_{xxyy}(-\overline{\omega},\omega+2\overline{\omega},-\overline{\omega})$$

$$+\hat{\chi}^{(3)}_{xxyy}(-\overline{\omega},-\overline{\omega},\omega+2\overline{\omega})\}\{\boldsymbol{e}(\boldsymbol{r})^*\cdot\hat{\boldsymbol{E}}(\boldsymbol{r},\omega+2\overline{\omega})'\}\boldsymbol{e}(\boldsymbol{r})^*\Big]\ . \tag{5.4}$$

Here, the abbreviations $\boldsymbol{p}(\boldsymbol{r})$ and $\boldsymbol{q}(\boldsymbol{r})$ stand for

$$\boldsymbol{p}(\boldsymbol{r})=\frac{3\varepsilon_o}{4\pi^2}\{\hat{\chi}^{(3)}_{xxyy}(\overline{\omega},\overline{\omega},-\overline{\omega})+\hat{\chi}^{(3)}_{xxyy}(\overline{\omega},-\overline{\omega},\overline{\omega})\}\{\boldsymbol{e}(\boldsymbol{r})\cdot\boldsymbol{e}(\boldsymbol{r})^*\}\boldsymbol{e}(\boldsymbol{r})$$

$$+\frac{3\varepsilon_o}{4\pi^2}\hat{\chi}^{(3)}_{xxyy}(-\overline{\omega},\overline{\omega},\overline{\omega})\{\boldsymbol{e}(\boldsymbol{r})\cdot\boldsymbol{e}(\boldsymbol{r})\}\boldsymbol{e}(\boldsymbol{r})^*\ , \tag{5.5}$$

$$\boldsymbol{q}(\boldsymbol{r})=\frac{3\varepsilon_o}{4\pi^2}\hat{\chi}^{(3)}_{xxyy}(\overline{\omega},\overline{\omega},\overline{\omega})\}\{\boldsymbol{e}(\boldsymbol{r})\cdot\boldsymbol{e}(\boldsymbol{r})\}\boldsymbol{e}(\boldsymbol{r})\ . \tag{5.6}$$

Expression (5.4) has to be substituted into the right-hand side of Maxwell's equation (4.11), together with the form (5.3) for $\hat{\boldsymbol{E}}(\boldsymbol{r},\omega)$.

We notice that the first two terms on the right-hand side of Eq. (5.4) contain the same δ-functions as Eq. (5.3), and they are responsible for the nonlinear contribution to $\boldsymbol{e}(\boldsymbol{r})$, as compared to an ordinary dielectric. The next two terms are δ-functions at $\omega=\pm3\overline{\omega}$, and these are responsible for third-harmonic generation in the medium. All terms inside the square brackets are proportional to a Fourier component of $\hat{\boldsymbol{E}}'$, at various frequencies. In deriving Eq. (5.4) we have not used the specific form of the pump fields, but only that they are monochromatic with frequency $\overline{\omega}$, and much stronger than the field to be conjugated.

6. SEPARATION OF EQUATIONS

The third-order polarization has the form

$$\hat{\boldsymbol{P}}(\boldsymbol{r},\omega)^{(3)} = \hat{\boldsymbol{P}}(\boldsymbol{r},\omega)' + \boldsymbol{p}(\boldsymbol{r})\delta(\omega-\overline{\omega}) + \boldsymbol{p}(\boldsymbol{r})^{*}\delta(\omega+\overline{\omega}) \ , \tag{6.1}$$

which is identical in form to Eq. (5.3). If we then write

$$\hat{\boldsymbol{B}}(\boldsymbol{r},\omega) = \hat{\boldsymbol{B}}(\boldsymbol{r},\omega)' + \boldsymbol{b}(\boldsymbol{r})\delta(\omega-\overline{\omega}) + \boldsymbol{b}(\boldsymbol{r})^{*}\delta(\omega+\overline{\omega}) \tag{6.2}$$

for the magnetic field, with

$$\hat{\boldsymbol{B}}(\boldsymbol{r},\omega)' = -\frac{i}{\omega}\nabla\times\hat{\boldsymbol{E}}(\boldsymbol{r},\omega)' \ , \tag{6.3}$$

$$\boldsymbol{b}(\boldsymbol{r}) = -\frac{i}{\omega}\nabla\times\boldsymbol{e}(\boldsymbol{r}) \ , \tag{6.4}$$

then Maxwell's equations are certainly satisfied if $\hat{\boldsymbol{E}}(\boldsymbol{r},\omega)'$ and $\boldsymbol{e}(\boldsymbol{r})$ obey the separate equations

$$\nabla\times(\nabla\times\hat{\boldsymbol{E}}(\boldsymbol{r},\omega)') - \varepsilon(\omega)\frac{\omega^2}{c^2}\hat{\boldsymbol{E}}(\boldsymbol{r},\omega)' = \frac{\omega^2}{c^2\varepsilon_o}\hat{\boldsymbol{P}}(\boldsymbol{r},\omega)' \ , \tag{6.5}$$

$$\nabla\times(\nabla\times\boldsymbol{e}(\boldsymbol{r})) - \varepsilon(\overline{\omega})\frac{\overline{\omega}^2}{c^2}\boldsymbol{e}(\boldsymbol{r}) = \frac{\overline{\omega}^2}{c^2\varepsilon_o}\boldsymbol{p}(\boldsymbol{r}) \ , \tag{6.6}$$

simultaneously.

We see from Eq. (5.5) that $\boldsymbol{p}(\boldsymbol{r})$ is determined by $\boldsymbol{e}(\boldsymbol{r})$, and is independent of the presence of $\hat{\boldsymbol{E}}(\boldsymbol{r},\omega)'$ in the medium. Therefore, the fields $\boldsymbol{e}(\boldsymbol{r})$ and $\boldsymbol{b}(\boldsymbol{r})$ satisfy the nonlinear Maxwell equations, with $\boldsymbol{p}(\boldsymbol{r})$ as the nonlinear term, and they do not couple to the weak field. At the sides $y = \pm L/2$ of the medium the quantities $(\varepsilon(\overline{\omega})\boldsymbol{e}(\boldsymbol{r}) + \boldsymbol{p}(\boldsymbol{r})/\varepsilon_o)_{\perp}$, $\boldsymbol{e}(\boldsymbol{r})_{\|}$ and $\boldsymbol{b}(\boldsymbol{r})$ must be continuous across the boundary. The external fields are given by the $\boldsymbol{e}(\boldsymbol{r})$ parts of the pump fields, which are

$$\boldsymbol{e}(\boldsymbol{r})_1 = \pi\,\boldsymbol{e}_z\,E_1\,e^{-i\bar{k}y} \ , \tag{6.7}$$

$$\boldsymbol{e}(\boldsymbol{r})_2 = \pi\,\boldsymbol{e}_z\,E_2\,e^{i\bar{k}y} \ , \tag{6.8}$$

for our particular choice of linearly-polarized pumps. We have to take into account, of course, that these fields also reflect at the boundaries. After solving for $\boldsymbol{e}(\boldsymbol{r})$, we can substitute the result into Eq. (5.4), which then gives us $\hat{\boldsymbol{P}}(\boldsymbol{r},\omega)'$ for the right-hand side of Eq. (6.5). But then Eqs. (6.3) and (6.5) form a set of regular nonlinear Maxwell equations for the weak fields $\hat{\boldsymbol{E}}(\boldsymbol{r},\omega)'$ and $\hat{\boldsymbol{B}}(\boldsymbol{r},\omega)'$, which now only depend parametrically on the solution $\boldsymbol{e}(\boldsymbol{r})$. In this fashion, the sets of equations for $\boldsymbol{e}(\boldsymbol{r})$ and $\hat{\boldsymbol{E}}(\boldsymbol{r},\omega)'$ are completely decoupled, which is a great simplification.

It is worthwhile to note at this point that the separation between the sets of equations for the strong and the weak fields is not a consequence of the neglect of the $(E')^3$ and $(E')^2 e$ terms in the nonlinear polarization. The fields $\hat{\boldsymbol{E}}(\boldsymbol{r},\omega)$, $\hat{\boldsymbol{B}}(\boldsymbol{r},\omega)$ and $\hat{\boldsymbol{P}}(\boldsymbol{r},\omega)^{(3)}$ will always have these δ-function contributions due to the pump fields, and these can always be singled out in a set of separate equations. We also mention that the $\hat{\boldsymbol{E}}'$ field inside the medium has to be matched across the boundaries $y = \pm L/2$ with an $\hat{\boldsymbol{E}}'$ field outside. As we shall see later, the production of phase-conjugated radiation is not energy conserving, and external energy has to be supplied. The $\hat{\boldsymbol{E}}(\boldsymbol{r},\omega)'$ component of the radiation which crosses the boundaries at $y = \pm L/2$, interferes with the pump fields and this gives rise to an effective depletion of the pump fields. We shall not take into account this effect, but refer to the literature for some of the consequences of pump depletion [85-88]. This is consistent with the assumption of a weak incident field, and the corresponding omission of the $(E')^3$ and $(E')^2 e$ terms, since pump depletion can only be significant in cases where the incident field has an intensity comparable to the intensity of the pump beams.

7. APPROXIMATIONS ON $\chi^{(3)}$

Maxwell's equation (6.5) is a wave equation for $\hat{\boldsymbol{E}}(\boldsymbol{r},\omega)'$, which has $\hat{\boldsymbol{P}}(\boldsymbol{r},\omega)'$ on the right-hand side as a source term. A non-zero $\hat{\boldsymbol{P}}'$ for a given frequency ω will therefore generate radiation $\hat{\boldsymbol{E}}'$ at that frequency. The general form of $\hat{\boldsymbol{P}}'$ ($\hat{\boldsymbol{P}}^{(3)}$ minus the two $\boldsymbol{p}$-terms) is given by Eq. (5.4). We shall assume that the incident field has a frequency spectrum, which is reasonably centered around $\omega \sim \overline{\omega}$, but it does not necessarily have to be in close resonance. In view of Eq. (3.4), the incident field then also has spectral components for $\omega \sim -\overline{\omega}$. Since this radiation propagates into the crystal, the weak field has at least a non-zero spectral distribution for $\omega \sim \pm\overline{\omega}$. The third, fifth and sixth terms in square brackets in Eq. (5.4) are proportional to $\hat{\boldsymbol{E}}(\boldsymbol{r},\omega)'$, and consequently $\hat{\boldsymbol{P}}(\boldsymbol{r},\omega)'$ is non-zero for $\omega \sim \pm\overline{\omega}$. The first and the fourth term are proportional to $\hat{\boldsymbol{E}}(\boldsymbol{r},\omega - 2\overline{\omega})'$, and if we take $\omega \sim 3\overline{\omega}$, then this becomes $\hat{\boldsymbol{E}}(\boldsymbol{r},\sim\overline{\omega})'$ which is non-zero due to the incident field. In the same way, the second and the seventh term give a contribution to $\hat{\boldsymbol{P}}'$ for $\omega \sim -3\overline{\omega}$, which is induced by the incident field. We see that the incoming field with frequencies $\omega \sim \pm\overline{\omega}$ generates a $\hat{\boldsymbol{P}}(\boldsymbol{r},\omega)'$ at $\omega \sim \pm\overline{\omega}$ and at $\omega \sim \pm 3\overline{\omega}$. As a source in the wave equation, this produces radiation $\hat{\boldsymbol{E}}(\boldsymbol{r},\omega)'$ at $\omega \sim \pm\overline{\omega}, \pm 3\overline{\omega}$. Then again, this field $\hat{\boldsymbol{E}}'$ induces polarization $\hat{\boldsymbol{P}}'$ at $\omega \sim \pm 5\overline{\omega}$, etc. The conclusion is that the nonlinear interaction generates radiation at the harmonics $\pm\omega, \pm 3\omega, \pm 5\omega, \ldots$ of the incident field, but not in the gaps between these peaks. The

unfortunate situation is that the wave equation (6.5) couples the spatial evolution and frequency dependence of all peaks.

In order to resolve this complication, we assume that the medium is such that if the third-order susceptibility $\hat{\chi}^{(3)}_{xxyy}(\omega_1,\omega_2,\omega_3)$ is vanishingly small if one of its arguments ω_1, ω_2 or ω_3 is in the neighborhood of $\pm 3\overline{\omega}$. Then it follows by inspection from Eq. (5.4), in the same way as argued above, that the equations for $\hat{\boldsymbol{E}}(\boldsymbol{r},\omega)'$ at $\omega \sim \overline{\omega}$ and $\omega \sim -\overline{\omega}$ couple together, but that the coupling with $\hat{\boldsymbol{E}}(\boldsymbol{r},\omega)'$ at higher harmonics disappears. This does not imply that there is no higher-harmonics generation due to the incident field or the pumps (the $\boldsymbol{q}$-terms), but only that the wave equations decouple.

Although the approximation above is sufficient for the further development of the theory, we make a few more assumptions in order to simplify the notation. First, we suppose that $\overline{\omega}$ is sufficiently far away from a resonance of the medium. This implies (page 58 of [84]) that $\hat{\chi}^{(3)}$ and the dielectric constant ε are real, and that they do not vary appreciably over a large frequency range around $\overline{\omega}$ and $-\overline{\omega}$. Second, we assume the validity of Kleinman's conjecture [89], which states that $\hat{\chi}^{(3)}_{xxyy}(\omega_1,\omega_2,\omega_3)$ is invariant under a permutation of its arguments. With these assumptions, the medium is described by only two parameters, which are

$$\varepsilon \equiv \varepsilon(\overline{\omega}) \ , \tag{7.1}$$

$$\chi \equiv \hat{\chi}^{(3)}_{xxyy}(\overline{\omega},\overline{\omega},-\overline{\omega}) \ , \tag{7.2}$$

and they obey

$$\varepsilon^* = \varepsilon > 0 \ , \quad \chi^* = \chi \ . \tag{7.3}$$

The additional restriction $\varepsilon > 0$ expresses that the medium must be non-metallic, as is obvious.

The polarizations for the strong and the weak fields now reduce to

$$\boldsymbol{p}(\boldsymbol{r}) = \chi \frac{3\varepsilon_o}{4\pi^2}\Big[2\{\boldsymbol{e}(\boldsymbol{r})\cdot\boldsymbol{e}(\boldsymbol{r})^*\}\boldsymbol{e}(\boldsymbol{r}) + \{\boldsymbol{e}(\boldsymbol{r})\cdot\boldsymbol{e}(\boldsymbol{r})\}\boldsymbol{e}(\boldsymbol{r})^*\Big] , \tag{7.4}$$

$$\begin{aligned}\hat{\boldsymbol{P}}(\boldsymbol{r},\omega)' = \chi \frac{3\varepsilon_o}{4\pi^2}\Big[&2\{\boldsymbol{e}(\boldsymbol{r})\cdot\boldsymbol{e}(\boldsymbol{r})^*\}\,\hat{\boldsymbol{E}}(\boldsymbol{r},\omega)' + 2\{\boldsymbol{e}(\boldsymbol{r})^*\cdot\hat{\boldsymbol{E}}(\boldsymbol{r},\omega)'\}\,\boldsymbol{e}(\boldsymbol{r}) \\ &+ 2\{\boldsymbol{e}(\boldsymbol{r})\cdot\hat{\boldsymbol{E}}(\boldsymbol{r},\omega)'\}\,\boldsymbol{e}(\boldsymbol{r})^* + \{\boldsymbol{e}(\boldsymbol{r})\cdot\boldsymbol{e}(\boldsymbol{r})\}\,\hat{\boldsymbol{E}}(\boldsymbol{r},\omega-2\overline{\omega})' \\ &+ 2\{\boldsymbol{e}(\boldsymbol{r})\cdot\hat{\boldsymbol{E}}(\boldsymbol{r},\omega-2\overline{\omega})'\}\,\boldsymbol{e}(\boldsymbol{r})\Big] \ , \quad \text{for } \omega \sim \overline{\omega} \ ,\end{aligned} \tag{7.5}$$

$$\hat{\boldsymbol{P}}(\boldsymbol{r},\omega)' = \chi \frac{3\varepsilon_o}{4\pi^2}\Big[2\{\boldsymbol{e}(\boldsymbol{r})\cdot\boldsymbol{e}(\boldsymbol{r})^*\}\,\hat{\boldsymbol{E}}(\boldsymbol{r},\omega)' + 2\{\boldsymbol{e}(\boldsymbol{r})^*\cdot\hat{\boldsymbol{E}}(\boldsymbol{r},\omega)'\}\,\boldsymbol{e}(\boldsymbol{r})$$

$$+ 2\{\boldsymbol{e}(\boldsymbol{r})\cdot\hat{\boldsymbol{E}}(\boldsymbol{r},\omega)'\}\,\boldsymbol{e}(\boldsymbol{r})^* + \{\boldsymbol{e}(\boldsymbol{r})^*\cdot\boldsymbol{e}(\boldsymbol{r})^*\}\,\hat{\boldsymbol{E}}(\boldsymbol{r},\omega+2\overline{\omega})'$$

$$+ 2\{\boldsymbol{e}(\boldsymbol{r})^*\cdot\hat{\boldsymbol{E}}(\boldsymbol{r},\omega+2\overline{\omega})'\}\,\boldsymbol{e}(\boldsymbol{r})^*\Big] \quad , \quad \text{for } \omega \sim -\overline{\omega} \ . \tag{7.6}$$

Notice that the last two expressions only hold for frequencies near the peaks $\omega \sim \overline{\omega}$ and $\omega \sim -\overline{\omega}$, respectively, rather than for the entire frequency range as in Eq. (5.4).

8. PUMP FIELDS

The pump fields are incident on the medium from the right and the left, as shown in Fig. 1. They partially reflect at the sides $y = \pm L/2$, and are partially transmitted in the medium. Since the pumps are linearly polarized in the *z*-direction, we try a solution of the form

$$\boldsymbol{e}(\boldsymbol{r}) = \pi\,\boldsymbol{e}_z\, f(y) \ . \tag{8.1}$$

The polarization, Eq. (7.4), becomes

$$\boldsymbol{p}(\boldsymbol{r}) = \frac{9}{4}\chi\,\pi\,\varepsilon_o \boldsymbol{e}_z\,|f(y)|^2\, f(y) \ , \tag{8.2}$$

and Maxwell's equation (6.6) simplifies to

$$\frac{d^2 f}{dy^2} + \bar{k}^2[\varepsilon + \tfrac{9}{4}\chi\,|f(y)|^2]f(y) = 0 \ . \tag{8.3}$$

The boundary conditions then require that *f(y)* and *df/dy* are continuous at $y = \pm L/2$.

We shall see in the next section that $|\chi|\,|f(y)|^2 << \varepsilon$, so the term $|\chi|\,|f(y)|^2$ can safely be neglected in Eq. (8.3). This is equivalent to neglecting the contribution of the nonlinear interaction to the propagation of the pump fields in the medium. Then the problem reduces to the problem of reflection and transmission of two plane waves incident on a layer of dielectric material [90]. Inside the medium we set

$$f(y) = \alpha_1\, e^{-i\bar{k}y\sqrt{\varepsilon}} + \alpha_2\, e^{i\bar{k}y\sqrt{\varepsilon}} \ , \tag{8.4}$$

with α_1 and α_2 to be determined, and this solution has to be matched to the external fields (6.7) and (6.8), and the reflected fields. We find explicitly

$$\alpha_{1,2} = \frac{2e^{\frac{1}{2}i\bar{k}L(\sqrt{\varepsilon}-1)}}{(\sqrt{\varepsilon}+1)^2 - (\sqrt{\varepsilon}-1)^2 e^{2i\bar{k}L\sqrt{\varepsilon}}} \left[(\sqrt{\varepsilon}+1)E_{1,2} + (\sqrt{\varepsilon}-1)E_{2,1} e^{i\bar{k}L\sqrt{\varepsilon}} \right] , \qquad (8.5)$$

in terms of the (complex) amplitudes E_1 and E_2 of the pump fields.

9. POLARIZATION OPERATOR

With the solution for $\boldsymbol{e}(\boldsymbol{r})$ from the previous section, we can now construct $\hat{\boldsymbol{P}}(\boldsymbol{r},\omega)'$ as given by Eqs. (7.5) and (7.6). First we substitute $\boldsymbol{e}(\boldsymbol{r}) = \pi \boldsymbol{e}_z f(y)$, which gives $\hat{\boldsymbol{P}}(\boldsymbol{r},\omega)'$ in terms of *f(y)*, and subsequently we use (8.4) for *f(y)*. Then we find that terms with factors $\exp(\pm 2i\bar{k}y\sqrt{\varepsilon})$ appear at various places. These exponentials vary with approximately half the pump-laser wavelength in their *y*-dependence. Such fast oscillations average out to zero quickly in their interaction with fields of twice their wavelength, and therefore we will neglect these contributions to the nonlinear polarization. We then obtain

$$\hat{\boldsymbol{P}}(\boldsymbol{r},\omega)' = \tfrac{3}{2}\varepsilon_o \chi \{(|\alpha_1|^2 + |\alpha_2|^2)\overleftrightarrow{P}\,\hat{\boldsymbol{E}}(\boldsymbol{r},\omega)' + \alpha_1\alpha_2 \overleftrightarrow{P}\,\hat{\boldsymbol{E}}(\boldsymbol{r},\omega - 2\overline{\omega})'\} ,$$

for $\omega \sim \overline{\omega}$, (9.1)

$$\hat{\boldsymbol{P}}(\boldsymbol{r},\omega)' = \tfrac{3}{2}\varepsilon_o \chi \{(|\alpha_1|^2 + |\alpha_2|^2)\overleftrightarrow{P}\,\hat{\boldsymbol{E}}(\boldsymbol{r},\omega)' + (\alpha_1\alpha_2)^* \overleftrightarrow{P}\,\hat{\boldsymbol{E}}(\boldsymbol{r},\omega + 2\overline{\omega})'\} ,$$

for $\omega \sim -\overline{\omega}$. (9.2)

Here we have introduced the polarization operator (tensor) $\overleftrightarrow{P}$, which is defined by its action on an arbitrary vector $\boldsymbol{v}$ according to

$$\overleftrightarrow{P}\boldsymbol{v} = \boldsymbol{v} + 2\boldsymbol{e}_z(\boldsymbol{e}_z \cdot \boldsymbol{v}) = \boldsymbol{v}_{\|} + 3\boldsymbol{v}_{\perp} . \qquad (9.3)$$

Here, the notation $\|$ and $\perp$ refers to the orientation with respect to the *xy*-plane, as it did in the boundary conditions. The expressions (9.1) and (9.2) have to be substituted into the wave equation (6.5) for $\hat{\boldsymbol{E}}(\boldsymbol{r},\omega)'$. We then notice that on the right-hand side the field $\hat{\boldsymbol{E}}(\boldsymbol{r},\omega)'$ appears, multiplied by $(3/2)\chi(|\alpha_1|^2 + |\alpha_2|^2)$. Therefore, this parameter accounts for the nonlinear interaction of $\hat{\boldsymbol{E}}(\boldsymbol{r},\omega)'$ with itself. On the other hand, the factor $(3/2)\chi\alpha_1\alpha_2$ is the coupling parameter for the interaction between $\hat{\boldsymbol{E}}(\boldsymbol{r},\omega)'$ and a different spectral component, $\hat{\boldsymbol{E}}(\boldsymbol{r},\omega \pm 2\overline{\omega})'$, of the field. The two coupling parameters can be varied independently by a proper choice of the amplitudes E_1 and E_2 of the pump beams. For instance, for a transparent medium (ε = 1) we have $\alpha_1 = E_1$ and $\alpha_2 = E_2$, which shows the independence of these parameters clearly. It is the parameter $(3/2)\chi\alpha_1\alpha_2$ which couples the spectral components with frequencies $\omega \sim \overline{\omega}$ and $\omega \sim \overline{\omega}$, and this interaction is responsible for the generation of

phase-conjugated radiation. If we want to maximize the efficiency, then $|\alpha_1\alpha_2|$ must be large compared to $|\alpha_1|^2 + |\alpha_2|^2$. This would require

$$|\alpha_1| = |\alpha_2| \ , \tag{9.4}$$

and with Eq. (8.4) this means that the two counterpropagating beams must have equal strength inside the medium. With Eq. (8.5) this becomes

$$\left| \frac{\sqrt{\varepsilon} + 1 + (\sqrt{\varepsilon} - 1) e^{i\bar{k}L\sqrt{\varepsilon}} (E_1 / E_2)}{(\sqrt{\varepsilon} + 1)(E_1 / E_2) + (\sqrt{\varepsilon} - 1) e^{i\bar{k}L\sqrt{\varepsilon}}} \right| = 1 \ , \tag{9.5}$$

in terms of the amplitude ratio E_1 / E_2 of the pump beams. We notice that this includes their phases as well, so Eq. (9.5) imposes a phase-matching condition on the beams. Two possible solutions are $E_1 / E_2 = \pm 1$. For a transparent medium, $\varepsilon = 1$, Eq. (9.5) reduces to $|E_1| = |E_2|$, and therefore two pumps of equal intensity is sufficient. Moreover, for $\varepsilon = 1$ we have $\alpha_1 = E_1$ and $\alpha_2 = E_2$.

Let us now introduce the dimensionless complex-valued coupling parameter

$$\gamma = \tfrac{3}{2} \chi \alpha_1 \alpha_2 \ , \tag{9.6}$$

and the real parameter

$$\gamma_o = |\gamma| \, \mathrm{sgn}(\chi) \ , \tag{9.7}$$

with obviously $|\gamma_o| = |\gamma|$. Then we can write

$$\gamma = \gamma_o \, e^{i\theta_p} \ , \quad \theta_p \text{ real}, \tag{9.8}$$

and the second coupling parameter becomes

$$\tfrac{3}{2} \chi (|\alpha_1|^2 + |\alpha_2|^2) = 2\gamma_o \ . \tag{9.9}$$

In terms of these parameters, the nonlinear polarization becomes

$$\hat{\boldsymbol{P}}(\boldsymbol{r}, \omega)' = \gamma_o \, \varepsilon_o \overleftrightarrow{P} \{2\hat{\boldsymbol{E}}(\boldsymbol{r}, \omega)' + e^{i\theta_p} \hat{\boldsymbol{E}}(\boldsymbol{r}, \omega - 2\overline{\omega})'\} \ , \ \omega \sim \overline{\omega} \ , \tag{9.10}$$

$$\hat{\boldsymbol{P}}(\boldsymbol{r}, \omega)' = \gamma_o \, \varepsilon_o \overleftrightarrow{P} \{2\hat{\boldsymbol{E}}(\boldsymbol{r}, \omega)' + e^{-i\theta_p} \hat{\boldsymbol{E}}(\boldsymbol{r}, \omega + 2\overline{\omega})'\} \ , \ \omega \sim -\overline{\omega} \ . \tag{9.11}$$

The phase θ_p depends in a complicated way on the phases of the pump beams, at least for $\varepsilon \neq 1$. In any case, any random fluctuations in the phases of the pumps are reflected in fluctuations of θ_p. If there is some phase noise in the pump beams, leading to a finite bandwidth of the lasers, then the factors $\exp(\pm i\theta_p)$ in the nonlinear polarization become random processes with zero average. In this fashion, the nonlinear interaction will be washed out since the second terms on the right-hand sides of Eqs. (9.10) and (9.11) will vanish, on average. Therefore, the pump frequency $\overline{\omega}$ has to be well-stabilized.

In practical situations the intensities of the pump beams will be almost equal, so that $|E_1| \approx |E_2|$. Then the coupling strength $|\gamma_o|$ has an order of magnitude of $|\gamma_o| \sim |\chi E_1^2|$, which is proportional to the laser intensity. Media where the nonlinear coupling is proportional to the pump intensity are called Kerr media, although here the dependence on the intensity is only parametric.

A typical value of a third-order susceptibility is $\chi \sim 10^{-22}$ m^2/V^2 (p. 531 of ref. 84), and an extremely strong pulsed laser has an intensity of 10^{18} W/m^2, which corresponds to an electric field strength of 3×10^{10} V/m, and a coupling parameter of $|\gamma_o| \sim 0.1$. This order of magnitude is a very upper limit. For moderate CW lasers or nanosecond pulses, values in the range of $|\gamma_o| \sim 10^{-5}$ - 10^{-8} are more realistic. In any case, the parameter $|\gamma_o|$ is always small compared to unity, and therefore the nonlinear polarization in the wave equation is a small term. Since this term is the one that is going to produce the phase-conjugated signal, it might seem that this scheme of four-wave mixing is not a very efficient way of generating phase-conjugated radiation. Such an opinion would be based on considering the term with $\hat{\boldsymbol{P}}(\boldsymbol{r},\omega)'$ as the source term in the wave equation. We shall see that the mechanism of generating a phase-conjugated signal by four-wave mixing is more subtle.

10. POSITIVE AND NEGATIVE FREQUENCY PARTS

For the remainder of this paper we shall only be concerned with the weak fields, and therefore we shall drop the primes on $\hat{\boldsymbol{E}}(\boldsymbol{r},\omega)'$, etc. It is worthwhile to note that $\hat{\boldsymbol{P}}(\boldsymbol{r},\omega)$, as given by Eqs. (9.10) and (9.11), obeys the relation

$$\hat{\boldsymbol{P}}(\boldsymbol{r},\omega)^* = \hat{\boldsymbol{P}}(\boldsymbol{r},-\omega) \ , \tag{10.1}$$

which guarantees that $\boldsymbol{P}(\boldsymbol{r},t)$ is real (section 3). If we want to find the Fourier inverse $\boldsymbol{P}(\boldsymbol{r},t)$, we can use either Eq. (3.2) or Eq. (3.5), with $\boldsymbol{E} \to \boldsymbol{P}$. Since $\hat{\boldsymbol{P}}(\boldsymbol{r},\omega)$ in Eq. (9.10) is given for positive ω only, it is easiest to find the positive frequency part first. We obtain

$$\boldsymbol{P}(\boldsymbol{r},t)^{(+)} = \gamma_o \overleftrightarrow{P} \{2\boldsymbol{E}(\boldsymbol{r},t)^{(+)} + e^{i\theta_p} e^{-2i\overline{\omega}t} \boldsymbol{E}(\boldsymbol{r},t)^{(-)}\} \ , \tag{10.2}$$

and then $\boldsymbol{P}(\boldsymbol{r},t)^{(-)}$ follows from a complex conjugation of the right-hand side. Most interesting to notice is that the positive frequency part of the polarization acquires a contribution which is proportional to the negative frequency component of the electric field. The factor $\exp(-2i\overline{\omega}t)$ assures that $\boldsymbol{P}(\boldsymbol{r},t)^{(+)}$ only has positive frequencies. We see that the

nonlinear interaction can transform a negative frequency field into a positive frequency field, which is reminiscent of time reversal and is the basis of the mechanism of phase conjugation by this device.

11. COUPLED WAVE EQUATIONS

For the remainder of this paper we shall only be concerned with the weak fields, and therefore we shall drop the primes on $\hat{\boldsymbol{E}}(\boldsymbol{r},\omega)'$, etc. When we substitute Eqs. (9.10) and (9.11) into the wave equation (6.5), we get

$$\nabla\times(\nabla\times\hat{\boldsymbol{E}}(\boldsymbol{r},\omega))-\frac{\omega^2}{c^2}(\varepsilon+2\gamma_o\overleftrightarrow{P})\hat{\boldsymbol{E}}(\boldsymbol{r},\omega)=\frac{\omega^2}{c^2}\overleftrightarrow{P}\begin{cases}\gamma\,\hat{\boldsymbol{E}}(\boldsymbol{r},\omega-2\overline{\omega}), & \omega\sim\overline{\omega}\\ \gamma^*\hat{\boldsymbol{E}}(\boldsymbol{r},\omega+2\overline{\omega}), & \omega\sim-\overline{\omega}\end{cases}. \tag{11.1}$$

This equations couples the spectral components of $\hat{\boldsymbol{E}}(\boldsymbol{r},\omega)$ at different frequencies. Suppose we consider a fixed frequency ω_a with

$$\omega_a\sim\overline{\omega}\ . \tag{11.2}$$

If we set $\omega=\omega_a$ in the top line of Eq. (11.1), then we see that $\hat{\boldsymbol{E}}(\boldsymbol{r},\omega_a)$ couples to $\hat{\boldsymbol{E}}(\boldsymbol{r},\omega_a-2\overline{\omega})$. We therefore introduce

$$\omega_b=\omega_a-2\overline{\omega}\,,\qquad \omega_b\sim-\overline{\omega}\ , \tag{11.3}$$

and if we take $\omega=\omega_b$ in the bottom line of Eq. (11.1) then we find that $\hat{\boldsymbol{E}}(\boldsymbol{r},\omega_b)$ couples to the spectral component $\hat{\boldsymbol{E}}(\boldsymbol{r},\omega_b+2\overline{\omega})$, which is $\hat{\boldsymbol{E}}(\boldsymbol{r},\omega_a)$. This shows that frequencies couple in pairs, with the frequencies related as ω_a and ω_b. Consequently, the electric field obeys the set of two coupled wave equations

$$\nabla\times(\nabla\times\hat{\boldsymbol{E}}(\boldsymbol{r},\omega_a))-\frac{\omega_a^2}{c^2}(\varepsilon+2\gamma_o\overleftrightarrow{P})\hat{\boldsymbol{E}}(\boldsymbol{r},\omega_a)=\gamma\frac{\omega_a^2}{c^2}\overleftrightarrow{P}\,\hat{\boldsymbol{E}}(\boldsymbol{r},\omega_b)\ , \tag{11.4}$$

$$\nabla\times(\nabla\times\hat{\boldsymbol{E}}(\boldsymbol{r},\omega_b))-\frac{\omega_b^2}{c^2}(\varepsilon+2\gamma_o\overleftrightarrow{P})\hat{\boldsymbol{E}}(\boldsymbol{r},\omega_b)=\gamma^*\frac{\omega_b^2}{c^2}\overleftrightarrow{P}\,\hat{\boldsymbol{E}}(\boldsymbol{r},\omega_a)\ . \tag{11.5}$$

It is important to notice that this set couples a spectral component with a positive frequency, ω_a, with a component with a negative frequency, ω_b, and such that

$$\omega_a+|\,\omega_b\,|=2\overline{\omega}\ , \tag{11.6}$$

indicating that the two frequencies are a distance $2\overline{\omega}$ apart. This, of course, reflects the fact that in a four-wave mixing process two photons with frequency $\overline{\omega}$ are involved. Figure 2 shows the four-wave mixing process, as it occurs at the atomic level inside the medium. Two pump photons are absorbed, while in between a photon with frequency ω_a is emitted. From energy conservation we then see that a second photon with frequency $|\omega_b|$ has to be emitted as the final stage of the process, with $|\omega_b|$ given by Eq. (11.6). Since ω_a is the frequency of the incident light (see below), we conclude that the incident wave is amplified in this process. It also shows that it takes two pump laser photons to create a single phase-conjugated, $|\omega_b|$, photon.

12. PLANE WAVES

When the source of the incident field is far away from the surface of the medium, the incident field will be a traveling plane wave. On the other hand, when the source is close to the *xy*-plane, then the radiation will consist of spherical waves, as happens for instance when an atomic dipole is located in close vicinity of the medium [65]. In that case, the incident field can be represented as an angular spectrum integral, which is a superposition of plane waves [91-93]. Apart from the usual traveling waves, the angular spectrum also contains evanescent waves, which are waves that decay exponentially along the *z*-axis and travel along the *xy*-plane. In order to cover this possibility, we shall allow the incident field to be either traveling or evanescent.

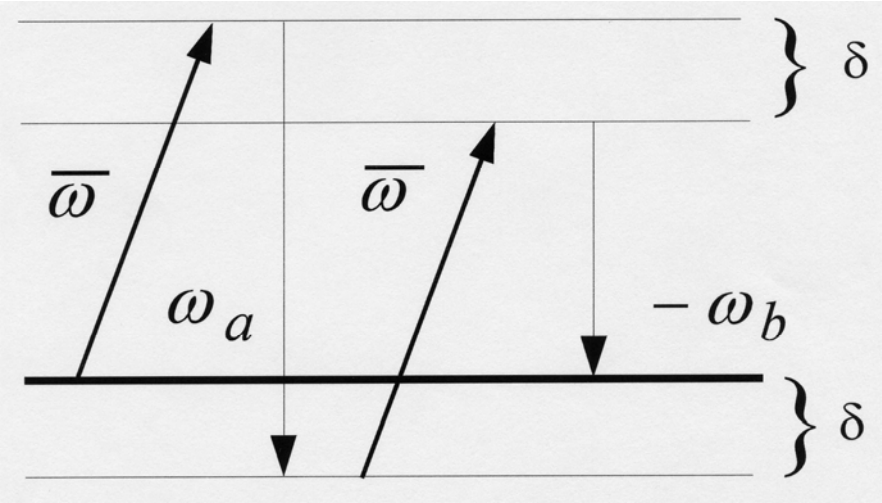

Figure 2: Energy level diagram for four-wave mixing in an atom. The thick line is the atomic ground state. An $\overline{\omega}$ pump photon is absorbed, bringing the atom to approximately an excited state (upper thin line). Then an ω_a photon is emitted, and subsequently a second $\overline{\omega}$ photon is absorbed. Finally, the atom returns to the ground state under emission of the phase-conjugated photon with frequency $-\omega_b$.

In order for this approach to be useful, it is necessary that the nonlinear medium supports plane-wave modes, which can be matched across the boundary to the incident field. Fortunately, these plane wave solutions do exist, and they have the form

$$\hat{\boldsymbol{E}}(\boldsymbol{r},\omega_a) = E\,\boldsymbol{a}\,e^{i\boldsymbol{k}\cdot\boldsymbol{r}} \quad , \quad \hat{\boldsymbol{E}}(\boldsymbol{r},\omega_b) = E\,\boldsymbol{b}\,e^{i\boldsymbol{k}\cdot\boldsymbol{r}} \quad , \tag{12.1}$$

with the polarization vectors $\boldsymbol{a}$ and $\boldsymbol{b}$ and the wave vector $\boldsymbol{k}$ to be determined. The overall constant E has to be the same in both waves in order to cancel out in the coupled wave equations (11.4) and (11.5). Both the ω_a-wave and the ω_b-wave have the same wave vector $\boldsymbol{k}$. For a traveling incident wave or a partial wave of the angular spectrum we have that the parallel component of the wave vector is real. It is only possible to match the waves across the boundary if all waves involved have wave vectors with the same parallel components. Therefore, we shall assume that the parallel component of $\boldsymbol{k}$ (its component in the xy-plane, $\boldsymbol{k}_{||}$) is real, and that it is the same $\boldsymbol{k}_{||}$ as of the incident wave, and consequently supposed to be given. The z-components of the various wave vectors are determined by the dispersion relation of either the vacuum or the medium, and they can be complex-valued.

Since ω_a is positive, the corresponding electric field in the time domain follows from Eqs. (3.5) and (3.7):

$$\boldsymbol{E}(\boldsymbol{r},t) \propto E\,\boldsymbol{a}\,e^{i(\boldsymbol{k}\cdot\boldsymbol{r}-\omega_a t)} + c.c. \quad , \tag{12.2}$$

which is a plane wave with wave vector $\boldsymbol{k}$. For the ω_b-wave we first use Eq. (3.4) to find the field at the positive frequency $-\omega_b = |\,\omega_b\,|$ as $\hat{\boldsymbol{E}}(\boldsymbol{r},-\omega_b) = \hat{\boldsymbol{E}}(\boldsymbol{r},\omega_b)^* = E^*\boldsymbol{b}^* \exp[-i(\boldsymbol{k}^*\cdot\boldsymbol{r})]$. The field in the time domain then has the form

$$\boldsymbol{E}(\boldsymbol{r},t) \propto E^*\boldsymbol{b}^*\,e^{i(-\boldsymbol{k}^*\cdot\boldsymbol{r}-|\omega_b|t)} + c.c. \quad , \tag{12.3}$$

and this is a plane wave with wave vector $-\boldsymbol{k}^*$. For a traveling wave, $\boldsymbol{k}$ is real, and hence the two waves form a counterpropagating pair. For an evanescent ω_a-wave, decaying in the $-z$-direction, the ω_b-wave is also evanescent, and it also decays in the $-z$-direction. These evanescent waves travel along the xy-plane, and since $\boldsymbol{k}_{||}$ is real, they counterpropagate.

13. Set of Equations for the Wave Vector

We shall introduce the dimensionless wave vector

$$\boldsymbol{\kappa} = \frac{c}{\omega_a}\boldsymbol{k} \quad , \tag{13.1}$$

with ω_a / c the wave number of an ω_a-wave in free space. Furthermore we define the dimensionless frequency parameter ρ as

$$\rho = -\frac{\omega_b}{\omega_a} = \frac{2\overline{\omega} - \omega_a}{\omega_a} \ , \tag{13.2}$$

which is positive. For plane waves on resonance with the pump frequency $\overline{\omega}$ we have $\overline{\omega} = \omega_a = -\omega_b$, and $\rho = 1$. In general, ρ will be close to unity, and ρ - 1 can be considered the dimensionless detuning from resonance. Then we substitute the solutions (12.1) into the wave equations (11.4) and (11.5), which gives

$$-(\boldsymbol{\kappa}\cdot\boldsymbol{a})\boldsymbol{\kappa} + \kappa^2\boldsymbol{a} - (\varepsilon + 2\gamma_o\overleftrightarrow{P})\boldsymbol{a} = \gamma\overleftrightarrow{P}\boldsymbol{b} \ , \tag{13.3}$$

$$-(\boldsymbol{\kappa}\cdot\boldsymbol{b})\boldsymbol{\kappa} + \kappa^2\boldsymbol{b} - \rho^2(\varepsilon + 2\gamma_o\overleftrightarrow{P})\boldsymbol{b} = \gamma^*\rho^2\overleftrightarrow{P}\boldsymbol{a} \ , \tag{13.4}$$

with $\kappa^2 = \boldsymbol{\kappa}\cdot\boldsymbol{\kappa}$. Here, ε, γ_o, γ and ρ are given, and the problem becomes to determine what solutions $\boldsymbol{a}$, $\boldsymbol{b}$, $\boldsymbol{\kappa}$ this set admits.

The action of the polarization operator $\overleftrightarrow{P}$ on a vector $\boldsymbol{v}$ yields a parallel and a perpendicular part, as shown in Eq. (9.3), and the set (13.3), (13.4) can be split accordingly. We then obtain the equivalent set of four equations

$$-(\boldsymbol{\kappa}\cdot\boldsymbol{a})\boldsymbol{\kappa}_\perp + (\kappa^2 - \varepsilon - 6\gamma_o)\boldsymbol{a}_\perp = 3\gamma\boldsymbol{b}_\perp \ , \tag{13.5}$$

$$-(\boldsymbol{\kappa}\cdot\boldsymbol{b})\boldsymbol{\kappa}_\perp + [\kappa^2 - \rho^2(\varepsilon + 6\gamma_o)]\boldsymbol{b}_\perp = 3\gamma^*\rho^2\boldsymbol{a}_\perp \ , \tag{13.6}$$

$$-(\boldsymbol{\kappa}\cdot\boldsymbol{a})\boldsymbol{\kappa}_\parallel + (\kappa^2 - \varepsilon - 2\gamma_o)\boldsymbol{a}_\parallel = \gamma\boldsymbol{b}_\parallel \ , \tag{13.7}$$

$$-(\boldsymbol{\kappa}\cdot\boldsymbol{b})\boldsymbol{\kappa}_\parallel + [\kappa^2 - \rho^2(\varepsilon + 2\gamma_o)]\boldsymbol{b}_\parallel = \gamma^*\rho^2\boldsymbol{a}_\parallel \ , \tag{13.8}$$

which have to be satisfied simultaneously for a solution $\boldsymbol{a}$, $\boldsymbol{b}$, $\boldsymbol{\kappa}$.

14. TRANSVERSE SOLUTION

For a linear medium, all plane-wave solutions are transverse ($\boldsymbol{k}$ 'perpendicular' to the polarization vector in the sense of $\boldsymbol{k}\cdot\boldsymbol{a} = 0$, although $\boldsymbol{k}$ can have complex components), so let us try the same here:

$$\boldsymbol{\kappa}\cdot\boldsymbol{a} = 0 \ , \quad \boldsymbol{\kappa}\cdot\boldsymbol{b} = 0 \ . \tag{14.1}$$

An obvious possibility for the solution of Eqs. (13.5) and (13.6) is then

$$\boldsymbol{a}_\perp = \boldsymbol{b}_\perp = 0 \ . \tag{14.2}$$

Then Eqs (13.7) and (13.8) become, in matrix form

$$\begin{pmatrix} \kappa^2 - (\varepsilon + 2\gamma_o) & -\gamma \\ -\gamma^* \rho^2 & \kappa^2 - \rho^2(\varepsilon + 2\gamma_o) \end{pmatrix} \begin{pmatrix} \boldsymbol{a}_{\parallel} \\ \boldsymbol{b}_{\parallel} \end{pmatrix} = 0 \ . \tag{14.3}$$

The solution $\boldsymbol{a}_{\parallel} = \boldsymbol{b}_{\parallel} = 0$ would give $\boldsymbol{a} = \boldsymbol{b} = 0$, so the only possibility is

$$\det \begin{pmatrix} \kappa^2 - (\varepsilon + 2\gamma_o) & -\gamma \\ -\gamma^* \rho^2 & \kappa^2 - \rho^2(\varepsilon + 2\gamma_o) \end{pmatrix} = 0 \ , \tag{14.4}$$

and this is

$$[\kappa^2 - (\varepsilon + 2\gamma_o)][\kappa^2 - \rho^2(\varepsilon + 2\gamma_o)] - \gamma_o^2 \rho^2 = 0 \ . \tag{14.5}$$

This relates the dimensionless wave number κ to the frequency parameter ρ, so this equation is the dispersion relation for this class of solutions.

Equation (14.5) is a quadratic equation for κ^2, so it has two solutions. We define the two branches, labeled 1 and 2, as the solutions

$$\kappa_s^{\binom{1}{2}} = \sqrt{\tfrac{1}{2}(\varepsilon + 2\gamma_o) \left\{ \rho^2 + 1 \mp \delta \sqrt{(\rho^2 - 1)^2 + \left(\frac{2\rho\gamma_o}{\varepsilon + 2\gamma_o} \right)^2} \right\}} \ , \tag{14.6}$$

where we have introduced the parameter δ

$$\delta = \begin{cases} 1, \quad for\ \rho > 1 \qquad (\omega_a < \overline{\omega}) \\ \\ -1, \quad for\ \rho < 1 \qquad (\omega_a > \overline{\omega}) \end{cases} , \tag{14.7}$$

for reasons explained below. Also, we write κ_s to indicate that it is a solution of the type considered in this section.

In an ordinary dielectric a wave with frequency ω_a would have a wave number $(\omega_a / c)\sqrt{\varepsilon}$, and for a wave with frequency $-\omega_b$ this would be $(-\omega_b / c)\sqrt{\varepsilon}$. With Eq. (13.1) this corresponds to $\kappa^2 = \varepsilon$ and $\kappa^2 = \rho^2 \varepsilon$, respectively. If we take the limit $\gamma_o \to 0$ in the solution (14.6) we find

$$\kappa_s^{(1)} \to \sqrt{\varepsilon} \ , \qquad \kappa_s^{(2)} \to \rho\sqrt{\varepsilon} \ , \tag{14.8}$$

which are the respective limits for an ω_a-wave and an ω_b-wave in a dielectric. This is a consequence of the introduction of δ in the solution (14.6). With this convention, the solution with label (1) is essentially the ω_a-wave $\hat{\boldsymbol{E}}(\boldsymbol{r}, \omega_a)$, and due to the nonlinear interaction the

ω_b component $\hat{\boldsymbol{E}}(\boldsymbol{r},\omega_b)$ can be excited. In the same way, the solution (2) is an ω_b-wave with an ω_a part mixed in when $\gamma \neq 0$. Figure 3 illustrates the solution of the dispersion relation (14.5) as a function of the frequency ω_a in units of $\overline{\omega}$:

$$\nu = \frac{\omega_a}{\overline{\omega}} \tag{14.9}$$

The discontinuity at $\rho = 1$, or $\nu = 1$, is due to the δ in the solution, and both curves jump by the amount of $2|\gamma_o|$.

15. NON-TRANSVERSE SOLUTION

In order to derive a second, independent, solution we start from Eqs. (13.3) and (13.4). First we take the dot product with $\boldsymbol{\kappa}$, and write the result as a single matrix equation. We then obtain the relation

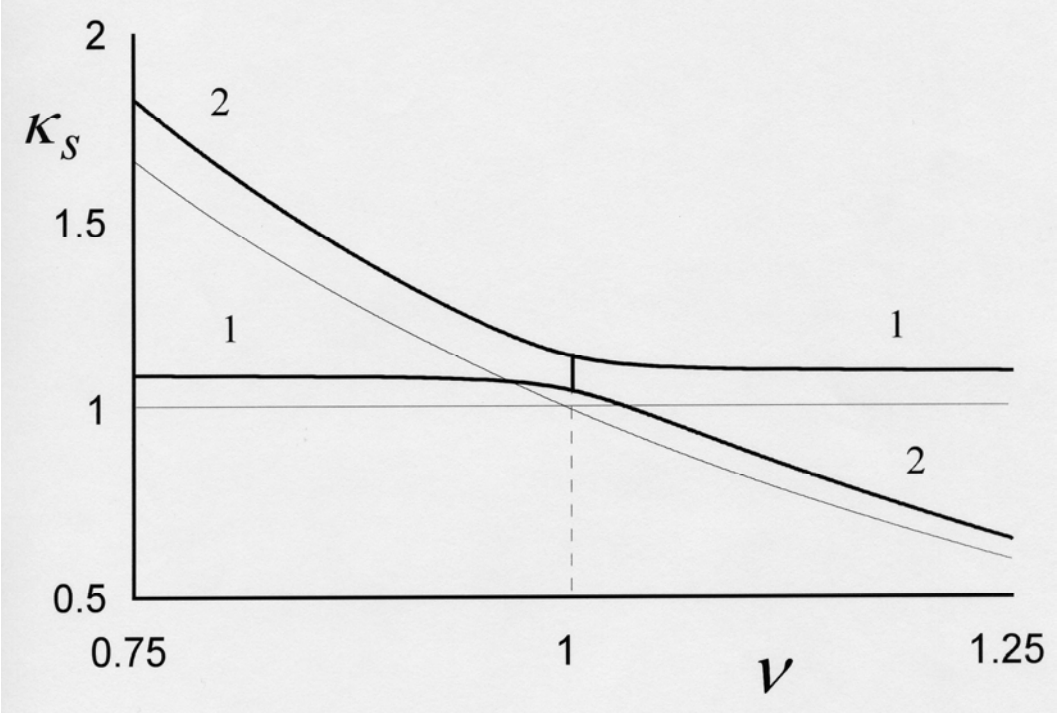

Figure 3: Dispersion relation for *s*-waves. Shown is the dimensionless wave number as a function of the dimensionless frequency. The thick curves are represented by the right-hand side of Eq. (14.6), for $\varepsilon = 1$ and $\gamma_o = 0.1$. The thin lines are the values for $\gamma_o \to 0$, which are $\sqrt{\varepsilon}$ for solution 1 and $\rho\sqrt{\varepsilon}$ for solution 2, as indicated by Eq. (14.8). Both curves have a discontinuity at $\nu = 1$.

$$M_a \begin{pmatrix} \boldsymbol{\kappa}\cdot\boldsymbol{a} \\ \boldsymbol{\kappa}\cdot\boldsymbol{b} \end{pmatrix} = M_b \begin{pmatrix} \kappa_\perp a_\perp \\ \kappa_\perp b_\perp \end{pmatrix} , \tag{15.1}$$

in terms of the matrices

$$M_a = \begin{pmatrix} \varepsilon + 2\gamma_o & \gamma \\ \gamma^* & \varepsilon + 2\gamma_o \end{pmatrix} , \tag{15.2}$$

$$M_b = -2 \begin{pmatrix} 2\gamma_o & \gamma \\ \gamma^* & 2\gamma_o \end{pmatrix} . \tag{15.3}$$

It is interesting to notice that both matrices have a non-vanishing determinant, and can therefore be inverted. Then Eq. (15.1) implies that Eq. (14.2) follows from Eq. (14.1) and vice versa. In other words, the solution of the previous section is the only transverse solution. Knowing this, we will now derive a solution which is necessarily not transverse, and thereby also automatically independent of the solution of the previous section.

When we take the dot product with $\boldsymbol{e}_z$ in Eqs. (13.5) and (13.6), multiply by $\kappa_\perp$, and put the result in matrix form, we find

$$M_c \begin{pmatrix} \kappa_\perp a_\perp \\ \kappa_\perp b_\perp \end{pmatrix} = \kappa_\perp^2 \begin{pmatrix} \boldsymbol{\kappa}\cdot\boldsymbol{a} \\ \boldsymbol{\kappa}\cdot\boldsymbol{b} \end{pmatrix} , \tag{15.4}$$

with

$$M_c = \begin{pmatrix} \kappa^2 - (\varepsilon + 6\gamma_o) & -3\gamma \\ -3\rho^2\gamma & \kappa^2 - \rho^2(\varepsilon + 6\gamma_o) \end{pmatrix} . \tag{15.5}$$

We notice that Eq. (15.4) relates the same 'variables' as Eq. (15.1), but in a different way. Then we eliminate $\kappa_\perp a_\perp$ and $\kappa_\perp b_\perp$ in Eq. (15.4) with the help of relation (15.1), which yields

$$(M_c\, M_b^{-1} M_a - \kappa_\perp^2) \begin{pmatrix} \boldsymbol{\kappa}\cdot\boldsymbol{a} \\ \boldsymbol{\kappa}\cdot\boldsymbol{b} \end{pmatrix} = 0 \ . \tag{15.6}$$

The solution $\boldsymbol{\kappa}\cdot\boldsymbol{a} = 0, \boldsymbol{\kappa}\cdot\boldsymbol{b} = 0$ are the *s*-waves from the previous section. A non-trivial solution exists if

$$\det (M_c\, M_b^{-1} M_a - \kappa_\perp^2 I) = 0 \ , \tag{15.7}$$

with I the 2×2 unit matrix. Equation (15.7) is the equivalent of Eq. (14.4) for the *s*-waves, so it provides the dispersion relation for this second class of solutions for the coupled waves. An interesting difference is that in Eq. (15.7) both κ^2 (through M_c) and $\kappa_\perp^2$ appear separately, whereas Eq. (14.4) only contains κ^2. As explained before, we shall take $\kappa_\parallel$ as an independent variable, and eliminate $\kappa_\perp^2=\kappa^2-\kappa_\parallel^2$. The solution of Eq. (15.7) is then found to be

$$\kappa_p^{\binom{1}{2}}=\sqrt{\gamma_o(2\varepsilon+9\gamma_o)y+\tfrac{1}{2}(\varepsilon+2\gamma_o)\left\{\rho^2+1\mp\delta\sqrt{(\rho^2-1)^2+(1+\varepsilon y)(\rho^2+\varepsilon y)\left(\frac{2\gamma_o}{\varepsilon+2\gamma_o}\right)^2}\right\}}\,, \tag{15.8}$$

with the abbreviation

$$y=\frac{2\kappa_\parallel^2}{(\varepsilon+3\gamma_o)(\varepsilon+9\gamma_o)}\,. \tag{15.9}$$

We notice that κ_p goes over in κ_s for $\kappa_\parallel\to 0$, both for the 1 and the 2 solution, and that for $\gamma_o\to 0$ we have

$$\kappa_p^{(1)}\to\sqrt{\varepsilon}\,,\qquad \kappa_p^{(2)}\to\rho\sqrt{\varepsilon}\,, \tag{15.10}$$

as in Eq. (14.8).

16. *S*-WAVES

It follows from Eq. (14.2) that the polarization vectors $\boldsymbol{a}$ and $\boldsymbol{b}$ for solutions of the first kind are perpendicular to the *z*-axis, and with a combination of Eqs. (14.1) and (14.2) we see that $\boldsymbol{\kappa}_\parallel\cdot\boldsymbol{a}=0,\boldsymbol{\kappa}_\parallel\cdot\boldsymbol{b}=0$. Therefore, vectors $\boldsymbol{a}$ and $\boldsymbol{b}$ are also perpendicular to $\boldsymbol{\kappa}_\parallel$, and therefore perpendicular to the plane defined by $\boldsymbol{\kappa}_\parallel$ and the *z*-axis (recall that we assume $\boldsymbol{\kappa}_\parallel$ to be real). Since all wave vectors have the same $\boldsymbol{k}_\parallel$, represented by the dimensionless $\boldsymbol{\kappa}_\parallel$, this is the plane of incidence of the incident wave, and the vectors $\boldsymbol{a}$ and $\boldsymbol{b}$ are perpendicular to that plane. Solutions of this type are said to be *s*-polarized, and we reflect that in the notation with a subscript *s* on the wave number κ, as in Eq. (14.6).

Given $\boldsymbol{\kappa}_\parallel$, we define the unit vector for *s*-polarization as

$$\boldsymbol{e}_s=\frac{1}{\kappa_\parallel}(\boldsymbol{\kappa}_\parallel\times\boldsymbol{e}_z)\,, \tag{16.1}$$

with $\kappa_\parallel$ the magnitude of $\boldsymbol{\kappa}_\parallel$. Then both $\boldsymbol{a}=\boldsymbol{a}_\parallel$ and $\boldsymbol{b}=\boldsymbol{b}_\parallel$ must be proportional to $\boldsymbol{e}_s$, and since the two equations in the matrix equation (14.3) are dependent by construction, $\boldsymbol{a}$ and $\boldsymbol{b}$

are only determined up to an overall, common, constant. We shall take this normalization constant different for the 1 and the 2 solutions of the dispersion relation. For $\kappa \equiv \kappa_s^{(1)}$ we set

$$\boldsymbol{a}_{1s} = \boldsymbol{e}_s \ , \quad \boldsymbol{b}_{1s} = \gamma^* \eta_1 \boldsymbol{e}_s \ , \tag{16.2}$$

whereas for the solution with $\kappa \equiv \kappa_s^{(2)}$ we take

$$\boldsymbol{a}_{2s} = \gamma \eta_2 \boldsymbol{e}_s \ , \quad \boldsymbol{b}_{2s} = \boldsymbol{e}_s \ , \tag{16.3}$$

with η_1 and η_2 to be determined. The factors γ^* and γ are taken out for later convenience. Then we substitute this in one of the equations of the set (14.3) and solve for η_1 and η_2. We obtain

$$\eta_1 = \frac{\rho^2}{\{\kappa_s^{(1)}\}^2 - \rho^2(\varepsilon + 2\gamma_o)} \ , \tag{16.4}$$

$$\eta_2 = \frac{1}{\{\kappa_s^{(2)}\}^2 - (\varepsilon + 2\gamma_o)} \ . \tag{16.5}$$

With the explicit expressions for $\kappa_s^{(1)}$ and $\kappa_s^{(2)}$ it can be verified that

$$\eta_1 = \frac{-2\rho^2}{(\varepsilon + 2\gamma_o)\left\{\rho^2 - 1 + \delta\sqrt{(\rho^2-1)^2 + \left(\dfrac{2\rho\gamma_o}{\varepsilon + 2\gamma_o}\right)^2}\right\}} \ , \tag{16.6}$$

and that the two parameters are related as

$$\eta_1 = -\rho^2 \eta_2 \ . \tag{16.7}$$

For $\gamma \to 0$ (nonlinear interaction turned off) we have $\kappa_s^{(1)} \to \sqrt{\varepsilon}$, Eq. (14.8), and therefore η_1 approaches the limit

$$\eta_1 \to \frac{\rho^2}{\varepsilon(1-\rho^2)} \ , \tag{16.8}$$

for $\rho \neq 1$. Then $\gamma^* \eta_1 \to 0$, and $\boldsymbol{b}_{1s} \to 0$. So, without the nonlinear interaction, only the ω_a-wave survives for the solution labeled with 1. It then follows from Eq. (16.3) that in this same limit the ω_a wave disappears in solution 2. Therefore, solutions 1 and 2 are essentially ω_a-

waves and ω_b-waves, respectively, and due to the nonlinear interaction they couple to the ω_b-wave and the ω_a-wave, respectively.

It is interesting to note that this conclusion requires $\rho \neq 1$. Conversely, we can consider the limit $\rho \to 1$ with γ finite. It can be verified from the results above that for $\rho \to 1$, η_1 approaches the limit

$$\eta_1 \to -\frac{\delta}{|\gamma|} \ , \tag{16.9}$$

and therefore the amplitude factor in $\boldsymbol{b}_{1s}$ is $|\gamma^* \eta_1| = 1$. This shows that for perfect resonance the ω_a- and ω_b-waves have the same amplitude, no matter how small the nonlinear interaction is. Due to the δ in Eq. (16.9), the value of η_1 is discontinuous across the resonance $\rho = 1$. Apparently, the limits $\gamma \to 0$ and $\rho \to 1$ do not commute. This also implies that the ω_a-wave (with the frequency of the incident wave) can be considered near resonance under condition $|\rho - 1| << |\gamma|$, and off resonance for $|\rho - 1| >> |\gamma|$. In terms of ω_a and $\overline{\omega}$ this is

$$|\omega_a - \overline{\omega}| << \tfrac{1}{2}\omega_a |\gamma| \ . \tag{16.10}$$

Since in the optical domain ω_a is very large, the coupling parameter γ can be relatively small. With the frequency parameter ν, Eq. (14.9), this resonance condition becomes $|\nu - 1| << \frac{1}{2}\nu|\gamma|$, and since $\nu \sim 1$ this is

$$|\nu - 1| << |\gamma| \ . \tag{16.11}$$

The various features of the amplitude parameter η_1 are shown in Fig. 4. Similar conclusions hold for the solution with $\kappa_s^{(2)}$.

17. *P*-WAVES

The right-hand side of Eq. (14.3) is zero for *s*-waves, because we imposed the condition $\boldsymbol{\kappa} \cdot \boldsymbol{a} = 0$, $\boldsymbol{\kappa} \cdot \boldsymbol{b} = 0$. Without this condition, Eqs. (13.7) and (13.8) become

$$\begin{pmatrix} \kappa_p^2 - (\varepsilon + 2\gamma_o) & -\gamma \\ -\gamma^* \rho^2 & \kappa_p^2 - \rho^2(\varepsilon + 2\gamma_o) \end{pmatrix} \begin{pmatrix} \boldsymbol{a}_{\parallel} \\ \boldsymbol{b}_{\parallel} \end{pmatrix} = \boldsymbol{\kappa}_{\parallel} \begin{pmatrix} \boldsymbol{\kappa} \cdot \boldsymbol{a} \\ \boldsymbol{\kappa} \cdot \boldsymbol{b} \end{pmatrix} \ , \tag{17.1}$$

where we have written $\kappa \equiv \kappa_p$ in the matrix to indicate that we are considering solutions of the second type. For *s*-waves, the determinant of this matrix was set equal to zero, so if the second solution is to be different, the determinant is now non-zero, and therefore has an inverse. This gives

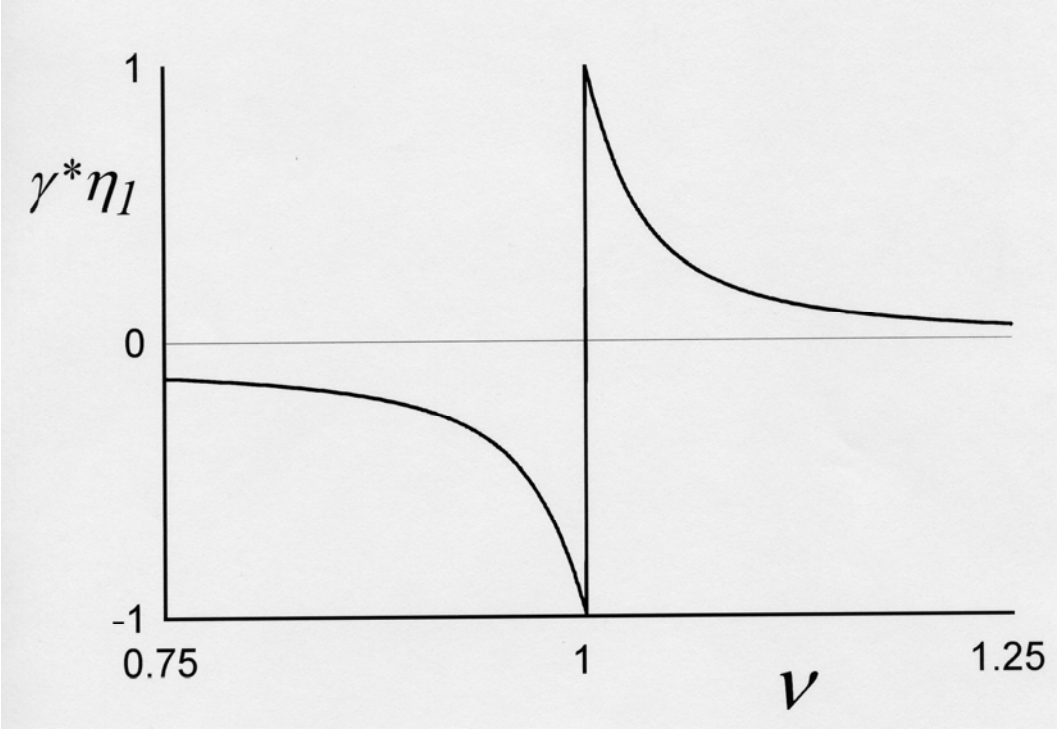

Figure 4: Illustration of the amplitude parameter η_1, multiplied by γ^*, as a function of the frequency ν, and for $\varepsilon = 1$, $\gamma = \gamma_o = 0.1$. At the resonance frequency $\nu = 1$, the value of $\gamma^*\eta_1$ jumps from -1 to 1, as follows from Eq. (16.9). The width of the graph is of the order of $\gamma_o = 0.1$.

$$\begin{pmatrix} \boldsymbol{a}_{\parallel} \\ \boldsymbol{b}_{\parallel} \end{pmatrix} = \boldsymbol{\kappa}_{\parallel} \begin{pmatrix} \kappa_p^2 - (\varepsilon + 2\gamma_o) & -\gamma \\ -\gamma^* \rho^2 & \kappa_p^2 - \rho^2(\varepsilon + 2\gamma_o) \end{pmatrix}^{-1} \begin{pmatrix} \boldsymbol{\kappa} \cdot \boldsymbol{a} \\ \boldsymbol{\kappa} \cdot \boldsymbol{b} \end{pmatrix}, \tag{17.2}$$

from which it follows that both $\boldsymbol{a}_{\parallel}$ and $\boldsymbol{b}_{\parallel}$ are proportional to $\boldsymbol{\kappa}_{\parallel}$. This is only possible when $\boldsymbol{a}$, $\boldsymbol{b}$ and $\boldsymbol{\kappa}$ all lie in the same plane. Since both $\boldsymbol{a}$ and $\boldsymbol{b}$ will have non-zero z-components, as follows from Eq. (15.1), we see that $\boldsymbol{a}$ and $\boldsymbol{b}$ lie in the plane defined by $\boldsymbol{\kappa}_{\parallel}$ and $\boldsymbol{e}_z$, e.g., the plane of incidence. Waves of this type are called *p*-polarized, in contrast to the *s*-polarized waves for which $\boldsymbol{a}$ and $\boldsymbol{b}$ were perpendicular to the plane of incidence. This clearly shows the independence of the two types of solutions.

In order to evaluate the polarization vectors $\boldsymbol{a}$ and $\boldsymbol{b}$ for *p*-polarization, we use the fact that these vectors must be linear combinations of $\boldsymbol{\kappa}_{\parallel}$ and $\boldsymbol{e}_z$. We write

$$\boldsymbol{a}_p = \alpha_{\perp} \boldsymbol{e}_z + \frac{\alpha_{\parallel}}{\kappa_{\parallel}} \boldsymbol{\kappa}_{\parallel}, \tag{17.3}$$

$$\boldsymbol{b}_p = \beta_\perp \boldsymbol{e}_z + \frac{\beta_\parallel}{\kappa_\parallel}\boldsymbol{\kappa}_\parallel \ , \tag{17.4}$$

in analogy to Eqs. (16.2) and (16.3). Here, the factors $\alpha_\perp$, $\alpha_\parallel$, $\beta_\perp$ and $\beta_\parallel$ remain to be determined, and since the dispersion relation has two branches there will be two solutions, 1 and 2, for each parameter, just as in the case of *s*-waves. The factors $\kappa_\parallel$ in the denominators have been split off for later convenience. In section 15, we eliminated $\kappa_\perp a_\perp$ and $\kappa_\perp b_\perp$ in favor of $\boldsymbol{\kappa}\cdot\boldsymbol{a}$ and $\boldsymbol{\kappa}\cdot\boldsymbol{b}$ in Eq. (15.4) by using Eq. (15.1), and this led to Eq. (15.6). Conversely, we can eliminate $\boldsymbol{\kappa}\cdot\boldsymbol{a}$ and $\boldsymbol{\kappa}\cdot\boldsymbol{b}$ in favor of $\kappa_\perp a_\perp$ and $\kappa_\perp b_\perp$, and this yields in the same way

$$(M_b^{-1} M_a M_c - \kappa_\perp^2)\begin{pmatrix}\kappa_\perp a_\perp \\ \kappa_\perp b_\perp\end{pmatrix} = 0 \ . \tag{17.5}$$

Since $(\boldsymbol{\kappa}\cdot\boldsymbol{a},\boldsymbol{\kappa}\cdot\boldsymbol{b}) \neq (0,0)$, as we imposed by Eq. (15.7), it follows from Eq. (15.1) that also $(\kappa_\perp a_\perp, \kappa_\perp b_\perp) \neq (0,0)$. The set (17.5) can only have a nontrivial solution if

$$\det\,(M_b^{-1} M_a M_c - \kappa_\perp^2 I) = 0 \ , \tag{17.6}$$

which must hold by construction. In any case, the two equations in (17.5) are dependent, and if we set $a_\perp = \alpha_\perp$, $b_\perp = \beta_\perp$, as in Eqs. (17.3) and (17.4), and let $\kappa_\perp \neq 0$, the set becomes

$$\alpha_\perp \left[\{\kappa_p^2 - (\varepsilon + 6\gamma_o)\}(\varepsilon + \gamma_o)(\varepsilon + 3\gamma_o) + 2\gamma_o(2\varepsilon + 3\gamma_o)(\kappa_p^2 - \kappa_\parallel^2)\right]$$

$$+ \gamma\,\beta_\perp \left[-3(\varepsilon + \gamma_o)(\varepsilon + 3\gamma_o) + 2\varepsilon(\kappa_p^2 - \kappa_\parallel^2)\right] = 0 \ , \tag{17.7}$$

$$\beta_\perp \left[\{\kappa_p^2 - \rho^2(\varepsilon + 6\gamma_o)\}(\varepsilon + \gamma_o)(\varepsilon + 3\gamma_o) + 2\gamma_o(2\varepsilon + 3\gamma_o)(\kappa_p^2 - \kappa_\parallel^2)\right]$$

$$+ \gamma^*\alpha_\perp \left[-3\rho^2(\varepsilon + \gamma_o)(\varepsilon + 3\gamma_o) + 2\varepsilon(\kappa_p^2 - \kappa_\parallel^2)\right] = 0 \ . \tag{17.8}$$

Just as for *s*-waves, we have a 1 solution and a 2 solution of the dispersion relation, which we would like to correspond to pure ω_a- and ω_b-waves, respectively, in the limit $\gamma \to 0$. For the solution of type 1 we set

$$\beta_\perp^{(1)} = \gamma^*\zeta_1\alpha_\perp^{(1)} \ , \tag{17.9}$$

in analogy to Eq. (16.2) for *s*-waves. Here the parameter ζ_1 is the equivalent of the resonance parameter η_1 for *s*-waves. The factor $\alpha_\perp^{(1)}$ is for normalization, and will be determined below. Then we have $\zeta_1 = \beta_\perp^{(1)}/(\gamma^* \alpha_\perp^{(1)})$, which can be found from either Eq. (17.7) or Eq. (17.8). We shall take Eq. (17.8), which gives

$$\zeta_1 = \frac{3\rho^2(\varepsilon+\gamma_o)(\varepsilon+3\gamma_o) - 2\varepsilon[(\kappa_p^{(1)})^2 - \kappa_\parallel^2]}{\{(\kappa_p^{(1)})^2 - \rho^2(\varepsilon+6\gamma_o)\}(\varepsilon+\gamma_o)(\varepsilon+3\gamma_o) + 2\gamma_o(2\varepsilon+3\gamma_o)[(\kappa_p^{(1)})^2 - \kappa_\parallel^2]} \ . \tag{17.10}$$

In this way, we have for $\gamma \to 0$

$$\zeta_1 \to \frac{3\rho^2 - 2(1-\kappa_\parallel^2/\varepsilon)}{\varepsilon(1-\rho^2)} \ , \tag{17.11}$$

for $\rho \neq 1$, and this is finite, as in Eq. (16.8). In order to find the parallel components $\alpha_\parallel^{(1)}$ and $\beta_\parallel^{(1)}$, we write Eq. (15.4) as

$$(M_c - \kappa_\perp^2 I)\begin{pmatrix} \kappa_\perp a_\perp \\ \kappa_\perp b_\perp \end{pmatrix} = \kappa_\perp^2 \begin{pmatrix} \boldsymbol{\kappa}_\parallel \cdot \boldsymbol{a}_\parallel \\ \boldsymbol{\kappa}_\parallel \cdot \boldsymbol{a}_\parallel \end{pmatrix} . \tag{17.12}$$

From Eq. (15.5) we then see that with $M_c - \kappa_\perp^2 I$, we effectively replace κ^2 by $\kappa_\parallel^2$ in matrix M_c, so that $M_c - \kappa_\perp^2 I$ only depends on the assumed given $\kappa_\parallel^2$. With Eqs. (17.3) and (17.4) the set (17.12) becomes

$$(M_c - \kappa_\perp^2 I)\begin{pmatrix} a_\perp \\ b_\perp \end{pmatrix} = \kappa_\perp \kappa_\parallel \begin{pmatrix} \alpha_\parallel \\ \beta_\parallel \end{pmatrix} , \tag{17.13}$$

both for the solutions of type 1 and type 2. The dispersion relation provides $\kappa \equiv \kappa_p$ and we assume $\kappa_{||}$ given. This only determines $\kappa_\perp^2$ and not $\kappa_\perp$ itself. Apparently, there are two solutions, which differ by a minus sign in their *z*-component of the wave vector. We shall come back to this point below, and assume for the time being that the choice of sign for $\kappa_\perp$ has been made. Equation (17.13) then yields, for the type 1 solution,

$$\alpha_\parallel^{(1)} = \frac{\alpha_\perp^{(1)}}{\kappa_\parallel \kappa_{p,\perp}^{(1)}} \left\{ \kappa_\parallel^2 - (\varepsilon+6\gamma_o) - 3\gamma_o^2 \zeta_1 \right\} , \tag{17.14}$$

$$\beta_\parallel^{(1)} = \gamma^* \frac{\alpha_\perp^{(1)}}{\kappa_\parallel \kappa_{p,\perp}^{(1)}} \left\{ \zeta_1[\kappa_\parallel^2 - \rho^2(\varepsilon+6\gamma_o)] - 3\rho^2 \right\} . \tag{17.15}$$

It finally remains to determine the parameter $\alpha_{\perp}^{(1)}$. We could simply take $\alpha_{\perp}^{(1)} = 1$, but it seems more elegant to use this freedom to normalize the polarization vector as

$$\boldsymbol{a}_{1p} \cdot \boldsymbol{a}_{1p} = 1 \ , \tag{17.16}$$

just as for *s*-waves, Eq. (16.2). We then find explicitly

$$\alpha_{\perp}^{(1)} = -\frac{\kappa_{\parallel}}{\sqrt{\kappa_{\parallel}^2 + \dfrac{\left\{\kappa_{\parallel}^2 - (\varepsilon + 6\gamma_o) - 3\gamma_o^2\zeta_1\right\}^2}{(\kappa_p^{(1)})^2 - \kappa_{\parallel}^2}}} \ . \tag{17.17}$$

The solution of type 2 follows in the same way. We now take

$$\alpha_{\perp}^{(2)} = \gamma\,\zeta_2\,\beta_{\perp}^{(2)} \ , \tag{17.18}$$

instead of Eq. (17.9), and with $\beta_{\perp}^{(2)}$ used for normalization. Along the same lines we now find

$$\zeta_2 = \frac{3(\varepsilon + \gamma_o)(\varepsilon + 3\gamma_o) - 2\varepsilon[(\kappa_p^{(2)})^2 - \kappa_{\parallel}^2]}{\{(\kappa_p^{(2)})^2 - (\varepsilon + 6\gamma_o)\}(\varepsilon + \gamma_o)(\varepsilon + 3\gamma_o) + 2\gamma_o(2\varepsilon + 3\gamma_o)[(\kappa_p^{(2)})^2 - \kappa_{\parallel}^2]} \ , \tag{17.19}$$

which behaves as

$$\zeta_2 \to -\frac{3 - 2(\rho^2 - \kappa_{\parallel}^2/\varepsilon)}{\varepsilon(1 - \rho^2)} \ , \tag{17.20}$$

for $\gamma \to 0$. The parallel components are now found to be

$$\alpha_{\parallel}^{(2)} = \gamma\frac{\beta_{\perp}^{(2)}}{\kappa_{\parallel}\kappa_{p,\perp}^{(2)}}\left\{\zeta_2[\kappa_{\parallel}^2 - (\varepsilon + 6\gamma_o)] - 3\right\} \ , \tag{17.21}$$

$$\beta_{\parallel}^{(2)} = \frac{\beta_{\perp}^{(2)}}{\kappa_{\parallel}\kappa_{p,\perp}^{(2)}}\left\{\kappa_{\parallel}^2 - \rho^2(\varepsilon + 6\gamma_o) - 3\gamma_o^2\rho^2\zeta_2\right\} \ , \tag{17.22}$$

and as normalization we now choose

$$\boldsymbol{b}_{2p} \cdot \boldsymbol{b}_{2p} = 1 \ , \tag{17.23}$$

which gives

$$\beta_{\perp}^{(2)} = -\frac{\kappa_{\|}}{\sqrt{\kappa_{\|}^2 + \dfrac{\left\{ \kappa_{\|}^2 - \rho^2(\varepsilon + 6\gamma_o) - 3\gamma_o^2 \rho^2 \zeta_2 \right\}^2}{(\kappa_p^{(2)})^2 - \kappa_{\|}^2}}} \ . \tag{17.24}$$

18. EXCITATION OF PLANE-WAVE MODES

The two counterpropagating waves $\hat{\boldsymbol{E}}(\boldsymbol{r}, \omega_a)$ and $\hat{\boldsymbol{E}}(\boldsymbol{r}, \omega_b)$, which are a solution of Maxwell's equations inside the medium, have the appearance of a traveling plane wave ($\hat{\boldsymbol{E}}(\boldsymbol{r}, \omega_a)$) and its phase-conjugate image ($\hat{\boldsymbol{E}}(\boldsymbol{r}, \omega_b)$), because the ω_b-wave travels in the opposite direction of the ω_a-wave. If a plane wave of the form

$$\hat{\boldsymbol{E}}(\boldsymbol{r}, \omega_a)_{inc} = E \, \boldsymbol{e}_{\sigma} \, e^{i\boldsymbol{k}\cdot\boldsymbol{r}} \ , \tag{18.1}$$

is incident on the medium from the region z > 0, then it will partially reflect and partially propagate into the medium, where it couples to the ω_b-wave due to the nonlinear interaction. This counterpropagating wave can leave the crystal again at the z = 0 interface, where it appears as the phase-conjugated replica of the incident field. We shall now consider the coupling of the wave (18.1) to the wave modes $\hat{\boldsymbol{E}}(\boldsymbol{r}, \omega_a)$ and $\hat{\boldsymbol{E}}(\boldsymbol{r}, \omega_b)$ inside the material.

In order for $\hat{\boldsymbol{E}}(\boldsymbol{r}, \omega_a)_{inc}$ to be a solution of Maxwell's equations in vacuum, we have the restrictions

$$k = \omega_a / c \ , \quad \boldsymbol{k} \cdot \boldsymbol{e}_{\sigma} = 0 \ , \tag{18.2}$$

for a given ω_a. The unit polarization vector $\boldsymbol{e}_{\sigma}$, with $\sigma = s$ or p, will be specified below, and the overall constant E is arbitrary. We shall assume that the parallel component, $\boldsymbol{k}_{\|}$, of $\boldsymbol{k}$ is given and real. When we write $\boldsymbol{k} = \boldsymbol{k}_{\|} + k_z \boldsymbol{e}_z$, then the first equation of (18.2) is satisfied if

$$k_z^2 = k^2 - \boldsymbol{k}_{\|} \cdot \boldsymbol{k}_{\|} \ , \tag{18.3}$$

which leaves us with two possible choices for k_z. For a wave traveling in the negative z-direction, we must obviously take the negative root of (18.3). In order to avoid longitudinal components in the spatial Fourier spectrum [94,95], which do not satisfy Maxwell's equations separately, we shall allow the incident field to have evanescent components [96-98] which decay in the negative z-direction. These waves are still transverse, but their wave vectors have an imaginary z-component. Since the wave has to decay in the negative z-direction, k_z must

be negative imaginary. Therefore, for a given ω_a and $\boldsymbol{k}_{||}$, the z-component of $\boldsymbol{k}$ must be chosen as

$$k_z = \begin{cases} -\sqrt{k^2 - k_{||}^2} \\ -i\sqrt{k_{||}^2 - k^2} \end{cases} . \tag{18.4}$$

In this notation it is understood that we take the solution for which the argument of the square root is positive.

Just as for the dispersion relations, we make the various quantities dimensionless. For the parallel component of the wave vector we define

$$\boldsymbol{\kappa}_{||} = \boldsymbol{k}_{||} / k \ , \tag{18.5}$$

just as in Eq. (13.1). Its magnitude lies in the range $0 \leq \kappa_{||} < \infty$. For $0 \leq \kappa_{||} < 1$ we have a traveling incident wave, and

$$\kappa_{||} = \sin\theta_i \ , \tag{18.6}$$

with θ_i the angle of incidence. For $\kappa_{||} > 1$ the incident wave is evanescent, with $1/\kappa_{||}$ a dimensionless measure of the distance over which the wave decays exponentially in the negative z-direction. We then introduce

$$\kappa_a = k_z / k \ , \tag{18.7}$$

which is explicitly

$$\kappa_a = \begin{cases} -\sqrt{1 - \kappa_{||}^2} \\ -i\sqrt{\kappa_{||}^2 - 1} \end{cases} . \tag{18.8}$$

The incoming wave couples with other waves inside and outside the medium, in a way which is determined by the boundary conditions at $z = 0$ and $z = -\Delta$. This same principle as in linear optics was first applied to nonlinear multiwave mixing in a layer by Bloembergen and Pershan [99,100]. Obviously, all appearing waves are plane waves which have a factor $\exp(i\boldsymbol{k}_i \cdot \boldsymbol{r})$, with $\boldsymbol{k}_i$ the wave vector of this particular wave. At the interface $z = 0$ this factor reduces to $\exp(i\boldsymbol{k}_{i,||} \cdot \boldsymbol{r})$, and it is easy to see that the boundary conditions can only be satisfied for all $\boldsymbol{r}$ in the xy-plane if this $\boldsymbol{r}$-dependent factor is the same for every wave. This implies that $\boldsymbol{k}_{i,||}$ must be the same for every wave, and consequently equal to $\boldsymbol{k}_{||}$ of the incident wave. The same argument holds for waves which have to be matched across the boundary $z = -\Delta$, and therefore every wave vector must have the form

$$\boldsymbol{k}_i = \boldsymbol{k}_{||} + k_{i,z}\,\boldsymbol{e}_z \ . \tag{18.9}$$

Besides that, every wave vector, either in vacuum or the medium, has to obey the dispersion relation for k_i^2, given its frequency. From this it follows that $k_{i,z}^2 = k_i^2 - k_{||}^2$ is fixed for every possible wave, and the only freedom we have is the choice of the sign of $k_{i,z}$.

The incident wave has positive frequency ω_a, which couples with ω_a-waves and negative-frequency ω_b-waves inside the medium. It can not be decided *à priori* which plane-wave modes will be excited by the incident field, so we have to consider all possible waves, inside and outside, with frequencies ω_a and ω_b and given $\boldsymbol{k}_{||}$. Let us first look at the region $z > 0$ (vacuum) and at frequency ω_a. Then the dispersion relation gives $k_{i,z}^2 = k^2 - k_{||}^2$, with solution (18.4) for the z-component of the wave vector of the incident wave. There is only one other solution, which is the usual specularly-reflected wave from linear optics. We shall call this the r-wave. The z-component of $\boldsymbol{k}_r$ can only be $k_{r,z} = -k_z$, which gives in terms of κ_a and $\kappa_{||}$

$$\boldsymbol{k}_r = k(\boldsymbol{\kappa}_{||} - \kappa_a \boldsymbol{e}_z) \ , \tag{18.10}$$

and compared to the wave vector of the incident field

$$\boldsymbol{k} = k(\boldsymbol{\kappa}_{||} + \kappa_a \boldsymbol{e}_z) \ , \tag{18.11}$$

the only difference is a minus sign in the z-component. This r-wave emanates from the medium and either travels in the specular direction or decays in the positive z-direction. For a traveling r-wave, the angle of reflection is of course equal to the angle of incidence. The various waves outside the medium are pictorially represented in Fig. 5. The arrows indicate the propagation direction in case of a traveling wave. When the wave is evanescent, it decays in the direction away from the material.

At frequency ω_b, the dispersion relation in vacuum is $k_i^2 = \omega_b^2 / c^2$, which admits two solutions for $k_{i,z}$. Considering $z > 0$ first, this ω_b-wave is generated by the nonlinear interaction in the medium, and leaves the crystal through the interface $z = 0$. Causality requires that we should only retain the solution which travels away from the medium, or in case of an evanescent wave, decays in the positive z-direction. Care should be exercised, however, since this is a negative frequency wave which travels in the direction opposite its wave vector. A moment of thought then shows that the wave vector must be

$$\boldsymbol{k}_{pc} = k(\boldsymbol{\kappa}_{||} + \kappa_b \boldsymbol{e}_z) \ , \tag{18.12}$$

in terms of the dimensionless parameter

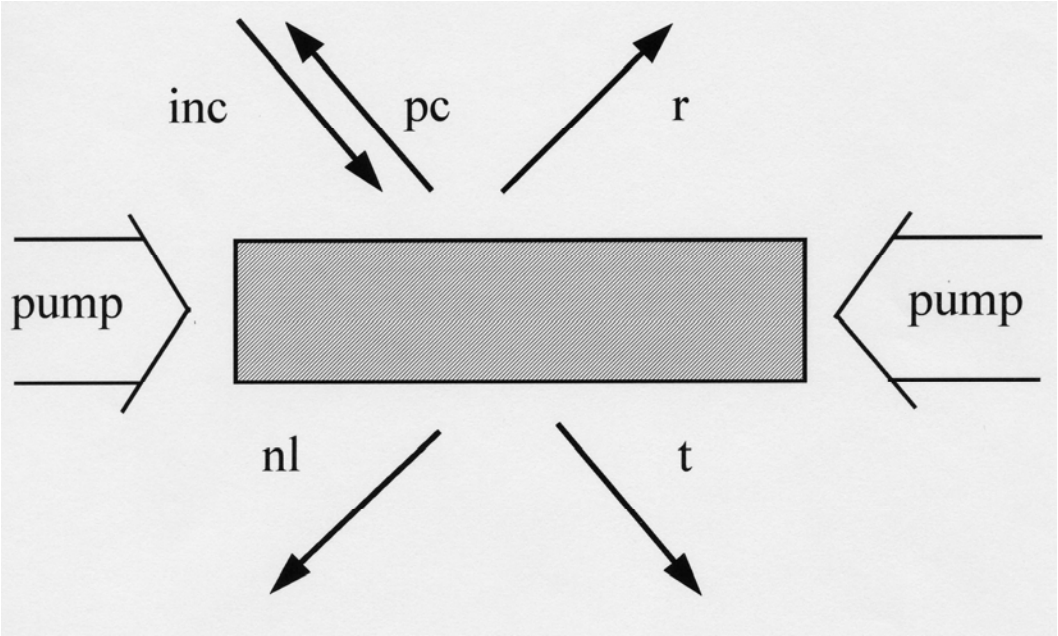

Figure 5: Illustration of the various waves present near the slab of nonlinear material. The arrows indicate the propagation directions of the various waves. For evanescent waves, the decay direction is away from the medium.

$$\kappa_b = \begin{cases} -\sqrt{\rho^2 - \kappa_{\|}^2} \\ i\sqrt{\kappa_{\|}^2 - \rho^2} \end{cases} . \tag{18.13}$$

The appearance of ρ accounts for the difference between ω_a and $|\omega_b|$. We call this the *pc*-wave, for obvious reasons. We notice that for traveling waves and $\rho \neq 1$ this $\boldsymbol{k}_{pc}$ is not identical to $\boldsymbol{k}$ of the incident wave. Since

$$k_{pc} = \frac{|\omega_b|}{c} = \rho k \ , \tag{18.14}$$

we have

$$\sin\theta_{pc} = \frac{\kappa_{\|}}{\rho} \ , \tag{18.15}$$

with θ_{pc} the angle of reflection of the *pc*-wave (for the case of a traveling wave). Comparison with Eq. (18.6) then shows that the angle of reflection is related to the angle of incidence according to

$$\rho \sin\theta_{pc} = \sin\theta_i \ , \tag{18.16}$$

or in terms of frequencies

$$|\omega_b| \sin\theta_{pc} = \omega_a \sin\theta_i \ . \tag{18.17}$$

Therefore, for $\omega_a \neq \overline{\omega}$ the *pc*-wave cannot be the exact phase-conjugated replica of the incident beam. For evanescent waves, phase conjugation never works (with the setup considered here) because the image of a wave which decays in the negative *z*-direction should be a wave which grows exponentially in the positive *z*-direction, as follows from the time-reversal argument. This would clearly violate causality. Nevertheless, we retain the possibility of evanescent incident waves, because of its relevance to applications in radiation theory. Figure 6 illustrates the various wave vectors for the case of traveling waves, and Fig. 7 shows the decay directions for the situation of evanescent waves. It should be noted that not all waves have to be either all traveling or all evanescent. Just as in linear optics, there can be situations where waves of both types appear for a given incident wave.

Next we consider the region $z < -\Delta$. Since this is also vacuum, the dispersion relations for the possible ω_a- and ω_b-waves are the same as in $z > 0$. For a given $\boldsymbol{k}_{||}$ this allows four possible wave vectors, but only two of these represent causal solutions. The ω_a-wave which travels or decays in the negative *z*-direction is the transmitted *t*-wave, with wave vector

$$\boldsymbol{k}_t = \boldsymbol{k} \ . \tag{18.18}$$

The possible ω_b-wave in $z < -\Delta$ is entirely due to the nonlinear interaction (in contrast to the ω_a-wave which is also present for a pure linear material), and we call this one the *nl*-wave. The solution which propagates or decays in the negative *z*-direction has wave vector

$$\boldsymbol{k}_{nl} = k(\boldsymbol{\kappa}_{||} - \kappa_b \boldsymbol{e}_z) \ . \tag{18.19}$$

When the incident wave is *s*-polarized, then every other wave is also *s*-polarized, and the same holds for *p*-polarization. Inside the medium, the dispersion relation is different for *s*- and *p*-waves, so we have to distinguish between the two situations by labeling the wave vectors of the various waves with σ (*s* or *p*). The dispersion relations were shown to have two branches, labeled 1 and 2, corresponding to an ω_a-wave and an ω_b-wave, respectively, in the limit $\gamma \to 0$. Since the dispersion relations only give κ_z^2, there are still two possibilities for the *z*-components of the wave vectors, which differ by a minus sign. Both solutions have to be retained, due to multiple reflections at the boundaries, as is most easily seen from Fig. 6. The four possible wave vectors for a given σ and $\boldsymbol{k}_{||}$ are then

$$\boldsymbol{k}_{1\sigma}^{\pm} = k(\boldsymbol{\kappa}_{||} \pm \kappa_{\alpha\sigma} \boldsymbol{e}_z) \ , \tag{18.20}$$

$$\boldsymbol{k}_{2\sigma}^{\pm} = k(\boldsymbol{\kappa}_{||} \pm \kappa_{\beta\sigma} \boldsymbol{e}_z) \ , \tag{18.21}$$

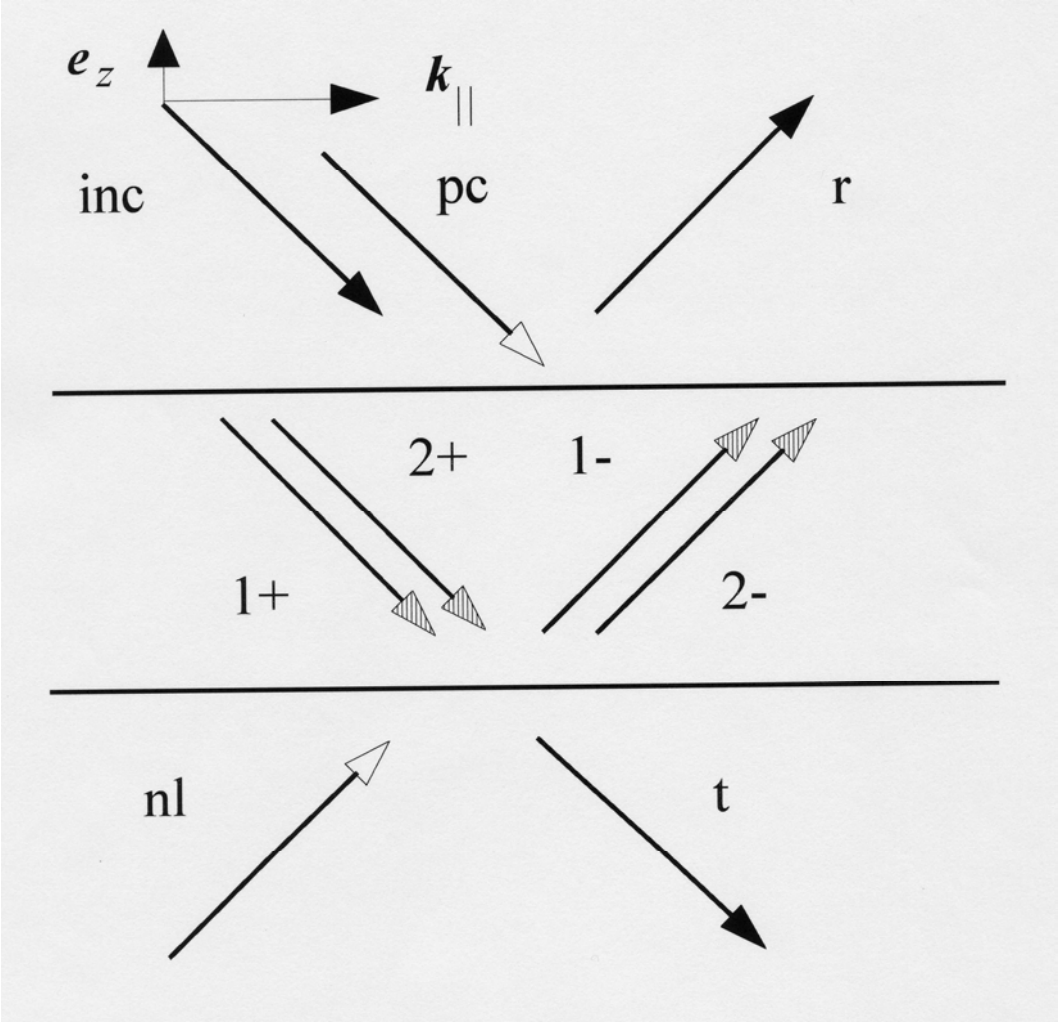

Figure 6: This diagram shows the plane of incidence, determined by k and e_z, and the wave vectors for the case of traveling waves of all fields that are present. All wave vectors have the same $k_{||}$, but they differ in their z-component. Arrows with a solid arrowhead are pure ω_a-waves, and they travel in the direction of the arrow. Arrows with a transparent arrowhead are pure ω_b-waves, which travel in the direction opposite the arrow. Inside the medium the arrowheads are shaded, and each of them represents a set of two counterpropagating waves, with frequencies ω_a and ω_b. In total, thirteen different waves are present simultaneously (plus the two pump beams which are not shown).

in terms of the dimensionless wave numbers

$$\kappa_{\alpha\sigma} = \begin{cases} -\sqrt{(\kappa_\sigma^{(1)})^2 - \kappa_{||}^2} \\ -i\sqrt{\kappa_{||}^2 - (\kappa_\sigma^{(1)})^2} \end{cases}, \tag{18.22}$$

$$\kappa_{\beta\sigma} = \begin{cases} -\sqrt{(\kappa_\sigma^{(2)})^2 - \kappa_{||}^2} \\ i\sqrt{\kappa_{||}^2 - (\kappa_\sigma^{(2)})^2} \end{cases} . \tag{18.23}$$

The four wave vectors are shown in Fig. 6 for traveling waves and Fig. 7 shows the direction of decay of the waves in case they are evanescent. When recalling that a single wave vector corresponds to a set of two counterpropagating waves, we see that the total number of waves inside the medium is eight, which brings the total number of waves that couple together to thirteen.

We see from Fig. 6 that in the limit $\gamma \to 0$, $\varepsilon \to 1$ (completely transparent medium) only the *inc*-, 1+- and *t*-waves will be present. For $\varepsilon \neq 1$ there are multiple reflections at the boundaries, so that the 1− -wave inside and the *r*-wave outside appear. When the nonlinear interaction is included, the $2\pm$ -waves come up, and the *pc*- and *nl*- waves leave the crystal. In addition, each 1 (2)-wave couples to an ω_b (ω_a)-wave, forming a counterpropagating pair. The sign convention for the wave vectors of the waves in the medium is chosen in such a way that for $\gamma \to 0$, $\varepsilon \to 1$, but ρ arbitrary, the wave vectors reduce to

$$\boldsymbol{k}_{1\sigma}^{+} \to \boldsymbol{k} = \boldsymbol{k}_t , \tag{18.24}$$

$$\boldsymbol{k}_{1\sigma}^{-} \to \boldsymbol{k}_r , \tag{18.25}$$

$$\boldsymbol{k}_{2\sigma}^{+} \to \boldsymbol{k}_{pc} , \tag{18.26}$$

$$\boldsymbol{k}_{2\sigma}^{-} \to \boldsymbol{k}_{nl} , \tag{18.27}$$

both for traveling and evanescent waves.

19. FIELDS

The incident field (18.1) gives rise to the excitation of plane-wave modes, which all have a spatial dependence of the form $\exp(i\boldsymbol{k}_i \cdot \boldsymbol{r})$ and with the wave vectors $\boldsymbol{k}_i$ given in the previous section. Next we have to specify the polarization vectors. For *s*-polarized waves in vacuum we take

$$\boldsymbol{e}_{s,i} = \frac{1}{\kappa_{||}} (\boldsymbol{\kappa}_{||} \times \boldsymbol{e}_z) , \tag{19.1}$$

as in Eq. (16.1), and this is the same for every wave. For *p*-polarized waves we choose

$$\boldsymbol{e}_{p,i} = \frac{1}{k_i} (\boldsymbol{k}_i \times \boldsymbol{e}_s) , \tag{19.2}$$

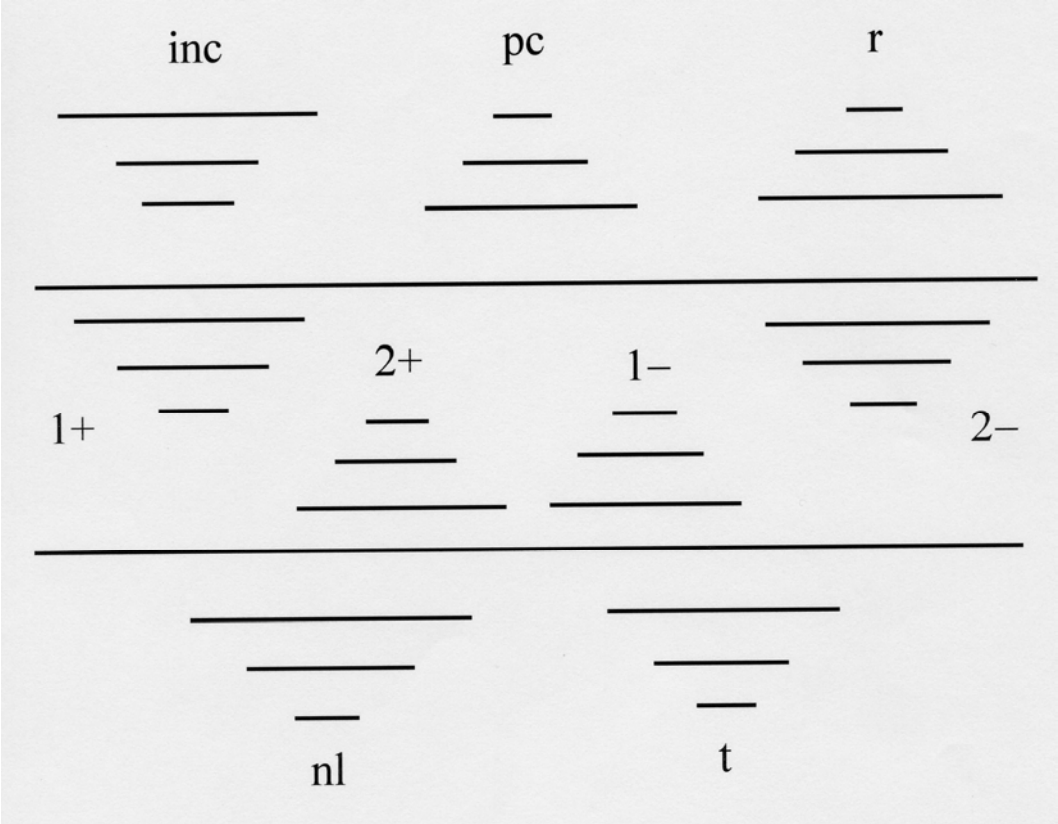

Figure 7: Illustration of the directions in which the various evanescent waves decay.

and we notice that this vector is complex for evanescent waves. These polarization vectors have the properties

$$\boldsymbol{e}_{\sigma,i}\cdot\boldsymbol{k}_i = 0 \ , \ \boldsymbol{e}_{\sigma,i}\cdot\boldsymbol{e}_{\sigma,i} = 0 \ , \tag{19.3}$$

e.g., the waves are transverse and the polarization vectors are unit vectors. Figure 23 in section 30 illustrates the directions of these vectors for the case of traveling waves.

The incident field has a (complex) amplitude factor E, and because the boundary conditions are linear in the field amplitudes, every wave will have this proportionality factor E. For the field in $z > 0$ we can then write

$$\hat{\boldsymbol{E}}(\boldsymbol{r},\omega_a) = E\left\{\boldsymbol{e}_\sigma\, e^{i\boldsymbol{k}\cdot\boldsymbol{r}} + R_\sigma\,\boldsymbol{e}_{\sigma,r}\, e^{i\boldsymbol{k}_r\cdot\boldsymbol{r}}\right\} , \tag{19.4}$$

$$\hat{\boldsymbol{E}}(\boldsymbol{r},\omega_b) = E\,P_\sigma\,\boldsymbol{e}_{\sigma,pc}\, e^{i\boldsymbol{k}_{pc}\cdot\boldsymbol{r}} \ , \tag{19.5}$$

which has only the two complex-valued dimensionless quantities R_σ and P_σ as unknowns. These are the Fresnel reflection coefficients for the *r*-wave and *pc*-wave, respectively, and

they have the significance of the relative amplitude (including the phase) of the two waves with respect to the incident wave. Notice that the phases of R_σ and P_σ depend on the phase convention for the polarization vectors $\boldsymbol{e}_{\sigma,i}$. Equations (19.4) and (19.5) cannot be added in order to give the total electric field in $z > 0$. The fields $\hat{\boldsymbol{E}}(\boldsymbol{r},\omega_a)$ and $\hat{\boldsymbol{E}}(\boldsymbol{r},\omega_b)$ are two frequency components of a, in general, continuous spectral distribution $\hat{\boldsymbol{E}}(\boldsymbol{r},\omega)$.

In the vacuum half-space $z < -\Delta$ there are only two plane waves, and the electric field at $\omega = \omega_a$ and $\omega = \omega_b$ can be written as

$$\hat{\boldsymbol{E}}(\boldsymbol{r},\omega_a) = E\,T_\sigma\,\boldsymbol{e}_{\sigma,t}\,e^{i\boldsymbol{k}_t\cdot\boldsymbol{r}} \quad , \tag{19.6}$$

$$\hat{\boldsymbol{E}}(\boldsymbol{r},\omega_b) = E\,N_\sigma\,\boldsymbol{e}_{\sigma,nl}\,e^{i\boldsymbol{k}_{nl}\cdot\boldsymbol{r}} \quad , \tag{19.7}$$

with T_σ and N_σ to be determined. These are the Fresnel transmission coefficient and the Fresnel coefficient for the emission of the *nl*-wave.

Inside the medium we have four sets of coupled waves, and each set has an ω_a-wave and an ω_b-wave. For the polarization vectors we have to take $\boldsymbol{a}_{1\sigma}$, $\boldsymbol{b}_{1\sigma}$, $\boldsymbol{a}_{2\sigma}$ and $\boldsymbol{b}_{2\sigma}$. The vectors $\boldsymbol{a}_{1\sigma}$ and $\boldsymbol{b}_{2\sigma}$ are unit vectors, but the other two contain an amplitude factor (the resonance parameters, like η_1 and η_2). The coupled wave equations are linear and so we can multiply each solution by an arbitrary complex number, keeping in mind that both the ω_a-wave and the ω_b-wave in a single set must be multiplied by the same factor, as in Eq. (12.1). With this notion, the field inside the medium attains the form

$$\begin{aligned}\hat{\boldsymbol{E}}(\boldsymbol{r},\omega_a) = E\Big\{ & Z^+_{1\sigma}\,\boldsymbol{a}^+_{1\sigma}\,e^{i\boldsymbol{k}^+_{1\sigma}\cdot\boldsymbol{r}} + Z^-_{1\sigma}\,\boldsymbol{a}^-_{1\sigma}\,e^{i\boldsymbol{k}^-_{1\sigma}\cdot\boldsymbol{r}} \\ & + Z^+_{2\sigma}\,\boldsymbol{a}^+_{2\sigma}\,e^{i\boldsymbol{k}^+_{2\sigma}\cdot\boldsymbol{r}} + Z^-_{2\sigma}\,\boldsymbol{a}^-_{2\sigma}\,e^{i\boldsymbol{k}^-_{2\sigma}\cdot\boldsymbol{r}}\Big\} \quad ,\end{aligned} \tag{19.8}$$

$$\begin{aligned}\hat{\boldsymbol{E}}(\boldsymbol{r},\omega_b) = E\Big\{ & Z^+_{1\sigma}\,\boldsymbol{b}^+_{1\sigma}\,e^{i\boldsymbol{k}^+_{1\sigma}\cdot\boldsymbol{r}} + Z^-_{1\sigma}\,\boldsymbol{b}^-_{1\sigma}\,e^{i\boldsymbol{k}^-_{1\sigma}\cdot\boldsymbol{r}} \\ & + Z^+_{2\sigma}\,\boldsymbol{b}^+_{2\sigma}\,e^{i\boldsymbol{k}^+_{2\sigma}\cdot\boldsymbol{r}} + Z^-_{2\sigma}\,\boldsymbol{b}^-_{2\sigma}\,e^{i\boldsymbol{k}^-_{2\sigma}\cdot\boldsymbol{r}}\Big\} \quad ,\end{aligned} \tag{19.9}$$

which has the Fresnel coefficients $Z^\pm_{1\sigma}$, $Z^\pm_{2\sigma}$ as unknowns. Each Fresnel coefficient describes the amount of excitation of a coupled set of waves, compared to the incident wave, but the relative strength of the two waves in a single set is fixed.

We have added a superscript + or − on the polarization vectors. These superscripts have the same significance as the $\pm$ in the notation for the wave vectors. As can be seen from Eqs.

(17.14), (17.15), (17.21) and (17.22), this sign comes into the definition of the parallel components of the polarization vectors for *p*-waves. Explicitly,

$$\kappa_{p,\perp}^{(1\pm)} = \pm \kappa_{\alpha p} \ , \tag{19.10}$$

$$\kappa_{p,\perp}^{(2\pm)} = \pm \kappa_{\beta p} \ . \tag{19.11}$$

For *s*-waves there is no dependence on this sign.

20. FRESNEL COEFFICIENTS

Maxwell's equations require that at the boundaries $z = 0$ and $z = -\Delta$ the fields $\hat{\boldsymbol{E}}_{||}$, $\hat{\boldsymbol{B}}$ and $(\varepsilon \hat{\boldsymbol{E}} + \hat{\boldsymbol{P}} / \varepsilon_o)_{\perp}$ are continuous, both for ω_a and for ω_b, and for $\sigma = s$ and $\sigma = p$. This yields two sets (one for each value of σ) of 12 linear equations for the 2×8 Fresnel coefficients, which shows that the sets are overdetermined. In this section we only look at the continuity of $\hat{\boldsymbol{E}}_{||}$ and $\hat{\boldsymbol{B}}$, which gives 8 equations with 8 unknowns, for each σ, and in the next section we shall discuss the third boundary condition.

At the boundary $z = -\Delta$, an exponential of the form $\exp(i\boldsymbol{k}_i \cdot \boldsymbol{r})$ gives effectively a phase factor $\exp(-ik_{i,z}\Delta)$, because $\exp(i\boldsymbol{k}_{||} \cdot \boldsymbol{r})$ factors out. We like to express this phase in dimensionless quantities. First we introduce the dimensionless layer thickness

$$l = k\Delta \ , \tag{20.1}$$

which equals the layer thickness in units of a wavelength of the incident field, apart from a factor of 2π. Then the phases can be written as

$$\phi_i = \kappa_i l \ , \tag{20.2}$$

in terms of the dimensionless *z*-components of the various wave vectors that were introduced in Sec. 18. The values of *i* can be $i = a$, b, $\alpha\sigma$ or $\beta\sigma$, with $\sigma = s$ or p. For a traveling wave this phase is real, but for an evanescent wave it is imaginary.

From the results for the electric field in the previous section we can obtain the corresponding expressions for the magnetic field with the help of Eq. (3.10). If we then write down the continuity equations for $\hat{\boldsymbol{E}}_{||}$ and $\hat{\boldsymbol{B}}$, both for ω_a and ω_b, and for $z = 0$ and $z = -\Delta$, work out the cross products of the form $\boldsymbol{k}_i \times \boldsymbol{e}_{\sigma,i}$, which appear in the equations for $\hat{\boldsymbol{B}}$, and rearrange the terms, then it follows that the equations divide into two sets of four equations, for a given σ. The Fresnel coefficients for the waves inside the medium are found to be a solution of the linear set

$$F_\sigma \begin{pmatrix} Z_{1\sigma}^{+} \\ Z_{1\sigma}^{-} \\ Z_{2\sigma}^{+} \\ Z_{2\sigma}^{-} \end{pmatrix} = \begin{pmatrix} 2\kappa_a \\ 0 \\ 0 \\ 0 \end{pmatrix}, \tag{20.3}$$

with the matrices F_s and F_p given below. After solving Eq. (20.3), the Fresnel coefficients for the waves in vacuum are found to be

$$\begin{pmatrix} R_\sigma \\ P_\sigma \\ T_\sigma\, e^{-i\phi_a} \\ N_\sigma\, e^{i\phi_b} \end{pmatrix} = \begin{pmatrix} -1 \\ 0 \\ 0 \\ 0 \end{pmatrix} + G_\sigma \begin{pmatrix} Z_{1\sigma}^{+} \\ Z_{1\sigma}^{-} \\ Z_{2\sigma}^{+} \\ Z_{2\sigma}^{-} \end{pmatrix}, \tag{20.4}$$

with the matrices G_s and G_p given below. Solving Eq. (20.3) numerically is trivial, but an analytical solution requires the inversion of the 4×4 matrices F_s and F_p. This analytical solution is presented partially in Sec. 22. Notice that in Eq. (20.4) we solve for $T_\sigma \exp(-i\phi_a)$ and $N_\sigma \exp(i\phi_b)$, rather than for T_σ and N_σ. The reason is that these quantities represent the values of the amplitudes of the *r*-wave and the *nl*-wave, respectively, at the surface $z = -\Delta$, where these waves leave the medium. On the other hand, T_σ and N_σ would be their amplitudes at $z = 0$ if the waves would be extrapolated into that region, as can be seen by setting $z = 0$ in Eqs. (19.6) and (19.7). Therefore, including the two exponentials gives us the physically meaningful quantities. For traveling waves, these exponentials are only phase factors, but for evanescent waves these are amplitude factors since the phases are imaginary.

The two matrices for *s*-waves are explicitly

$$F_s = \begin{pmatrix} \kappa_a + \kappa_{\alpha s} & \kappa_a - \kappa_{\alpha s} \\ \gamma^* \eta_1 (\kappa_b - \kappa_{\alpha s}) & \gamma^* \eta_1 (\kappa_b + \kappa_{\alpha s}) \\ (\kappa_a - \kappa_{\alpha s}) e^{-i\phi_{\alpha s}} & (\kappa_a + \kappa_{\alpha s}) e^{i\phi_{\alpha s}} \\ \gamma^* \eta_1 (\kappa_b + \kappa_{\alpha s}) e^{-i\phi_{\alpha s}} & \gamma^* \eta_1 (\kappa_b - \kappa_{\alpha s}) e^{i\phi_{\alpha s}} \end{pmatrix}$$

$$\begin{pmatrix} \gamma \eta_2 (\kappa_a + \kappa_{\beta s}) & \gamma \eta_2 (\kappa_a - \kappa_{\beta s}) \\ \kappa_b - \kappa_{\beta s} & \kappa_b + \kappa_{\beta s} \\ \gamma \eta_2 (\kappa_a - \kappa_{\beta s}) e^{-i\phi_{\beta s}} & \gamma \eta_2 (\kappa_a + \kappa_{\beta s}) e^{i\phi_{\beta s}} \\ (\kappa_b + \kappa_{\beta s}) e^{-i\phi_{\beta s}} & (\kappa_b - \kappa_{\beta s}) e^{i\phi_{\beta s}} \end{pmatrix}, \tag{20.5}$$

$$G_s = \begin{pmatrix} 1 & 1 & \gamma\eta_2 & \gamma\eta_2 \\ \gamma^*\eta_1 & \gamma^*\eta_1 & 1 & 1 \\ e^{-i\phi_{\alpha s}} & e^{i\phi_{\alpha s}} & \gamma\eta_2 e^{-i\phi_{\beta s}} & \gamma\eta_2 e^{i\phi_{\beta s}} \\ \gamma^*\eta_1 e^{-i\phi_{\alpha s}} & \gamma^*\eta_1 e^{i\phi_{\alpha s}} & e^{-i\phi_{\beta s}} & e^{i\phi_{\beta s}} \end{pmatrix} , \tag{20.6}$$

which contain only the dimensionless wave numbers, the various phases and the resonance parameters η_1 and η_2. For *p*-waves the situation is more involved, due to the complicated expressions for the polarization vectors. With the abbreviations

$$q_1 = -\frac{\alpha_\perp^{(1)}}{\kappa_\parallel}\{\varepsilon + 6\gamma_o + 3\gamma_0^2\,\zeta_1\} , \tag{20.7}$$

$$q_2 = -\rho\frac{\alpha_\perp^{(1)}}{\kappa_\parallel}\{\zeta_1(\varepsilon + 6\gamma_o) + 3\} , \tag{20.8}$$

$$q_3 = -\frac{\beta_\perp^{(2)}}{\kappa_\parallel}\{\zeta_2(\varepsilon + 6\gamma_o) + 3\} , \tag{20.9}$$

$$q_4 = -\rho\frac{\beta_\perp^{(2)}}{\kappa_\parallel}\{\varepsilon + 6\gamma_o + 3\gamma_0^2\,\zeta_2\} , \tag{20.10}$$

$$\overline{q}_1 = \frac{\alpha_\perp^{(1)}}{\kappa_\parallel\,\kappa_{\alpha p}^2}\{\kappa_\parallel^2 - (\varepsilon + 6\gamma_o) - 3\gamma_0^2\,\zeta_1\} , \tag{20.11}$$

$$\overline{q}_2 = \rho\frac{\alpha_\perp^{(1)}}{\kappa_\parallel\,\kappa_{\alpha p}^2}\{\zeta_1[\kappa_\parallel^2 - \rho^2(\varepsilon + 6\gamma_o)] - 3\rho^2\} , \tag{20.12}$$

$$\overline{q}_3 = \frac{\beta_\perp^{(2)}}{\kappa_\parallel\,\kappa_{\beta p}^2}\{\zeta_2[\kappa_\parallel^2 - (\varepsilon + 6\gamma_o)] - 3\} , \tag{20.13}$$

$$\overline{q}_4 = \rho\frac{\beta_\perp^{(2)}}{\kappa_\parallel\,\kappa_{\beta p}^2}\{\kappa_\parallel^2 - \rho^2(\varepsilon + 6\gamma_o) - 3\gamma_0^2\,\rho^2\zeta_2\} , \tag{20.14}$$

the two matrices attain the form

$$F_p = \begin{pmatrix} q_1\kappa_a + \bar{q}_1\kappa_{\alpha p} & q_1\kappa_a - \bar{q}_1\kappa_{\alpha p} \\ \gamma^*(q_2\kappa_b - \bar{q}_2\kappa_{\alpha p}) & \gamma^*(q_2\kappa_b + \bar{q}_2\kappa_{\alpha p}) \\ (q_1\kappa_a - \bar{q}_1\kappa_{\alpha p})e^{-i\phi_{\alpha p}} & (q_1\kappa_a + \bar{q}_1\kappa_{\alpha p})e^{i\phi_{\alpha p}} \\ \gamma^*(q_2\kappa_b + \bar{q}_2\kappa_{\alpha p})e^{-i\phi_{\alpha p}} & \gamma^*(q_2\kappa_b - \bar{q}_2\kappa_{\alpha p})e^{i\phi_{\alpha p}} \end{pmatrix}$$

$$\begin{pmatrix} \gamma(q_3\kappa_a + \bar{q}_3\kappa_{\beta p}) & \gamma(q_3\kappa_a - \bar{q}_3\kappa_{\beta p}) \\ q_4\kappa_b - \bar{q}_4\kappa_{\beta p} & q_4\kappa_b + \bar{q}_4\kappa_{\beta p} \\ \gamma(q_3\kappa_a - \bar{q}_3\kappa_{\beta p})e^{-i\phi_{\beta p}} & \gamma(q_3\kappa_a + \bar{q}_3\kappa_{\beta p})e^{i\phi_{\beta p}} \\ (q_4\kappa_b + \bar{q}_4\kappa_{\beta p})e^{-i\phi_{\beta p}} & (q_4\kappa_b - \bar{q}_4\kappa_{\beta p})e^{i\phi_{\beta p}} \end{pmatrix}, \tag{20.15}$$

$$G_p = \begin{pmatrix} q_1 & q_1 & \gamma q_3 & \gamma q_3 \\ \gamma^* q_2 & \gamma^* q_2 & q_4 & q_4 \\ q_1 e^{-i\phi_{\alpha p}} & q_1 e^{i\phi_{\alpha p}} & \gamma q_3 e^{-i\phi_{\beta p}} & \gamma q_3 e^{i\phi_{\beta p}} \\ \gamma^* q_2 e^{-i\phi_{\alpha p}} & \gamma^* q_2 e^{i\phi_{\alpha p}} & q_4 e^{-i\phi_{\beta p}} & q_4 e^{i\phi_{\beta p}} \end{pmatrix}. \tag{20.16}$$

21. THIRD BOUNDARY CONDITION

The Fresnel coefficients in the previous section were obtained by matching the fields across the two boundaries of the medium with the requirement that $\hat{\boldsymbol{E}}_{\|}$ and $\hat{\boldsymbol{B}}$, both for ω_a and ω_b and for $z = 0$ and $z = -\Delta$, must be continuous. Maxwell's equations impose a third boundary condition, namely that $(\varepsilon\hat{\boldsymbol{E}} + \hat{\boldsymbol{P}}/\varepsilon_o)_\perp$ must be continuous. In the case of *s*-polarization all fields are parallel to the surface $z = 0$, and therefore this condition holds trivially, but for *p*-waves this gives an additional set of equations for the Fresnel coefficients, and this set has to be satisfied simultaneously with the set of the previous section. From Eqs. (9.10) and (9.11) we derive

$$(\varepsilon\hat{\boldsymbol{E}}(\boldsymbol{r},\omega_a) + \hat{P}(\boldsymbol{r},\omega_a)/\varepsilon_o)_\perp = (\varepsilon + 6\gamma_o)\hat{\boldsymbol{E}}(\boldsymbol{r},\omega_a)_\perp + 3\gamma\,\hat{\boldsymbol{E}}(\boldsymbol{r},\omega_b)_\perp\,, \tag{21.1}$$

$$(\varepsilon\hat{\boldsymbol{E}}(\boldsymbol{r},\omega_b) + \hat{P}(\boldsymbol{r},\omega_b)/\varepsilon_o)_\perp = (\varepsilon + 6\gamma_o)\hat{\boldsymbol{E}}(\boldsymbol{r},\omega_b)_\perp + 3\gamma^*\,\hat{\boldsymbol{E}}(\boldsymbol{r},\omega_a)_\perp\,. \tag{21.2}$$

Therefore, the right-hand side of Eq. (21.1), evaluated for the field inside the medium, must match $\hat{\boldsymbol{E}}(\boldsymbol{r},\omega_a)_\perp$ outside, both at $z = 0$ and $z = -\Delta$. In the same way, the right-hand side of Eq. (21.2) must match $\hat{\boldsymbol{E}}(\boldsymbol{r},\omega_b)$ in vacuum.

This third boundary condition leads to a set of four equations, and when written out we get factors of the type $(\varepsilon + 6\gamma_o)\alpha_\perp + 3\gamma\,\beta_\perp$ in Eq. (21.1), and similar ones in Eq. (21.2). It turns out that the equations do not resemble any of the other equations which we used to solve for the Fresnel coefficients. However, the eight q parameters in the *p*-wave matrices are

complicated functions of ρ, ε, γ and $\kappa_{\|}$, and they can be written in many alternative forms. With the matrix methods of Secs. 15 and 17 we can derive

$$(\varepsilon + 6\gamma_o)\alpha_\perp + 3\gamma\,\beta_\perp = \kappa_{\|}(\kappa_{\|}\alpha_\perp - \kappa_\perp \alpha_{\|}) \ , \tag{21.3}$$

$$(\varepsilon + 6\gamma_o)\beta_\perp + 3\gamma^* \alpha_\perp = \frac{\kappa_{\|}}{\rho^2}(\kappa_{\|}\beta_\perp - \kappa_\perp \beta_{\|}) \ , \tag{21.4}$$

which holds for the polarization vector components of both the 1 and the 2 solutions. The left-hand sides are factors which appear in the four new boundary equations, and the right-hand sides resemble cross products. Indeed, for any wave vector $\boldsymbol{k}_i$, with i = 1+, 1–, 2+ or 2–, we have

$$\boldsymbol{k}_i \times \boldsymbol{a} = k\,\boldsymbol{e}_s\,(\kappa_{\|}\alpha_\perp - \kappa_\perp \alpha_{\|}) \ , \tag{21.5}$$

and a similar relation can be found for $\boldsymbol{k}_i \times \boldsymbol{b}$. On the other hand, the parameters q_i from the previous section came from the continuity conditions for $\hat{\boldsymbol{B}}$, which also involve cross products. For instance, q_1 came from

$$\boldsymbol{k}_{Ip}^{\pm} \times \boldsymbol{a}_{Ip}^{\pm} = -k\,q_1\,\boldsymbol{e}_s \ . \tag{21.6}$$

Combination of Eqs. (21.3) - (21.6) then gives

$$q_1 = -\frac{1}{\kappa_{\|}}\{(\varepsilon + 6\gamma_o)\alpha_\perp^{(1)} + 3\gamma\,\beta_\perp^{(1)}\} \ , \tag{21.7}$$

as an alternative form of q_1. It appears, after deriving similar relations for the other q parameters, that the third boundary condition for p-waves gives a set of four equations which is identical to the four equations that follow from the continuity of the magnetic field.

22. ANALYTICAL SOLUTION

The Fresnel coefficients P_s and P_p determine the amplitude, phase and polarization of the phase-conjugated wave. For most practical applications only these two Fresnel coefficients are of relevance, although sometimes also R_s and R_p are important because they represent radiation which is also scattered into the region $z > 0$, although under a different angle. Eliminating the Fresnel coefficients $Z_{1\sigma}^{\pm}$ and $Z_{2\sigma}^{\pm}$ for the field in the medium from Eqs. (20.3) and (20.4) gives explicitly

$$\begin{pmatrix} R_\sigma \\ P_\sigma \\ T_\sigma\, e^{-i\phi_a} \\ N_\sigma\, e^{i\phi_b} \end{pmatrix} = \begin{pmatrix} -1 \\ 0 \\ 0 \\ 0 \end{pmatrix} + G_\sigma F_\sigma^{-1} \begin{pmatrix} 2\kappa_a \\ 0 \\ 0 \\ 0 \end{pmatrix}, \tag{22.1}$$

for the fields outside. The most cumbersome part in the analytical evaluation of the right-hand side of Eq. (22.1) is the inversion of the two matrices F_s and F_p.

We have computed the 16 Fresnel coefficients analytically. For the purpose of illustration we give the expressions for P_s and R_s here. All Fresnel coefficients are given in the Appendix, although in a slightly different form. First we introduce the abbreviations

$$\Lambda_{\alpha s} = (\kappa_a + \kappa_{\alpha s})^2\, e^{i\phi_{\alpha s}} - (\kappa_a - \kappa_{\alpha s})^2\, e^{-i\phi_{\alpha s}}, \tag{22.2}$$

$$\Lambda_{\beta s} = (\kappa_b - \kappa_{\beta s})^2\, e^{i\phi_{\beta s}} - (\kappa_b + \kappa_{\beta s})^2\, e^{-i\phi_{\beta s}}. \tag{22.3}$$

Then the determinant of F_s is found to be

$$\begin{aligned} \det(F_s) = &-\Lambda_{\alpha s}\Lambda_{\beta s} - \gamma_o^2\,\eta_1\eta_2 \Big[8\kappa_{\alpha s}\kappa_{\beta s}(\kappa_a + \kappa_b)^2 \\ &- 2\{(\kappa_a + \kappa_{\alpha s})(\kappa_b - \kappa_{\alpha s})\, e^{i\phi_{\alpha s}} - (\kappa_a - \kappa_{\alpha s})(\kappa_b + \kappa_{\alpha s})\, e^{-i\phi_{\alpha s}}\} \\ &\times \{(\kappa_a + \kappa_{\beta s})(\kappa_b - \kappa_{\beta s})\, e^{i\phi_{\beta s}} - (\kappa_a - \kappa_{\beta s})(\kappa_b + \kappa_{\beta s})\, e^{-i\phi_{\beta s}}\} \\ &+ \gamma_o^2\,\eta_1\eta_2\, \{(\kappa_b - \kappa_{\alpha s})^2\, e^{i\phi_{\alpha s}} - (\kappa_b + \kappa_{\alpha s})^2\, e^{-i\phi_{\alpha s}}\} \\ &\times \{(\kappa_a + \kappa_{\beta s})^2\, e^{i\phi_{\beta s}} - (\kappa_a - \kappa_{\beta s})^2\, e^{-i\phi_{\beta s}}\} \Big], \end{aligned} \tag{22.4}$$

and the two Fresnel coefficients are

$$\begin{aligned} R_s = \frac{1}{\det(F_s)} \Big\{ &-\Lambda_{\beta s}(\kappa_a^2 - \kappa_{\alpha s}^2)(e^{i\phi_{\alpha s}} - e^{-i\phi_{\alpha s}}) \\ &-\gamma_o^2\,\eta_1\eta_2 \Big[8\kappa_{\alpha s}\kappa_{\beta s}(\kappa_a^2 - \kappa_b^2) - 2\, e^{i(\phi_{\alpha s} + \phi_{\beta s})}(\kappa_a^2 - \kappa_{\alpha s}\kappa_{\beta s})(\kappa_b - \kappa_{\alpha s})(\kappa_b - \kappa_{\beta s}) \\ &+ 2\, e^{i(\phi_{\alpha s} - \phi_{\beta s})}(\kappa_a^2 + \kappa_{\alpha s}\kappa_{\beta s})(\kappa_b - \kappa_{\alpha s})(\kappa_b + \kappa_{\beta s}) \end{aligned}$$

$$+2e^{-i(\phi_{\alpha s}-\phi_{\beta s})}(\kappa_a^2+\kappa_{\alpha s}\kappa_{\beta s})(\kappa_b+\kappa_{\alpha s})(\kappa_b-\kappa_{\beta s})$$

$$-2e^{-i(\phi_{\alpha s}+\phi_{\beta s})}(\kappa_a^2-\kappa_{\alpha s}\kappa_{\beta s})(\kappa_b+\kappa_{\alpha s})(\kappa_b+\kappa_{\beta s})$$

$$+\gamma_o^2\eta_1\eta_2(\kappa_a^2-\kappa_{\beta s}^2)\{(\kappa_b-\kappa_{\alpha s})^2e^{i\phi_{\alpha s}}-(\kappa_b+\kappa_{\alpha s})^2e^{-i\phi_{\alpha s}}\}$$

$$\times(e^{i\phi_{\beta s}}-e^{-i\phi_{\beta s}})\Big]\Big\}\,, \tag{22.5}$$

$$P_s=-\frac{2\gamma^*\eta_1\kappa_a}{\det(F_s)}\Big\{4(1+\gamma_o^2\eta_1\eta_2)\kappa_{\alpha s}\kappa_{\beta s}(\kappa_a+\kappa_b)$$

$$+(\kappa_{\alpha s}-\kappa_{\beta s})e^{i(\phi_{\alpha s}+\phi_{\beta s})}[(\kappa_a+\kappa_{\alpha s})(\kappa_b-\kappa_{\beta s})-\gamma_o^2\eta_1\eta_2(\kappa_a+\kappa_{\beta s})(\kappa_b-\kappa_{\alpha s})]$$

$$-(\kappa_{\alpha s}+\kappa_{\beta s})e^{i(\phi_{\alpha s}-\phi_{\beta s})}[(\kappa_a+\kappa_{\alpha s})(\kappa_b+\kappa_{\beta s})-\gamma_o^2\eta_1\eta_2(\kappa_a-\kappa_{\beta s})(\kappa_b-\kappa_{\alpha s})]$$

$$+(\kappa_{\alpha s}+\kappa_{\beta s})e^{-i(\phi_{\alpha s}-\phi_{\beta s})}[(\kappa_a-\kappa_{\alpha s})(\kappa_b-\kappa_{\beta s})-\gamma_o^2\eta_1\eta_2(\kappa_a+\kappa_{\beta s})(\kappa_b+\kappa_{\alpha s})]$$

$$-(\kappa_{\alpha s}-\kappa_{\beta s})e^{-i(\phi_{\alpha s}+\phi_{\beta s})}[(\kappa_a-\kappa_{\alpha s})(\kappa_b+\kappa_{\beta s})-\gamma_o^2\eta_1\eta_2(\kappa_a-\kappa_{\beta s})(\kappa_b+\kappa_{\alpha s})]\Big\}\,. \tag{22.6}$$

It does not appear to be possible to simplify these expressions in general, but later we shall consider some special limits of practical relevance, and derive simple expressions for all sixteen Fresnel coefficients. These results will exhibit the main features of the Fresnel coefficients, but not all the tiny details which are hidden in the full solution.

23. OFF RESONANCE

In order to shed some light on the structure and parameter dependence of the Fresnel coefficients, we consider some special limits. Inspection of the four matrices which determine the Fresnel coefficients shows that they contain three kinds of parameters. First there are the dimensionless z-components of the wave vectors (κ_a, κ_b, $\kappa_{\alpha\sigma}$ and $\kappa_{\beta\sigma}$), which are mainly determined by the angle of incidence and the dielectric constant. Then we have the phase factors $\exp(\pm i\phi_{\alpha\sigma})$ and $\exp(\pm i\phi_{\beta\sigma})$, which are the only parameters that depend on the dimensionless layer thickness l. Third, there are factors proportional to the nonlinear coupling constant γ, or its complex conjugate. As it turns out, for s-waves these factors only

appear in the combination $\gamma^* \eta_1$ and $\gamma \eta_2$, whereas for *p*-waves we get $\gamma^* q_2$, $\gamma^* \bar{q}_2$, γq_3 and $\gamma \bar{q}_3$. It was shown in Sec. 16 that these factors account for the resonance behavior in the coupling to the second wave in the counterpropagating sets, depending on whether $|\rho - 1|$ is much smaller or larger than $|\gamma|$. This same frequency dependence governs the resonance structure of the matrices F_σ and G_σ, and thereby the Fresnel coefficients.

In this section we consider the situation where the frequency ω_a of the incident field is far off resonance with the pump frequency $\bar{\omega}$, which means $|\rho - 1| >> |\gamma|$, and we use the fact that $|\gamma|$ is very small, say $10^{-5} \sim 10^{-8}$. From Eq. (16.8) we then see that $\gamma^* \eta_1 \to 0$, and similarly every other matrix element which is proportional to γ or γ^* vanishes. In this limit, half the number of matrix elements in F_σ and G_σ are zero, and Eqs. (20.3) and (20.4) are easily solved for the Fresnel coefficients. For *p*-waves we also need

$$q_1, q_4 \to \sqrt{\varepsilon}\,, \qquad \bar{q}_1, \bar{q}_4 \to 1/\sqrt{\varepsilon}\,, \tag{23.1}$$

in this limit. We find

$$P_\sigma = Z_{2\sigma}^{\pm} = N_\sigma e^{i\phi_b} = 0\,, \tag{23.2}$$

which shows that all ω_b-waves disappear. Especially, $P_\sigma = 0$ indicates that we can only generate a phase conjugated wave when ω_a is sufficiently close to the resonance frequency $\bar{\omega}$, as could have been expected. The nonzero Fresnel coefficients for *s*-waves are found to be

$$Z_{1s}^{\pm} = \pm \frac{2\kappa_a(\kappa_a \pm \kappa_{\alpha s})}{\Lambda_{\alpha s}} e^{\pm i\phi_{\alpha s}}\,, \tag{23.3}$$

$$R_s = \frac{\kappa_a^2 - \kappa_{\alpha s}^2}{\Lambda_{\alpha s}} (e^{i\phi_{\alpha s}} - e^{-i\phi_{\alpha s}})\,, \tag{23.4}$$

$$T_s e^{-i\phi_a} = \frac{4\kappa_a \kappa_{\alpha s}}{\Lambda_{\alpha s}}\,, \tag{23.5}$$

and similar expressions can be derived for the *p*-wave coefficients. We recognize this solution as the Fresnel coefficients for an ordinary dielectric layer [101, 102], and consequently the nonlinear interaction has no effect at all in this limit.

Far off resonance, the set (20.3) of four coupled equations splits in two decoupled sets of two equations for $Z_{1\sigma}^{+}$ and $Z_{1\sigma}^{-}$ and a set of two equations for $Z_{2\sigma}^{+}$ and $Z_{2\sigma}^{-}$. The same holds for Eq. (20.4). Since the second set in Eq. (20.3) is homogeneous, it only admits the solution $Z_{2\sigma}^{+} = Z_{2\sigma}^{-} = 0$, and with Eq. (20.4) we then find $P_\sigma = N_\sigma \exp(i\phi_b) = 0$. The other set in Eq. (20.3) is inhomogeneous, and has nonzero $Z_{1\sigma}^{+}$ and $Z_{1\sigma}^{-}$ as solutions, leading to nonzero values for R_σ and $T_\sigma \exp(-i\phi_a)$. When ω_a is closer to resonance, the 4×4 set does not decouple anymore into a set for ω_a-waves and a set for ω_b-waves.

24. TRAVELING WAVES ON RESONANCE

Let us now consider the opposite situation of perfect resonance, $\rho \to 1$, and $|\gamma|$ very small compared to unity. Since the limits $\rho \to 1$ and $\gamma \to 0$ do not commute, this limit is understood as $|\rho - 1| << |\gamma|$, as shown in Sec. 16. The relative width of the resonance is $\Delta\omega_a / \omega_a \approx |\gamma|$, as indicated by Eq. (16.10), so that we could call $|\gamma|$ the relative bandwidth of the phase conjugator. In order to simplify the notation somewhat we shall from now on assume that $\gamma_o > 0$, and with Eq. (9.7) this is equivalent to assuming that χ is positive.

With Eqs. (14.8) and (15.10) we find that the solutions of the dispersion relations in the medium reduce to

$$\kappa_\sigma^{\binom{1}{2}} = \sqrt{\varepsilon} \ . \tag{24.1}$$

From Eqs. (16.7) and (16.9) we find that the resonance parameters for *s*-waves become

$$\eta_1 = -\eta_2 = -\frac{\delta}{\gamma_o} \ , \tag{24.2}$$

in this resonance limit. For *p*-waves we find for the resonance parameters

$$\zeta_1 = -\zeta_2 = -\frac{\delta}{\gamma_o} \ . \tag{24.3}$$

These relations indicate that for a set of coupled waves in the medium, the ω_a-wave and the ω_b-wave have equal amplitude. For the *q*-parameters that have a resonant nature we obtain

$$q_2 = -q_3 = -\frac{\delta\sqrt{\varepsilon}}{\gamma_o}, \qquad \overline{q}_2 = -\overline{q}_3 = -\frac{\delta}{\gamma_o\sqrt{\varepsilon}} \ , \tag{24.4}$$

and the other *q*-parameters become

$$q_1 = q_4 = \sqrt{\varepsilon} \ , \qquad \overline{q}_1 = \overline{q}_4 = \frac{1}{\sqrt{\varepsilon}} \ . \tag{24.5}$$

We shall furthermore assume that the incident wave is traveling, so that $0 \le \kappa_{||} < 1$. Since $\rho = 1$, also the other four waves in vacuum are traveling. With $\kappa_{||} = \sin\theta_i$, the dimensionless wave numbers κ_a, Eq. (18.8), and κ_b, Eq. (18.3), then simplify to

$$\kappa_a = \kappa_b = -\sqrt{1 - \kappa_{||}^2} = -\cos\theta_i \ . \tag{24.6}$$

For the wave numbers inside the medium we find from Eqs. (18.22) and (18.23) the limits

$$\kappa_{\alpha\sigma} = \begin{cases} -\sqrt{\varepsilon - \kappa_{\|}^2} \\ -i\sqrt{\kappa_{\|}^2 - \varepsilon} \end{cases} , \tag{24.7}$$

$$\kappa_{\beta\sigma} = \begin{cases} -\sqrt{\varepsilon - \kappa_{\|}^2} \\ i\sqrt{\kappa_{\|}^2 - \varepsilon} \end{cases} . \tag{24.8}$$

Depending on whether $\kappa_{\|} < \varepsilon$ or $\kappa_{\|} > \varepsilon$, we have traveling or evanescent waves, respectively, inside the medium.

Since for most materials we have $\varepsilon > 1$, the condition $\kappa_{\|} < \varepsilon$ is automatically satisfied, and we shall assume this in the remainder of this section. We then have

$$\kappa_{\alpha\sigma} = \kappa_{\beta\sigma} = -\sqrt{\varepsilon - \sin^2\theta_i} . \tag{24.9}$$

The major simplification comes from the identities $\kappa_a = \kappa_b$ and $\kappa_{\alpha\sigma} = \kappa_{\beta\sigma}$, as can be seen from the analytical solution. All kinds of terms with $\kappa_{\alpha s} - \kappa_{\beta s}$ disappear, and factors of $(\kappa_a + \kappa_{\alpha s})(\kappa_b - \kappa_{\beta s})$ simplify to 1-ε. Also, the appearance of the resonance parameters reduces to $\gamma_o^2 \eta_1 \eta_2 = -1$. In the matrices F_σ and G_σ also the phases $\phi_{\alpha\sigma} = \kappa_{\alpha\sigma} l$ and $\phi_{\beta\sigma} = \kappa_{\beta\sigma} l$, with l the layer thickness parameter, appear. Since l can be a very large number, we cannot say $\phi_{\alpha s} - \phi_{\beta s} = 0$, even though $\kappa_{\alpha s} - \kappa_{\beta s} = 0$. The reason is that the last identity only holds up to order γ_o, and $\gamma_o l$ can easily, and will, remain finite.

Even with the above simplifications, the explicit solution for the Fresnel coefficients is still rather complicated, and we shall only give the results for the waves outside the medium. First we introduce the quantities

$$D_\sigma = \frac{1}{16}\det(F_\sigma) , \quad \sigma = s, p , \tag{24.10}$$

which are explicitly

$$D_s = (\kappa_a^4 + \kappa_{\alpha s}^4)\sin\phi_{\alpha s}\sin\phi_{\beta s} + 2\kappa_a^2\kappa_{\alpha s}^2(1 + \cos\phi_{\alpha s}\cos\phi_{\beta s}) , \tag{24.11}$$

$$D_p = \frac{1}{\varepsilon^2}(\varepsilon^4\kappa_a^4 + \kappa_{\alpha p}^4)\sin\phi_{\alpha p}\sin\phi_{\beta p} + 2\kappa_a^2\kappa_{\alpha p}^2(1 + \cos\phi_{\alpha p}\cos\phi_{\beta p}) . \tag{24.12}$$

Then the Fresnel coefficients become

$$R_s = \frac{1-\varepsilon}{D_s}\{(\kappa_a^2+\kappa_{\alpha s}^2)\sin\phi_{\alpha s}\sin\phi_{\beta s} + i\kappa_a\kappa_{\alpha s}\sin(\phi_{\alpha s}+\phi_{\beta s})\}\,, \tag{24.13}$$

$$R_p = \frac{(\varepsilon-1)\{\varepsilon-\kappa_{||}^2(\varepsilon+1)\}}{\varepsilon^2 D_p}\{(\varepsilon^2\kappa_a^2+\kappa_{\alpha p}^2)\sin\phi_{\alpha p}\sin\phi_{\beta p} + i\varepsilon\kappa_a\kappa_{\alpha p}\sin(\phi_{\alpha p}+\phi_{\beta p})\}\,, \tag{24.14}$$

$$P_s = \frac{-i\delta e^{-i\theta_p}\kappa_a\kappa_{\alpha s}(\kappa_a^2+\kappa_{\alpha s}^2)}{D_s}\sin(\phi_{\alpha s}-\phi_{\beta s})\,, \tag{24.15}$$

$$P_p = \frac{-i\delta e^{-i\theta_p}\kappa_a\kappa_{\alpha p}(\varepsilon^2\kappa_a^2+\kappa_{\alpha p}^2)}{\varepsilon D_p}\sin(\phi_{\alpha p}-\phi_{\beta p})\,, \tag{24.16}$$

$$T_s e^{-i\phi_a} = \frac{\kappa_a\kappa_{\alpha s}}{D_s}\{2\kappa_a\kappa_{\alpha s}(\cos\phi_{\alpha s}+\cos\phi_{\beta s}) - i(\kappa_a^2+\kappa_{\alpha s}^2)(\sin\phi_{\alpha s}+\sin\phi_{\beta s})\}\,, \tag{24.17}$$

$$T_p e^{-i\phi_a} = \frac{\kappa_a\kappa_{\alpha p}}{\varepsilon D_p}\{2\varepsilon\kappa_a\kappa_{\alpha p}(\cos\phi_{\alpha p}+\cos\phi_{\beta p}) - i(\varepsilon^2\kappa_a^2+\kappa_{\alpha p}^2)(\sin\phi_{\alpha p}+\sin\phi_{\beta p})\}\,, \tag{24.18}$$

$$N_s e^{i\phi_b} = (1-\varepsilon)\frac{i\delta e^{-i\theta_p}}{D_s}\kappa_a\kappa_\alpha(\sin\phi_{\alpha s}-\sin\phi_{\beta s})\,, \tag{24.19}$$

$$N_p e^{i\phi_b} = (\varepsilon-1)\{\varepsilon-\kappa_{||}^2(\varepsilon+1)\}\frac{i\delta e^{-i\theta_p}}{\varepsilon D_p}\kappa_a\kappa_{\alpha p}(\sin\phi_{\alpha p}-\sin\phi_{\beta p})\,. \tag{24.20}$$

As a first observation we notice that for a transparent medium ($\varepsilon = 1$) the *r*-wave and the *nl*-wave disappear, both for *s*- and *p*-polarization,

$$R_\sigma = 0\,, \qquad N_\sigma e^{i\phi_b} = 0\,, \tag{24.21}$$

and it can be shown that also $Z_{1\sigma}^- = Z_{2\sigma}^- = 0$. Therefore, all waves with their $\boldsymbol{k}$-vector up in Fig. 6 vanish. Outside the medium we then only have the phase conjugated and transmitted waves, apart from the incident wave. A second feature appears when $\varepsilon - \kappa_{||}^2(\varepsilon+1) = 0$. Then

$$R_p = 0\,, \qquad N_p e^{i\phi_b} = 0\,, \tag{24.22}$$

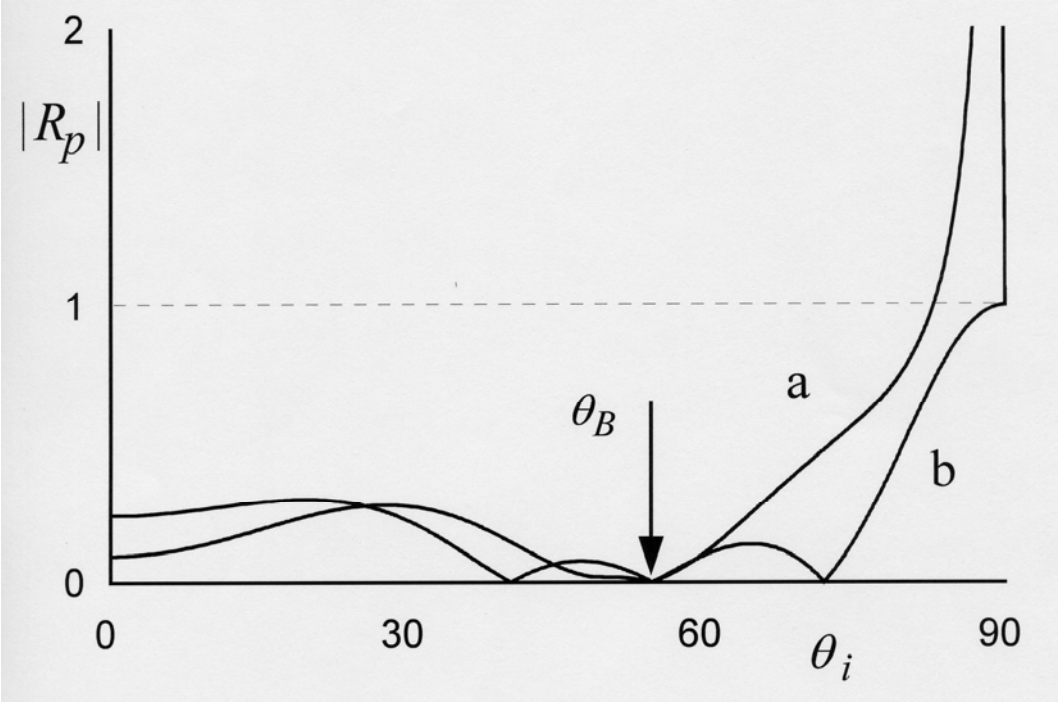

Figure 8: Fresnel reflection coefficient $|R_p|$ as a function of the angle of incidence (in degrees). Curve (a) is for reflection at a phase conjugator ($\nu = 0.99999$, $\gamma = 0.05$, $l = 15$, $\varepsilon = 2$) and curve (b) is for reflection at an ordinary dielectric layer, so effectively for $\gamma = 0$. Both curves have a zero at the Brewster angle, which is here $\theta_B = \arctan\sqrt{\varepsilon} = 54.7^o$. For the linear case this is exact, and for the nonlinear case we found from the data that $|R_p|$ vanishes at 54.4^o. This small difference is due to the fact that for the nonlinear case the formula for the Brewster angle follows from the approximation of perfect resonance. Also interesting to see is that near 90^o the nonlinear reflection coefficient is much larger than unity, which represents amplification with respect to the incident field. For linear media, this can obviously never happen.

and it can be shown that also $Z_{1\sigma}^{-} = Z_{2\sigma}^{-} = 0$. This corresponds to an angle of incidence θ_B equal to

$$\theta_B = \arctan(\sqrt{\varepsilon}) \ , \tag{24.23}$$

which is the Brewster angle from linear optics. At this angle, the *pc*-wave is still present. Figure 8 illustrates the disappearance of the *r*-wave for *p*-polarization at the Brewster angle. Also shown is the reflection coefficient for $\gamma = 0$ (linear case). We mention here that all graphs are made with the exact numerical solution, and not with approximated formulas.

25. RESONANCE IN A TRANSPARENT MEDIUM

The phase-conjugate reflectivity has a tendency to diminish with an increasing dielectric constant ε, as illustrated in Fig. 9. The oscillations are due to the fact that ε appears in the phases $\phi_{\alpha\sigma}$ and $\phi_{\beta\sigma}$. In this section we consider the same case as in the previous section (traveling waves on resonance), and in addition we assume that the medium is transparent, e.g., $\varepsilon = 1$. From Eqs. (24.6) and (24.9) we then see that all wave numbers are equal:

$$\kappa_a = \kappa_b = \kappa_{\alpha\sigma} = \kappa_{\beta\sigma} = -\cos\theta_i \ . \tag{25.1}$$

We already found in the previous section that for $\varepsilon = 1$ we have

$$Z_{1\sigma}^{-} = 0\,, \qquad Z_{2\sigma}^{-} = 0\,, \qquad R_\sigma = 0\,, \qquad N_\sigma\, e^{i\phi_b} = 0 \ . \tag{25.2}$$

The remaining Fresnel coefficients can be simplified to

$$Z_{1\sigma}^{+} = \frac{1}{2}\frac{1 + e^{i(\phi_{\alpha\sigma} - \phi_{\beta\sigma})}}{1 + \cos(\phi_{\alpha\sigma} - \phi_{\beta\sigma})} \ , \tag{25.3}$$

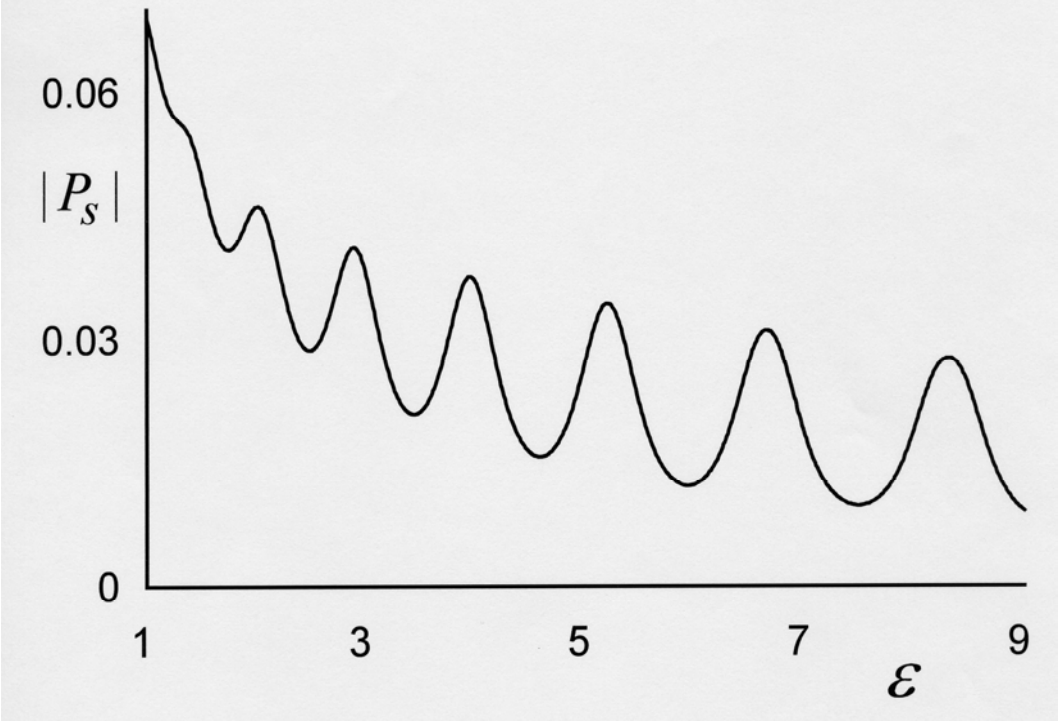

Figure 9: Absolute value of the Fresnel reflection coefficient for an *s*-polarized phase-conjugated wave, as a function of the dielectric constant ε. The parameters are $\nu = 0.99$, $\gamma = 0.01$, $\theta_i = 45^o$ and $l = 10$.

$$Z_{2\sigma}^{+} = \delta e^{-i\theta_p} (Z_{1\sigma}^{+})^{*} \ , \tag{25.4}$$

$$P_{\sigma} = -i\delta e^{-i\theta_p} \tan\{\tfrac{1}{2}(\phi_{\alpha\sigma} - \phi_{\beta\sigma})\} \ , \tag{25.5}$$

$$T_{\sigma} e^{-i\phi_a} = \frac{e^{-i\phi_{\alpha\sigma}} + e^{-i\phi_{\beta\sigma}}}{1 + \cos(\phi_{\alpha\sigma} - \phi_{\beta\sigma})} \ , \tag{25.6}$$

and it is interesting to note that the coefficients for *s*-waves and *p*-waves have the same appearance.

We already found that on resonance the two waves in each counterpropagating pair have the same intensity. We now see from Eq. (25.4) that $|Z_{1\sigma}^{+}| = |Z_{2\sigma}^{+}|$, which implies that all four waves that are excited in the medium in this limit have the same intensity. The intensities of each wave, with respect to the incident wave, can be simplified to

$$|Z_{1\sigma}^{+}|^2 = |Z_{2\sigma}^{+}|^2 = \frac{1}{2}\frac{1}{1+\cos\phi_{\sigma}} \ , \tag{25.7}$$

$$|P_{\sigma}|^2 = \frac{1-\cos\phi_{\sigma}}{1+\cos\phi_{\sigma}} \ , \tag{25.8}$$

$$|T_{\sigma} e^{-i\phi_a}|^2 = \frac{2}{1+\cos\phi_{\sigma}} \ , \tag{25.9}$$

where we introduced the abbreviation

$$\phi_{\sigma} = \phi_{\alpha\sigma} - \phi_{\beta\sigma} \ . \tag{25.10}$$

As mentioned before, the dependence on the layer thickness *l* comes in through these phases, and therefore $\kappa_{\alpha\sigma} = \kappa_{\beta\sigma}$ does not imply $\phi_{\sigma} = 0$. We should expand $\kappa_{\alpha\sigma}$ and $\kappa_{\beta\sigma}$ up to leading order in γ_o, and then consider $\gamma_o l$ finite. We then find explicitly

$$\phi_s = \frac{\delta}{\cos\theta_i}\gamma_o l \ , \tag{25.11}$$

$$\phi_p = \frac{\delta}{\cos\theta_i}(1 + 2\sin^2\theta_i)\gamma_o l \ . \tag{25.12}$$

The intensities depend only on ϕ_σ through $\cos\phi_\sigma$, and therefore the factors δ in Eqs. (25.11) and (25.12) are irrelevant. It is interesting to notice that the relative intensities obey the inequalities

$$|Z^+_{1,2\sigma}|^2 \geq \frac{1}{4} \ , \tag{25.13}$$

$$|T_\sigma e^{-i\phi_a}|^2 \geq 1 \ , \tag{25.14}$$

$$0 \leq |P_\sigma|^2 < \infty \ , \tag{25.15}$$

which shows in particular that the transmitted wave is always amplified, as compared to the incident field. Therefore, the process of reflection and transmission of the incident light is not energy conserving, and always more energy is produced than is provided by the incident wave. Of course, the difference is supplied by the pumps, which leads to depletion. Also interesting to notice is that

$$|T_\sigma e^{-i\phi_a}|^2 = 4|Z^+_{1\sigma}|^2 \ . \tag{25.16}$$

The phase-conjugate reflectivity $|P_\sigma|^2$ can be anything in between zero and infinity. Of course, $|P_\sigma|^2 \to \infty$ is a consequence of taking the limit $\gamma \to 0$, whereas a more detailed analysis would show $|P_\sigma|^2 \sim 1/\gamma_o^2$. Occurrence of a reflectivity larger than unity indicates amplification of the phase-conjugated signal with respect to the input, and an appearance of a value of $|P_\sigma|^2$ far in excess of unity is sometimes termed self oscillation. Both phenomena have been observed experimentally by Pepper, Fekete and Yariv [103] in liquid CS_2. We can write the reflection and transmission intensities in the alternative forms

$$|P_\sigma|^2 = \tan^2(\tfrac{1}{2}\phi_\sigma) \ , \tag{25.17}$$

$$|T_\sigma|^2 = \sec^2(\tfrac{1}{2}\phi_\sigma) \ , \tag{25.18}$$

which are the usual expressions, derived in a very simplified way from the beginning. The behavior of $|P_\sigma|^2$, as predicted by Eq. (25.17) has been qualitatively verified by experiment [103].

Only a phase-conjugated and a transmitted signal are emitted by the medium. Their total relative intensity is $|P_\sigma|^2 + |T_\sigma|^2$, and for an energy-conserving process, like for linear non-absorbing media, this sum would equal unity. However, it follows from Eqs. (25.8) and (25.9) that the two emission intensities are related as

$$|T_\sigma|^2 - |P_\sigma|^2 = 1 \ , \tag{25.19}$$

for any angle of incidence and polarization, and any l and γ_o .

Combination of the results from above gives the expressions for the Fresnel reflection coefficients

$$P_s = -i\,e^{-i\theta_p}\tan\left\{\frac{\gamma_o\, l}{2\cos\theta_i}\right\}\,, \tag{25.20}$$

$$P_p = -i\,e^{-i\theta_p}\tan\left\{\frac{\gamma_o\, l}{2\cos\theta_i}(1+2\sin^2\theta_i)\right\}\,, \tag{25.21}$$

which shows explicitly the dependence on l, γ_o and the angle of incidence. We see from Eq. (25.8) that self oscillation ($P_\sigma \to \infty$) occurs if $\phi_\sigma = (2n+1)\pi$ with n integer. For a given angle of incidence, the layer thickness must be

$$l = \frac{\pi}{\gamma_o}(2n+1)\cos\theta_i\,, \quad s\text{-waves}, \tag{25.22}$$

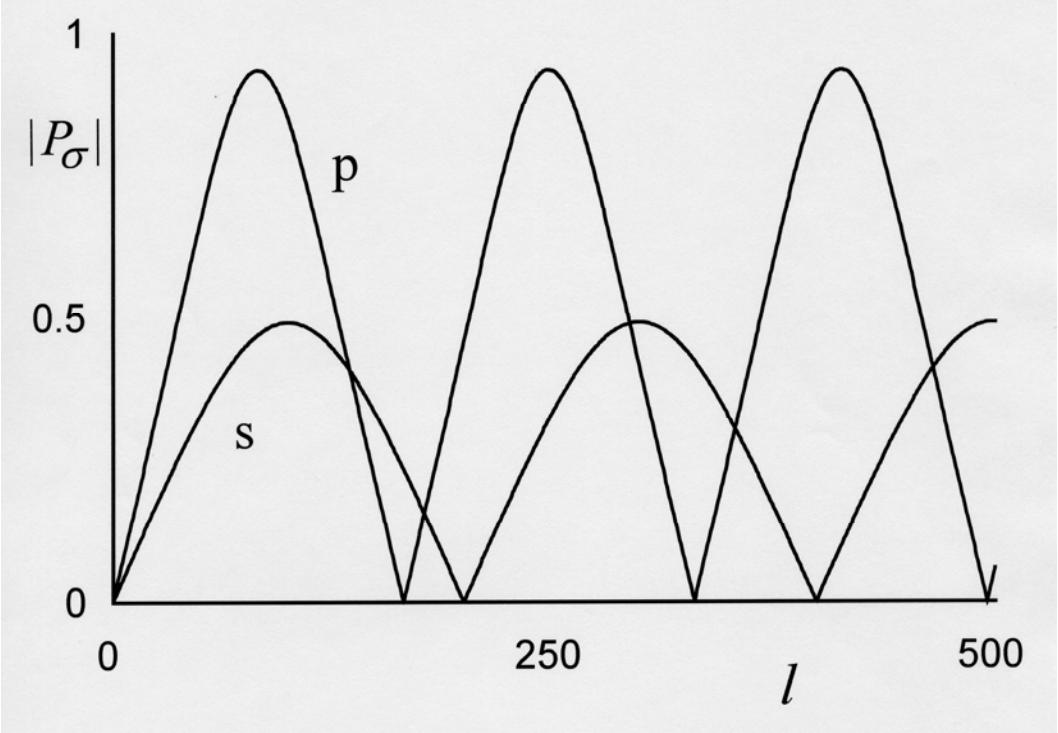

Figure 10: Absolute value of the Fresnel reflection coefficients for the *pc*-wave, both for *s*- and *p*-polarization, as a function of the layer thickness *l*. The parameters are ν = 1.01, γ = 0.01, θ_i = 45° and ε = 1.

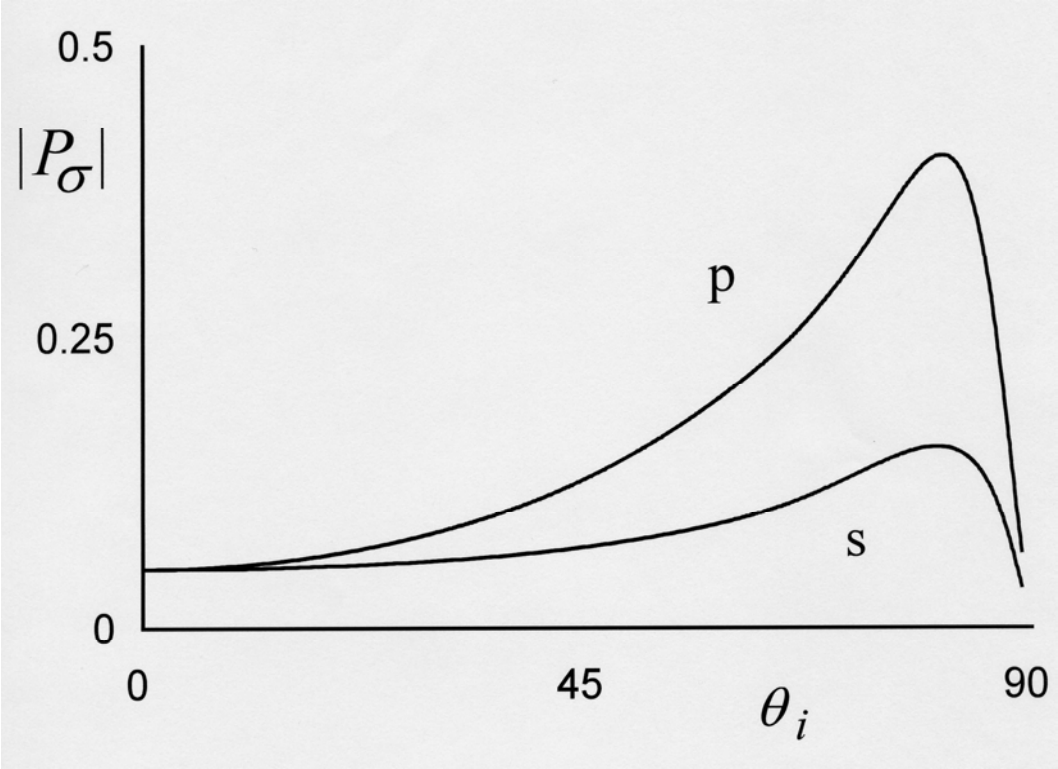

Figure 11: Absolute value of the Fresnel reflection coefficients for the *pc*-wave, both for *s*- and *p*-polarization, as a function of the angle of incidence θ_i . The parameters are $\nu = 0.99$, $\gamma = 0.01$, $\varepsilon = 1$ and $l = 10$.

$$l = \frac{\pi}{\gamma_o}(2n+1)\frac{\cos\theta_i}{1+2\sin^2\theta_i} \quad , \quad p\text{-waves,} \tag{25.23}$$

with $n = 0, 1, 2, \ldots$. The successive values of l are equidistant, and these l-values are different for *s*-waves and *p*-waves. The minimum value of l for *s*-waves is $l = (\pi/\gamma_o)\cos\theta_i$, which is $l \sim 1/\gamma_o$. Since realistic values of γ_o are $10^{-5} \sim 10^{-8}$, this requires a medium with a thickness of at least a few centimeters. Figure 10 shows the dependence of the reflection coefficients on the layer thickness for a given angle of incidence.

In practice, the layer thickness is fixed and the maxima are displayed in the angle-of-incidence dependence of the Fresnel coefficients. From Eqs. (25.22) and (25.23) we find for the locations of the maxima

$$\cos\theta_i = \frac{l\gamma_o}{\pi}\frac{1}{2n+1} \quad , \quad s\text{-waves} \, , \tag{25.24}$$

$$\cos\theta_i = \frac{l\gamma_o}{\pi}\frac{6}{2n+1+\sqrt{(2n+1)^2+24(l\gamma_o/\pi)^2}} \quad , \quad p\text{-waves} \, , \tag{25.25}$$

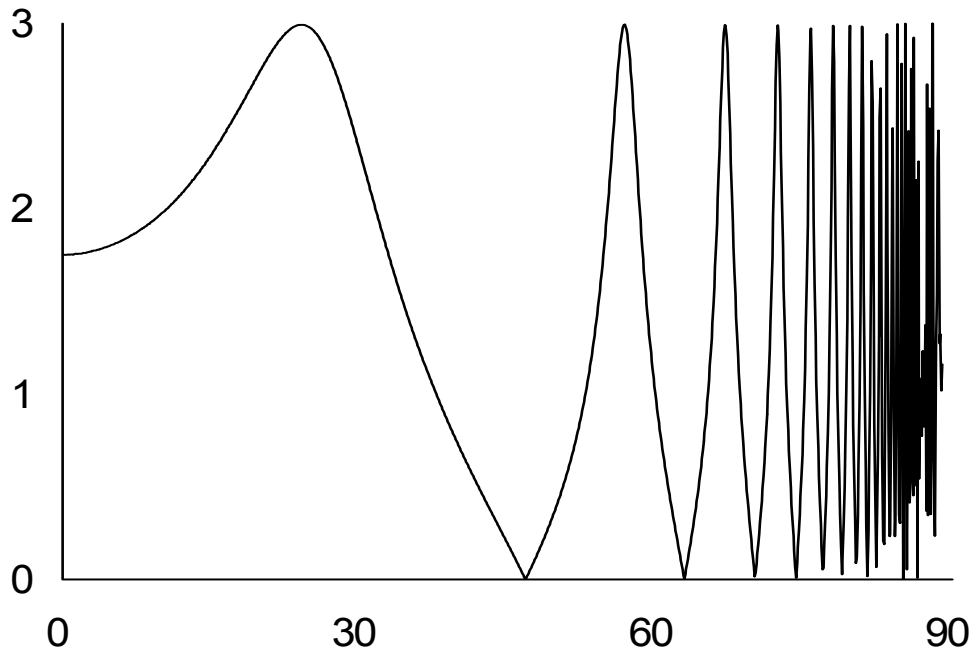

Figure 12: Absolute value of the Fresnel reflection coefficient $|P_S|$ for an *s*-polarized *pc*-wave as a function of the angle of incidence θ_i. The parameters are $\nu - 1 = 10^{-4}$, $\gamma = 6 \times 10^{-4}$, $\varepsilon = 1$ and $l = 13{,}603$. For these values, the resonances are predicted by Eq. (25.24) to appear for $n = 1, 2, \ldots$ at $\theta_i = 30.0^o, 58.7^o, 68.2^o, 73.2^o, 76.3^o, 78.5^o, 80.1^o, \ldots$. It is seen that there is some discrepancy, for instance at 30^o. Near 90^o, there are an infinite number of oscillations, which cannot be resolved adequately in a graph.

with $n = 0, 1, 2, \ldots$. However, if $l\gamma_o/\pi$ is larger than unity, for instance, then there is no solution θ_i for *s*-waves with $n = 0$. In general, there is a minimum $n = n_o$ (can be different for *s*- and *p*-waves) which gives the smallest angle θ_i for which a maximum occurs. Every $n > n_o$ then also gives a solution, so there are an infinite number of solutions which cluster at $\theta_i = 90^o$ (because the right-hand sides go to zero for $n \to \infty$). Figure 11 shows $|P_S|$ and $|P_p|$ as a function of θ_i, and for parameters $\gamma = 0.01$, $\nu = 0.99$, $\varepsilon = 1$ and $l = 10$. Here we have $\gamma \sim \nu$, and therefore this does not correspond to the resonance limit $|\nu - 1| << |\gamma|$ considered in this section. For these parameters, the maxima predicted by Eqs. (25.24) and (25.25) are 88^o and 84^o for *s*-waves and *p*-waves, respectively. Figure 12 is drawn with parameters closer to resonance, and the fast oscillations near 90^o clearly appear, but the peaks are not exactly at the locations predicted by Eqs. (25.24). Then in Fig. 13, we truly have

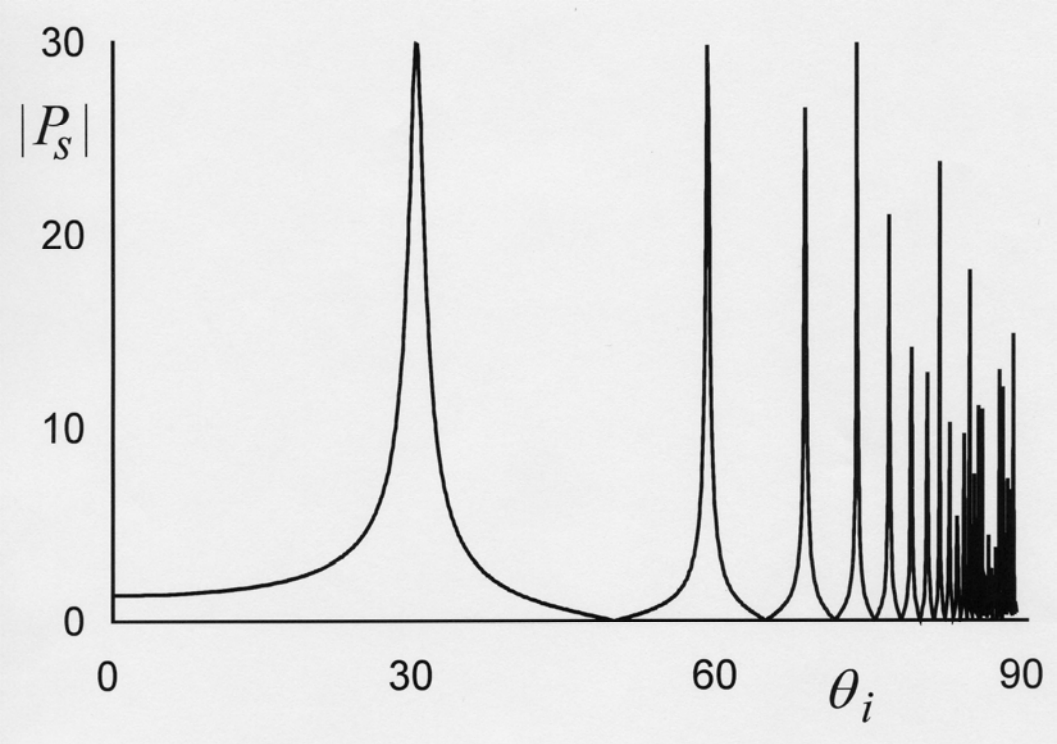

Figure 13: Same as Fig. 12, but now with ν - 1 = 10^{-5}. The value of this ν - 1 is a factor of 10 closer to resonance, and we see that the peaks appear exactly where predicted. The resonances are also much sharper, and their peak values are about a factor of 10 higher.

$|\nu-1|<<|\gamma|$, and the maxima are in the correct positions. Also, the values of the maxima increases with decreasing $|\nu-1|$, and the lines become narrower. The values of the maxima will be calculated in the next section.

26. FREQUENCY DEPENDENCE IN A TRANSPARENT MEDIUM

In the previous section we studied the case of perfect resonance in a transparent medium, for which the Fresnel coefficients reduced to very simple forms. In this section we retain the possibility that ω_a is not necessarily close to resonance, and in this way the results will be a generalization of the results from the previous section. We shall assume again that the medium is transparent, γ is small and all waves are traveling. Far off resonance the medium is effectively vacuum, which implies $Z_{1\sigma}^{+}=T_\sigma=1$ and that all other Fresnel coefficients vanish.

The resonant behavior is governed by the parameters η_1 and η_2 for *s*-waves and by ζ_1 and ζ_2 for *p*-waves, whereas the wave numbers κ_a, κ_b, $\kappa_{\alpha\sigma}$ and $\kappa_{\beta\sigma}$ in the matrices F_s and F_p are more or less geometrical factors. Care should be exercised in approximating the phase factors $\exp(\pm i\phi_{\alpha\sigma})$ and $\exp(\pm i\phi_{\alpha\sigma})$, so for the time being we leave them as they

stand. Let us first consider η_1 and η_2, which are related according to $\eta_1 = -\rho^2\eta_2$. Far off resonance the values of η_1 and η_2 are finite, but on resonance they are proportional to $1/\gamma_o$. Then we recall that η_1 and η_2 are always multiplied by γ^* and γ, respectively, which means that far off resonance their contribution is negligible. Therefore, for $|\rho - 1| >> \gamma_o$ we can approximate η_1 and η_2 by any finite value, and for $|\rho - 1| << \gamma_o$ we can replace the relation $\eta_1 = -\rho^2\eta_2$ by

$$\eta_1 = -\eta_2 \ . \tag{26.1}$$

Since off resonance the values of η_1 and η_2 are irrelevant, we can use approximation (26.1) for the entire frequency range. In Eq. (16.6) we can set $\varepsilon + 2\gamma_o = 1$. Then we notice that the factor $(2\rho\gamma_o)^2$ under the square root sign only contributes for $|\rho - 1| << \gamma_o$, and therefore we can replace it by $4\gamma_o^2$. The parameters η_1 and η_2 only contribute for $\rho \sim 1$, so that we can also set $\rho^2 - 1 \approx 2(\rho - 1)$, if necessary. Combining everything gives

$$\eta_2 = \frac{1}{\rho - 1 + \delta\sqrt{(\rho-1)^2 + \gamma_o^2}} \ , \tag{26.2}$$

which is considerably simpler.

For *p*-waves the matrices F_p and G_p contain the parameters q_i and $\bar{q}_i$, i = 1,..,4, which depend on the resonance parameters ζ_1 and ζ_2. Along the same lines as above, although much more involved, we can derive that $\zeta_1 \approx -\zeta_2$, and

$$\zeta_2 = \frac{1 + 2\kappa_{||}^2}{\rho - 1 + \delta\sqrt{(\rho-1)^2 + \gamma_o^2(1 + 2\kappa_{||}^2)^2}} \ . \tag{26.3}$$

For the *q*-parameters we find

$$q_1 = \bar{q}_1 = q_4 = \bar{q}_4 = 1 \ , \tag{26.4}$$

$$-q_2 = -\bar{q}_2 = q_3 = \bar{q}_3 = \zeta_2 \ , \tag{26.5}$$

which leaves us with ζ_2 as the only resonance parameter for *p*-waves. The wave numbers $\kappa_{\alpha\sigma}$ and $\kappa_{\beta\sigma}$ depend in a complicated way on the various parameters, but the deviation from their vacuum values κ_a and κ_b, respectively, is of the order of γ_o. Since there is no resonance behavior in the wave numbers, we can set

$$\kappa_{\alpha\sigma} = \kappa_a \ , \qquad \kappa_{\beta\sigma} = \kappa_b \ , \tag{26.6}$$

to a good approximation. This approximation can be made in the matrices F_s and F_p, but not in the corresponding phase factors $\phi_{\alpha\sigma}$ and $\phi_{\beta\sigma}$.

If we substitute all approximations in the matrices F_s and F_p, then it appears that the equations for *s*-waves and *p*-waves are identical in form. The *p*-wave matrices follow from the *s*-wave matrices through the substitution

$$\eta_2 \to \zeta_2 \,, \qquad \phi_{\alpha s} \to \phi_{\alpha p} \,, \qquad \phi_{\beta s} \to \phi_{\beta p} \,, \tag{26.7}$$

and the same holds for the resulting Fresnel coefficients. Within the approximations of this section, the following Fresnel coefficients vanish

$$Z^-_{1\sigma} = 0 \,, \qquad Z^-_{2\sigma} = 0 \,, \qquad R_\sigma = 0 \,, \qquad N_\sigma \, e^{i\phi_b} = 0 \,, \tag{26.8}$$

which generalizes Eq. (25.2). The remaining Fresnel coefficients are

$$Z^+_{1s} = \frac{e^{i(\phi_{\alpha s} - \phi_{\beta s})}}{\gamma_o^2 \, \eta_2^2 + e^{i(\phi_{\alpha s} - \phi_{\beta s})}} \,, \tag{26.9}$$

$$Z^+_{2s} = \frac{\gamma^* \eta_2}{\gamma_o^2 \, \eta_2^2 + e^{i(\phi_{\alpha s} - \phi_{\beta s})}} \,, \tag{26.10}$$

$$P_s = \gamma^* \eta_2 \, \frac{1 - e^{i(\phi_{\alpha s} - \phi_\beta)}}{\gamma_o^2 \, \eta_2^2 + e^{i(\phi_{\alpha s} - \phi_{\beta s})}} \,, \tag{26.11}$$

$$T_s \, e^{-i\phi_a} = \frac{(1 + \gamma_o^2 \, \eta_2^2) e^{-i\phi_{\beta s}}}{\gamma_o^2 \, \eta_2^2 + e^{i(\phi_{\alpha s} - \phi_{\beta s})}} \,, \tag{26.12}$$

and this generalizes Eqs. (25.3)-(25.6). The results for *p*-waves follow then from Eq. (26.7). Far off resonance, η_2 remains finite, and therefore $\gamma^* \eta_2 \to 0$ and $\gamma_o^2 \, \eta_2^2 \to 0$. We then have $Z^+_{1s} = T_s = 1$ (because then $\phi_a = \phi_{\alpha s}$), and the other Fresnel coefficients vanish, as it should be. On the other hand, on resonance we have $\gamma^* \eta_2 = \delta \exp(-i\theta_p)$ and $\gamma_o^2 \, \eta_2^2 = 1$, and in this limit we recover the results from the previous section.

We see from Eq. (26.11) that $P_s = 0$ for $\exp[i(\phi_{\alpha s} - \phi_{\beta s})] = 1$, and it is easy to verify that $|\, P_s \,|$ is maximum for $\exp[i(\phi_{\alpha s} - \phi_{\beta s})] = -1$, which is $\phi_{\alpha s} - \phi_{\beta s} = (2n+1)\pi$, n integer. For a fixed value of the frequency, this leads again to conditions for the layer thickness or angle of incidence that optimizes the *pc*-wave, as in Eqs. (25.22) and (25.24), respectively. Under the same condition, the absolute values of the other Fresnel coefficients are also maximum, and the Fresnel coefficients themselves are given by

$$Z_{1s}^{+} = \frac{1}{1-\gamma_o^2 \eta_2^2} \ , \tag{26.13}$$

$$Z_{2s}^{+} = \frac{\gamma^* \eta_2}{\gamma_o^2 \eta_2^2 - 1} \ , \tag{26.14}$$

$$P_s = \gamma^* \eta_2 \frac{2}{\gamma_o^2 \eta_2^2 - 1} \ , \tag{26.15}$$

$$T_s \, e^{-i\phi_a} = e^{-i\phi_{\alpha s}} \frac{1+\gamma_o^2 \eta_2^2}{1-\gamma_o^2 \eta_2^2} \ . \tag{26.16}$$

For perfect resonance, we have $\gamma_o^2 \eta_2^2 = 1$, and all Fresnel coefficients are infinite, but for $\rho \neq 1$ they remain finite. Seen as a function of the angle of incidence, the condition $\phi_{\alpha s} - \phi_{\beta s} = (2n+1)\pi$ determines the values of θ_i where the maxima appear, similar to Eq. (25.24) for the case of resonance. Here the condition also involves ρ, since these phases depend on ρ. However, the values of the maxima, as given by the absolute values of the right-

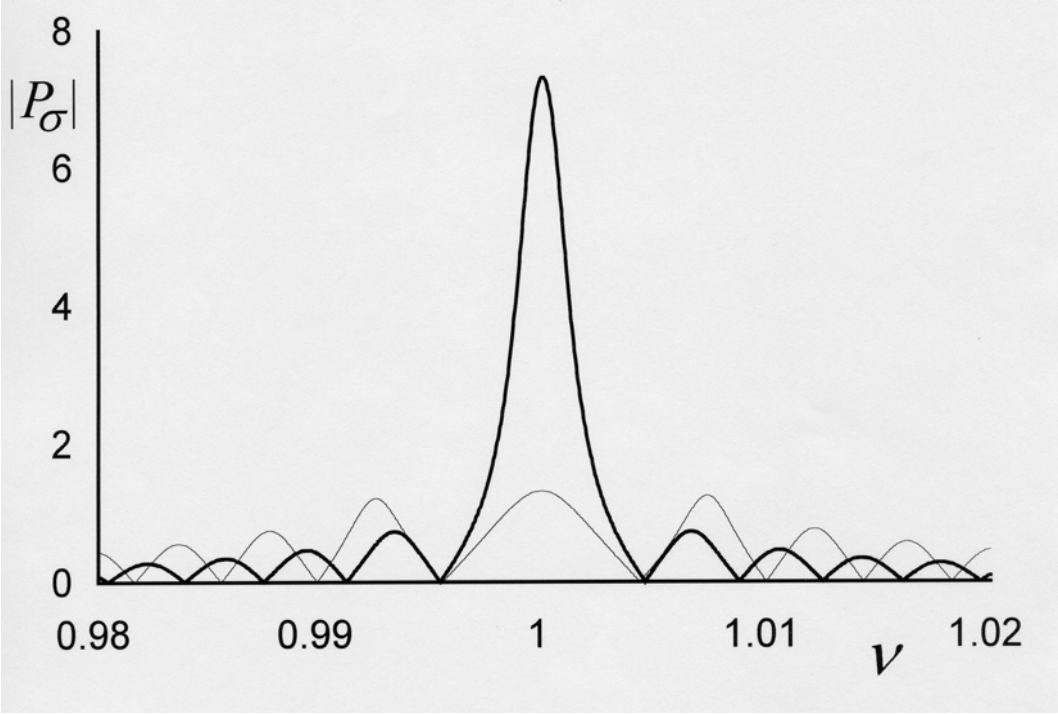

Figure 14: Illustration of the frequency dependence of $|P_s|$ (thick line) and $|P_p|$ (thin line) for $\varepsilon = 1$, $\gamma = 0.01$, $l = 660$ and $\theta_i = 45^0$. The peak heights are clearly different for *s*- and *p*-waves.

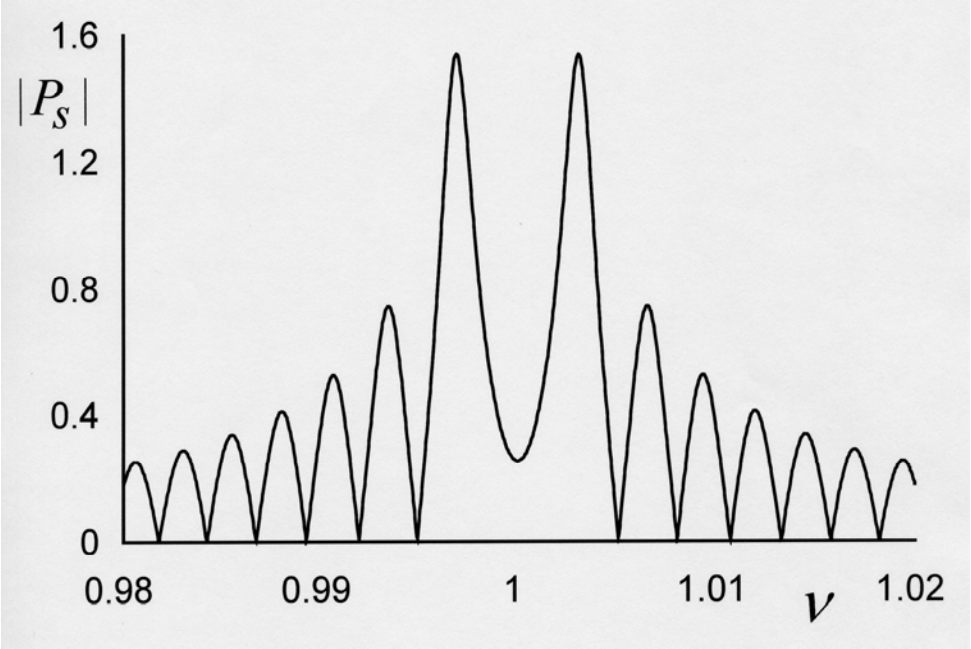

Figure 15: Graph of $|P_s|$ as a function of ν, for the same parameters as for Fig. 14, except here $l = 942$. This change in l turns the strong maximum at $\nu = 1$ into a minimum.

hand sides of Eqs. (26.13)-(26.16), do not depend on the layer thickness or the angle of incidence. This explains why all peaks in Figs. 12 and 13 appear to have the same height. For *p*-waves this is only approximately true, since ζ_2 replaces η_2, and we see from Eq. (26.3) that ζ_2 has a dependence on θ_i through $\kappa_{\|} = \sin\theta_i$. For the parameters of Fig. 12 we have from Eq. (26.2) $\eta_2 = -1201.3$, and with Eq. (26.15) this yields $|P_s| = 3.00$, in excellent agreement with the graph. Similarly, for Fig. 13 we find $\eta_2 = -1612.0$ and $|P_s| = 30.0$.

The relation $\phi_{\alpha s} - \phi_{\beta s} = (2n+1)\pi$ also predicts maxima for certain values of ρ, because these phases depend on ρ, although in a complicated way. Figure 14 shows a typical frequency dependence of the reflection coefficients $|P_s|$ and $|P_p|$. We see a strong resonance near $\nu = 1$, and the peaks have a width of order of γ_o. Since γ_o can be very small, a phase conjugator can be used to construct a narrow-band frequency filter [104]. We also see the appearance of side bands. The peak heights of the peaks at the resonance $\nu = 1$ should be given by Eqs. (25.20) and (25.21), but the value of $\gamma_o = 0.01$ is too large for the approximations of Sec. 25 to hold. The very sensitive dependence on the various parameters is illustrated with Fig. 15, where, compared to Fig. 14, only the value of the layer thickness is changed slightly. We see that the strong peak at $\nu = 1$ has disappeared, and has now become a minimum. Figure 16 shows the same graph, but then for *p*-waves. Here, the peak at the resonance frequency has come back, but it is still much weaker than the two nearest side bands. This possible disappearance of the *pc*-signal at resonance was confirmed experimentally [105].

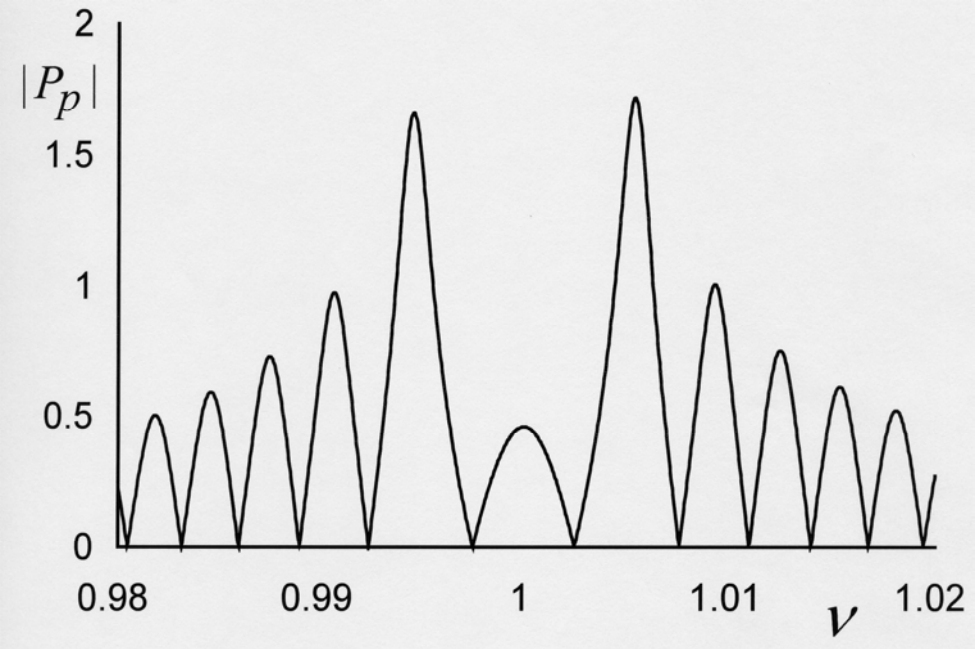

Figure 16: Same as Fig. 15, but here for *p*-waves. We see that for *p*-waves the maximum at $\nu = 1$ does not disappear, but it is considerably smaller than the first side bands.

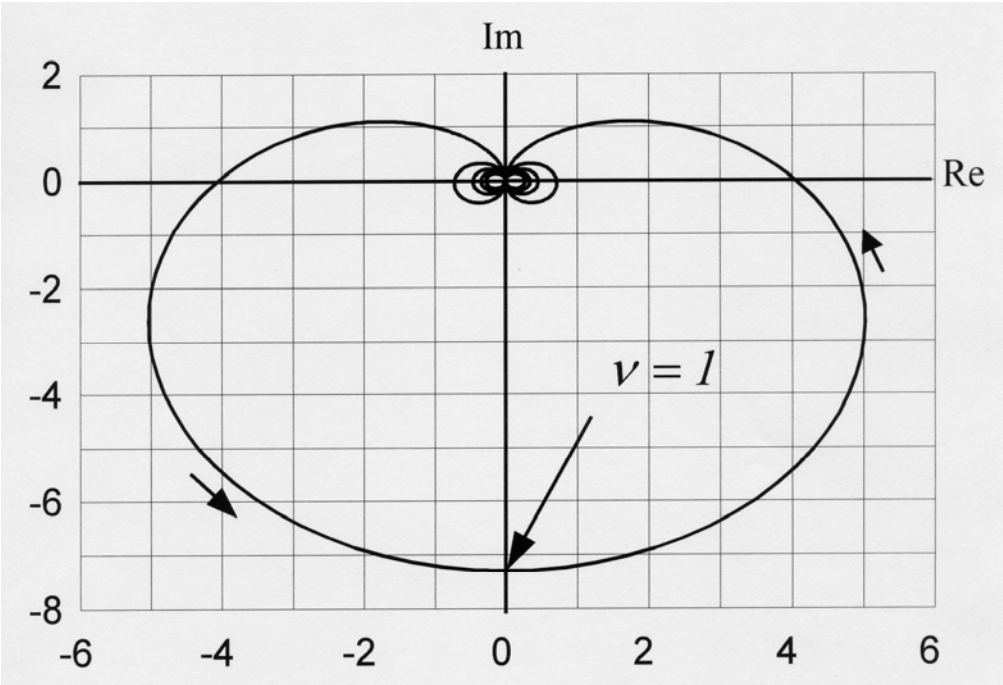

Figure 17: Polar diagram of P_s in the complex plane for the same parameters as in Fig. 14. At resonance, $\nu = 1$, the value of P_s is negative imaginary, as indicated by Eq. (25.20) (we have $\theta_p = 0$). The arrows indicate the direction of increasing ν.

An interesting way of depicting the Fresnel coefficients as a function of the frequency is by a representation as a polar plot in the complex plane. Figures 17 and 18 show the polar diagrams of P_s for the same parameters as in Figs. 14 and 15, respectively. The value of P_s at resonance is on the negative imaginary axis, as follows from Eq. (25.20). As the frequency increases or decreases, the curve spirals into the origin. After every turn of 360^o, the curve goes through the origin, which corresponds to a zero of the graphs in Figs. 14 and 15. We see that in the complex plane, the value of P_s varies smoothly throughout the plane, and in a non-trivial way, as has been known for a while [106].

For the intensities of the various waves on resonance we found the inequalities (25.14) and (25.15). For arbitrary ρ we have from Eqs. (26.12)

$$|T_s|^2 = \frac{(1+\gamma_o^2\eta_2^2)^2}{(1+\gamma_o^2\eta_2^2)^2 - 2\gamma_o^2\eta_2^2\{1-\cos(\phi_{\alpha s}-\phi_{\beta s})\}} \geq 1 \ , \tag{26.17}$$

which is larger than unity at any frequency. For the phase-conjugated wave we find from Eq. (26.11)

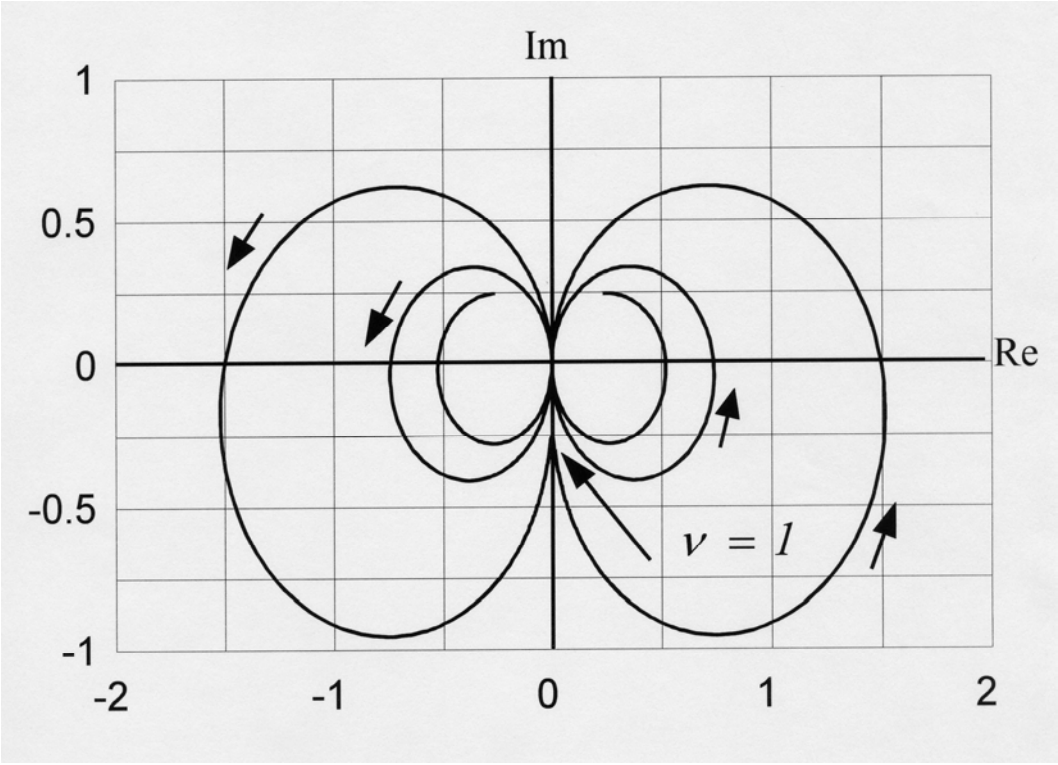

Figure 18: Same as Fig. 17, but for the parameters of Fig. 15, and the frequency range limited to $0.99 \leq \nu \leq 1.01$. The resonance value is still on the negative imaginary axis, but it does not correspond to a maximum of $|P_s|$ anymore.

$$|P_s|^2 = 2\gamma_o^2\eta_2^2 \frac{1-\cos(\phi_{\alpha s}-\phi_{\beta s})}{(1+\gamma_o^2\eta_2^2)^2 - 2\gamma_o^2\eta_2^2\{1-\cos(\phi_{\alpha s}-\phi_{\beta s})\}} \ , \tag{26.18}$$

which can be anything in between zero and infinity. Most remarkably is that from Eqs. (26.17) and (26.18) we obtain

$$|T_s|^2 - |P_s|^2 = 1 \ , \tag{26.19}$$

as Eq. (25.19) for the limit of close resonance. Since the results for *p*-waves follow from the substitutions shown in Eq. (26.7), this identity also holds for *p*-waves.

Finally, we mention that P_s from Eq. (26.11) can be written in the alternative form

$$P_s = -i\gamma^*\eta_2 \frac{\sin[\frac{1}{2}(\phi_{\alpha s}-\phi_{\beta s})]}{\cos[\frac{1}{2}(\phi_{\alpha s}-\phi_{\beta s})] + \frac{1}{2}(\gamma_o^2\eta_2^2 - 1)e^{-\frac{1}{2}i(\phi_{\alpha s}-\phi_{\beta s})}} \ , \tag{26.20}$$

which displays more clearly that P_s reduces to the earlier result (25.5) in the limit $\rho \to 1$.

27. SPECULAR WAVE

The most essential features of the amplitudes of the various waves are exhibited in the approximate solutions (25.2)-(25.6), and the expressions from the previous section incorporate the main characteristics for off-resonance excitation. Nevertheless, Eq. (26.15) still predicts $P_s = \infty$ for a peak located at perfect resonance, whereas the exact solution remains finite. Considerable deviations from the previous results can already occur for values of γ as low as 10^{-3}. In this section we look at the value of R_s, which is predicted to vanish by Eqs. (25.2) and (26.8). Figure 19 shows $|R_s|$ as a function of ν, and for $\gamma = 0.01$. We see that $|R_s|$ is not really small, due to the finite γ, and another interesting feature is that the maximum appears well off resonance. Figure 20 shows the polar diagram in the complex plane of R_s as a function of ν, and for the same parameters as in Fig. 19. This apparent erratic frequency dependence only follows from considering the exact solution for finite but small γ. Figure 21 shows $|R_s|$ as a function of the angle of incidence, and we notice that a sharp peak appears near $\theta_i = 75^o$. For this graph we took $\nu - 1 = 0.0015$. For smaller values of $\nu - 1$, the sub-peaks near 90^o disappear, and the main peak gets sharper and higher, and moves closer to 90^o. Obviously, such subtleties require a more detailed analysis of the solution for R_s than given by the approximations presented in this paper, for which we only find $R_s = 0$.

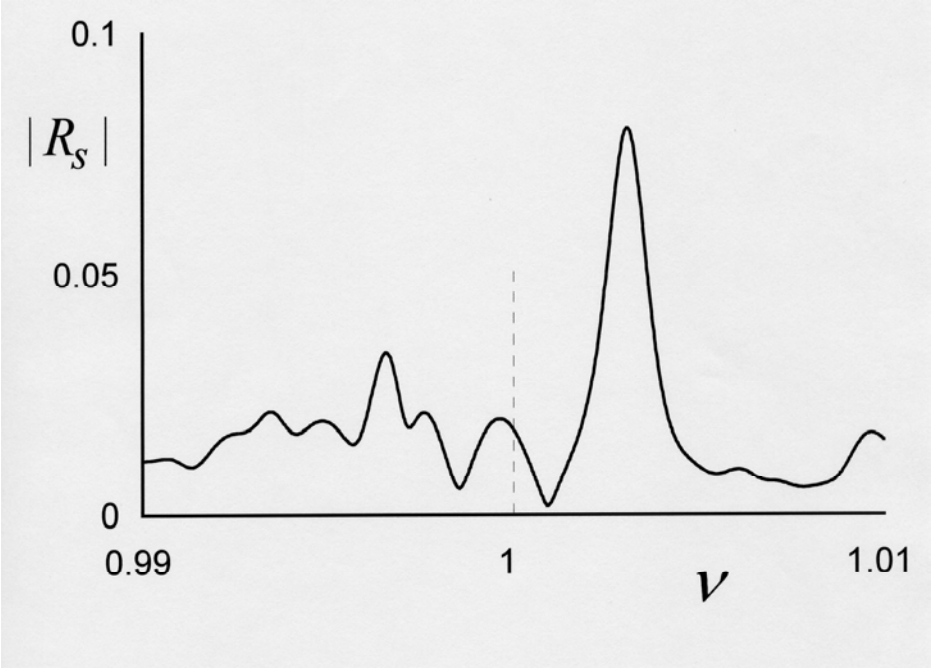

Figure 19: Graph of the absolute value of the reflection coefficient for *s*-waves, as a function of the frequency ν. The parameters are $\varepsilon = 1$, $\gamma = 0.01$, $l = 942$ and $\theta_i = 45^o$, which are the same as for Fig. 15.

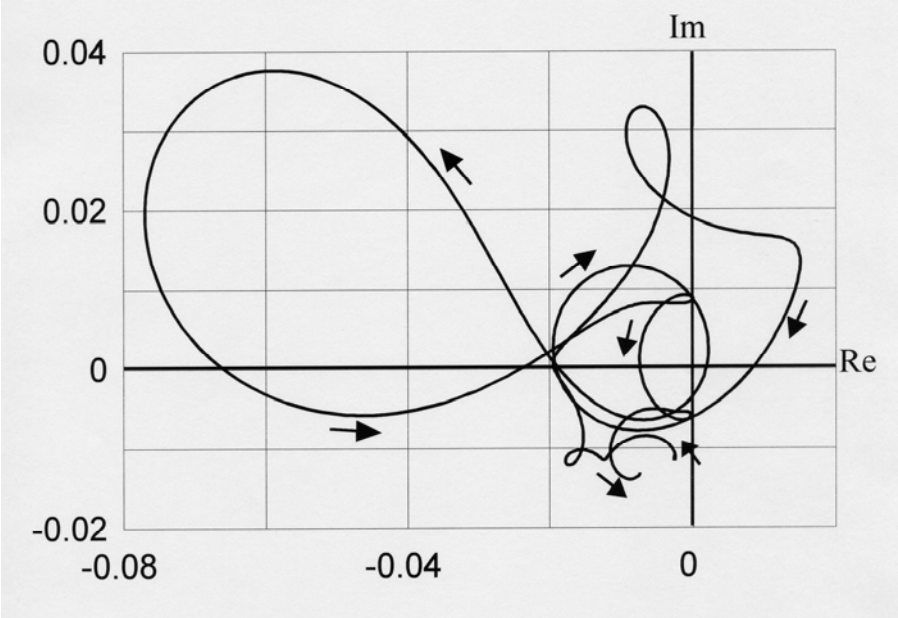

Figure 20: Polar diagram in the complex plane for R_S as a function of ν, with $0.99 \leq \nu \leq 1.01$, and for the same parameters as in Fig. 19.

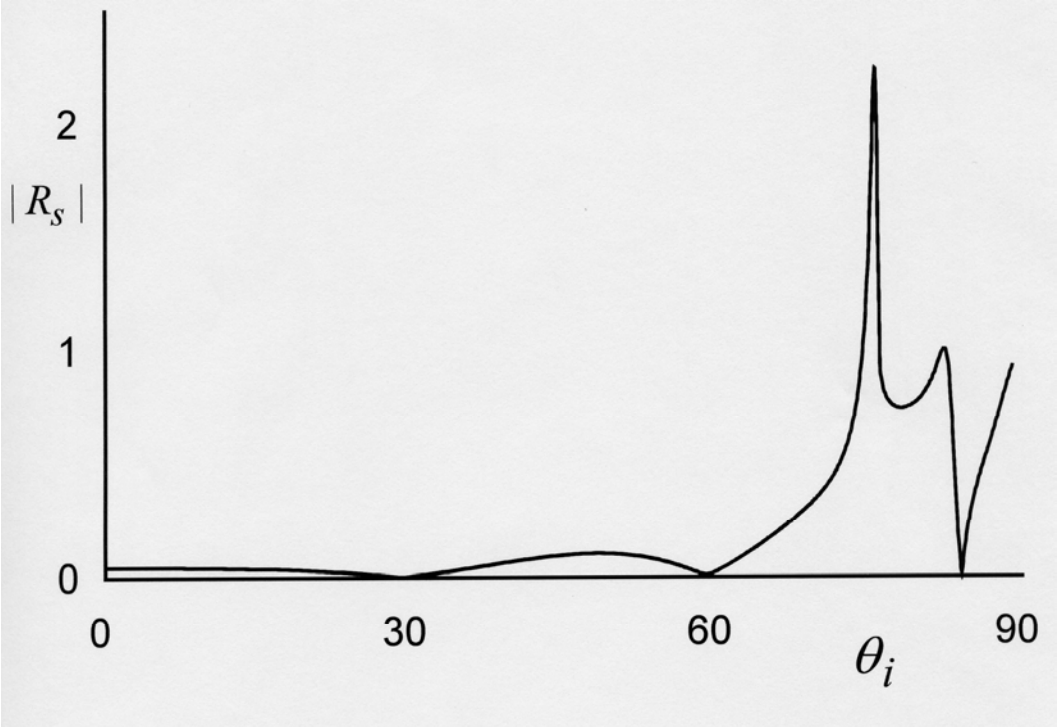

Figure 21: Illustration of $|R_s|$ as a function of the angle of incidence, for $\varepsilon = 1$, $\gamma = 0.05$, $l = 10$ and $\nu = 1.0015$.

28. EVANESCENT WAVES

In the general solution, both traveling and evanescent waves are included in one formalism, but it appears that the approximate expressions for the Fresnel coefficients are different in form for evanescent waves than for traveling waves. In this section we consider $\kappa_{||} > 1$, e.g., the incident wave is evanescent, and a transparent medium ($\varepsilon = 1$) with γ small, which is the same situation as in Sec. 26. We shall also assume that the layer thickness is many wavelengths. Since we shall allow for an arbitrary frequency detuning, it can happen that the ω_b-waves are traveling (κ_b real and κ_a imaginary). However, it turns out that in that case the Fresnel coefficients for the traveling waves are zero, up to order γ_o. The same conclusion holds for a traveling incident wave and other evanescent waves, so that either all waves are traveling or all are evanescent. Along similar lines as in Sec. 26 we find

$$Z_{1\sigma}^{-} = 0\,, \quad Z_{2\sigma}^{+} = 0\,, \quad R_\sigma = 0\,, \quad P_\sigma = 0\,, \quad N_\sigma e^{i\phi_b} = 0\,, \quad T_\sigma e^{-i\phi_a} = 0\,, \tag{28.1}$$

and for *s*-waves we obtain

$$Z_{1s}^{+} = \frac{1}{1 + \gamma_o^2 \eta_2^2}\,, \tag{28.2}$$

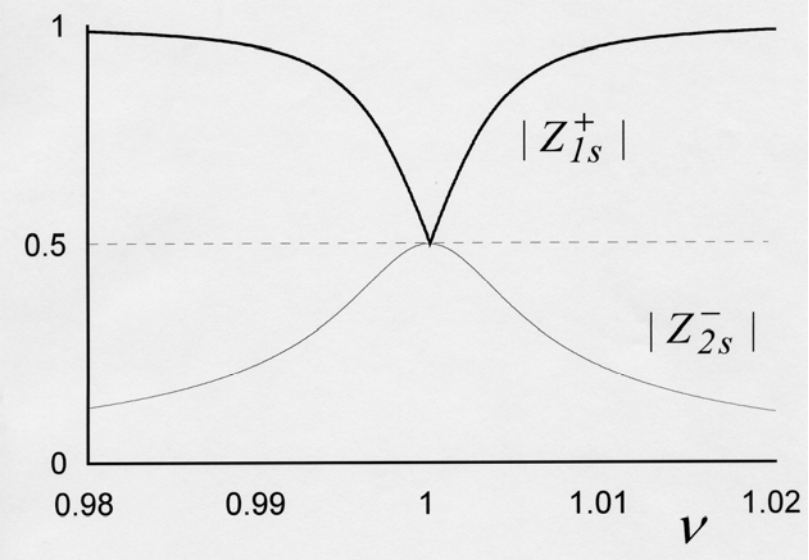

Figure 22: The two non-zero Fresnel coefficients for evanescent waves, as a function of the frequency. The parameters are $\varepsilon = 1$, $\gamma = 0.01$, $l = 10$ and $\kappa_{||} = 2$.

$$Z_{2s}^{-} = \frac{\gamma^{*}\eta_2}{1+\gamma_o^2\eta_2^2} \ . \tag{28.3}$$

The results for *p*-waves follow from the substitution $\eta_2 \to \zeta_2$, as in Eq. (26.7). Referring to Fig. 7, we notice that the only waves, other than the incident wave, inside the medium survive, which are the ones that seem to emanate from the surface $z = 0$. Far off resonance we find $Z_{1s}^{+} \to 1$, $Z_{2s}^{-} \to 0$, as it should be. On resonance we have $\gamma_o^2\eta_2^2 = 1$, and Eqs. (28.2) and (28.3) reduce to

$$Z_{1s}^{+} = \frac{1}{2}, \qquad Z_{2s}^{-} = \frac{1}{2}\delta\, e^{-i\theta_p} \ , \tag{28.4}$$

showing that both waves have equal intensity. The frequency dependence is entirely accounted for by η_2, unlike for traveling waves where we also had a ρ dependence in the phases $\phi_{\alpha s}$ and $\phi_{\beta s}$. For *s*-waves there is no dependence on $\kappa_{||}$, but for *p*-waves the parameter ζ_2 has a $\kappa_{||}$ dependence, as can be seen in Eq. (26.3). Figure 22 shows the two Fresnel coefficients as a function of the frequency.

29. BICHROMATIC SOLUTION OF PLANE WAVES

The set of coupled wave equations, Eqs. (11.4) and (11.5), expresses that the electric field $\hat{\boldsymbol{E}}(\boldsymbol{r},\omega)$ (which is in general a continuous function of ω), evaluated at $\omega=\omega_a$ and at $\omega=\omega_b$, must be related according to these equations. In analogy to the monochromatic solutions in linear optics, it might seem that here we can find a bichromatic solution, such that $\hat{\boldsymbol{E}}(\boldsymbol{r},\omega)\propto\delta(\omega-\omega_a)$ around $\omega=\omega_a$, $\hat{\boldsymbol{E}}(\boldsymbol{r},\omega)\propto\delta(\omega-\omega_b)$ around $\omega=\omega_b$, and zero elsewhere. If we would substitute this into the more general equation (11.1), then the left-hand side would be proportional to $\delta(\omega-\omega_a)$ and the right-hand side to $\delta(\omega-\omega_b)$, which shows that the two delta functions would not cancel. Also, a solution of this form does not obey the condition (3.4) for $\hat{\boldsymbol{E}}(\boldsymbol{r},\omega)$. Equation (3.4) expresses that if we are given the field at $\omega=\omega_a$, then we also know the field at $\omega=-\omega_a$, and vice versa. A bichromatic solution must have the form

$$\hat{\boldsymbol{E}}(\boldsymbol{r},\omega)=\hat{\boldsymbol{E}}(\boldsymbol{r},\omega_a)\delta(\omega-\omega_a)+\hat{\boldsymbol{E}}(\boldsymbol{r},\omega_a')\delta(\omega-\omega_a')$$

$$+\hat{\boldsymbol{E}}(\boldsymbol{r},\omega_b)\delta(\omega-\omega_b)+\hat{\boldsymbol{E}}(\boldsymbol{r},\omega_b')\delta(\omega-\omega_b')\ . \tag{29.1}$$

Here we have introduced $\omega_a'=-\omega_b$ and $\omega_b'=-\omega_a$, so that ω_a and ω_a' are positive and ω_b and ω_b' are negative. Then we have $\omega_a+\omega_a'=2\overline{\omega}$ and $\omega_b+\omega_b'=-2\overline{\omega}$, which shows that ω_a and ω_a' are symmetrically located around $\overline{\omega}$, and ω_b and ω_b' have $-\overline{\omega}$ in their middle. In the notation of Eq. (29.1) it should be understood that $\hat{\boldsymbol{E}}(\boldsymbol{r},\omega_a)$ is meant to be the amplitude of $\hat{\boldsymbol{E}}(\boldsymbol{r},\omega)$ at $\omega=\omega_a$, and not $\hat{\boldsymbol{E}}(\boldsymbol{r},\omega\equiv\omega_a)$. When we substitute the right-hand side of Eq. (29.1) into the top line of Eq. (11.1), then both the right-hand side and the left-hand side have a term proportional to $\delta(\omega-\omega_a)$ and a term proportional to $\delta(\omega-\omega_a')$. Therefore, we can separate the equations for ω_a and ω_a', and then the delta functions cancel. The equation at ω_a is then exactly Eq. (11.4). In the same way, the bottom line of Eq. (11.1) reproduces Eq. (11.5). Then, from $\hat{\boldsymbol{E}}(\boldsymbol{r},\omega)^*=\hat{\boldsymbol{E}}(\boldsymbol{r},-\omega)$ we have the relations

$$\hat{\boldsymbol{E}}(\boldsymbol{r},\omega_a')=\hat{\boldsymbol{E}}(\boldsymbol{r},\omega_b)^*\ ,\qquad \hat{\boldsymbol{E}}(\boldsymbol{r},\omega_b')=\hat{\boldsymbol{E}}(\boldsymbol{r},\omega_a)^*\ . \tag{29.2}$$

For the positive frequency part of the field, only the contributions of ω_a and ω_a' contribute, and with Eq. (3.5) we find

$$\boldsymbol{E}(\boldsymbol{r},t)^{(+)}=\frac{1}{2\pi}\left[\hat{\boldsymbol{E}}(\boldsymbol{r},\omega_a)e^{-i\omega_a t}+\hat{\boldsymbol{E}}(\boldsymbol{r},\omega_b)^*e^{-i\omega_a' t}\right]\ , \tag{29.3}$$

in terms of a solution $\hat{\boldsymbol{E}}(\boldsymbol{r},\omega_a)$, $\hat{\boldsymbol{E}}(\boldsymbol{r},\omega_b)$ of the set (11.4), (11.5). For the field itself we add the negative frequency part, as in Eq. (3.7), and this is equivalent to

$$\boldsymbol{E}(\boldsymbol{r},t)=\frac{1}{\pi}\mathrm{Re}\left[\hat{\boldsymbol{E}}(\boldsymbol{r},\omega_a)e^{-i\omega_a t}+\hat{\boldsymbol{E}}(\boldsymbol{r},\omega_b)^{*}e^{-i\omega_a' t}\right], \tag{29.4}$$

in view of Eq. (3.6).

For the situation where the layer is illuminated by a monochromatic polarized plane wave of the form (18.1), the solution for $\hat{\boldsymbol{E}}(\boldsymbol{r},\omega_a)$ and $\hat{\boldsymbol{E}}(\boldsymbol{r},\omega_b)$ in $z > 0$ takes the form as given by Eqs. (19.4) and (19.5). Then the field in $z > 0$ is explicitly

$$\boldsymbol{E}(\boldsymbol{r},t)=\frac{1}{\pi}\mathrm{Re}\left[E\,\boldsymbol{e}_\sigma\,e^{i(\boldsymbol{k}\cdot\boldsymbol{r}-\omega_a t)}+E\,R_\sigma\,\boldsymbol{e}_{\sigma,r}\,e^{i(\boldsymbol{k}_r\cdot\boldsymbol{r}-\omega_a t)}+E^{*}P_\sigma^{*}\,\boldsymbol{e}_{\sigma,pc}^{*}\,e^{i(-\boldsymbol{k}_{pc}^{*}\cdot\boldsymbol{r}-\omega_a' t)}\right]. \tag{29.5}$$

This shows clearly that the frequency of the *pc*-wave is ω_a'. If the wave is traveling, then its wave vector is real, and equal to $-\boldsymbol{k}_{pc}$. For $\rho\approx 1$ we have $-\boldsymbol{k}_{pc}\approx-\boldsymbol{k}$, as shown in Sec. 18, and therefore the incident wave and the phase conjugated wave are almost counterpropagating indeed. Interference between the two waves gives rise to observable fringes [107,108].

30. HELICITY

When the incident field is *s*- (*p*-) polarized, then all other waves are also *s*- (*p*-) polarized. As pointed out in Sec. 1, below Eq. (1.4), a well-operating phase conjugator does not only reverse the propagation direction of the incident wave, but it also conjugates the polarization vector, if complex. As pointed out by others [109,110], this implies that a phase conjugator should preserve the handedness, or helicity, of the wave. Whether or not the phase conjugator under discussion does that is hidden in the *s*-*p* formalism. In order to investigate this question, we first consider the reflection of a polarized plane wave with arbitrary polarization.

Equation (29.5) represents the field in $z > 0$ for either *s*- or *p*-polarized waves. Since the coupled wave equations are linear in the fields, an arbitrary superposition of solutions is again a solution. We replace E by E_σ and sum over σ. The first term on the right-hand side of Eq. (29.5) then contains the factor $\sum_\sigma E_\sigma\,\boldsymbol{e}_\sigma$, which we write as

$$\sum_\sigma E_\sigma\,\boldsymbol{e}_\sigma=\pi\,E_o\,\boldsymbol{\varepsilon}\ , \tag{30.1}$$

with $E_o > 0$, and $\boldsymbol{\varepsilon}$ normalized as $\boldsymbol{\varepsilon}\cdot\boldsymbol{\varepsilon}^{*}=1$. Then E_o is the amplitude of the incident field and $\boldsymbol{\varepsilon}$ is the polarization vector. Given E_o and $\boldsymbol{\varepsilon}$, E_σ follows from

$$E_\sigma=\pi\,E_o(\boldsymbol{\varepsilon}\cdot\boldsymbol{e}_\sigma)\ , \tag{30.2}$$

since the polarization vectors $\boldsymbol{e}_\sigma$ are normalized as $\boldsymbol{e}_\sigma\cdot\boldsymbol{e}_\sigma=1$ (without the star). So we set $E\to\pi\,E_o(\boldsymbol{\varepsilon}\cdot\boldsymbol{e}_\sigma)$ in Eq. (29.5) and sum over σ. This yields

$$\boldsymbol{E}(\boldsymbol{r},t) = E_o \mathrm{Re}\left[\boldsymbol{\varepsilon}\, e^{i(\boldsymbol{k}\cdot\boldsymbol{r}-\omega_a t)} + e^{i(\boldsymbol{k}_r\cdot\boldsymbol{r}-\omega_a t)} \sum_{\sigma=s,p} R_\sigma (\boldsymbol{\varepsilon}\cdot\boldsymbol{e}_\sigma)\boldsymbol{e}_{\sigma,r} \right.$$

$$\left. + e^{i(-\boldsymbol{k}^*_{pc}\cdot\boldsymbol{r}-\omega_a' t)} \sum_{\sigma=s,p} P^*_\sigma (\boldsymbol{\varepsilon}^*\cdot\boldsymbol{e}^*_\sigma)\boldsymbol{e}^*_{\sigma,pc} \right], \tag{30.3}$$

where we have used

$$\sum_{\sigma=s,p} (\boldsymbol{\varepsilon}\cdot\boldsymbol{e}_\sigma)\boldsymbol{e}_\sigma = \boldsymbol{\varepsilon} \ . \tag{30.4}$$

Then we introduce the (unnormalized) polarization vectors for the *r*-wave and the *pc*-wave by

$$\boldsymbol{\varepsilon}_r = \sum_{\sigma=s,p} R_\sigma (\boldsymbol{\varepsilon}\cdot\boldsymbol{e}_\sigma)\boldsymbol{e}_{\sigma,r} \ , \tag{30.5}$$

$$\boldsymbol{\varepsilon}_{pc} = \sum_{\sigma=s,p} P^*_\sigma (\boldsymbol{\varepsilon}^*\cdot\boldsymbol{e}^*_\sigma)\boldsymbol{e}^*_{\sigma,pc} \ . \tag{30.6}$$

The three contributions to the field of Eq. (30.3) are then

$$\boldsymbol{E}(\boldsymbol{r},t)_{inc} = E_o \ \mathrm{Re}\ \boldsymbol{\varepsilon}\, e^{i(\boldsymbol{k}\cdot\boldsymbol{r}-\omega_a t)} \ , \tag{30.7}$$

$$\boldsymbol{E}(\boldsymbol{r},t)_r = E_o \ \mathrm{Re}\ \boldsymbol{\varepsilon}_r\, e^{i(\boldsymbol{k}_r\cdot\boldsymbol{r}-\omega_a t)} \ , \tag{30.8}$$

$$\boldsymbol{E}(\boldsymbol{r},t)_{pc} = E_o \ \mathrm{Re}\ \boldsymbol{\varepsilon}_{pc}\, e^{i(-\boldsymbol{k}^*_{pc}\cdot\boldsymbol{r}-\omega_a' t)} \ , \tag{30.9}$$

in obvious notation.

In order to see what happens to the helicity upon reflection, let us consider traveling waves, and normal incidence. Let us take the *x*- and *y*- directions as the directions of the unit *p*- and *s*- polarization vectors of the incident wave. It then follows from Fig. 23 that the other *p*-polarization vectors are $\boldsymbol{e}_{p,pc} = \boldsymbol{e}_x$ and $\boldsymbol{e}_{p,r} = -\boldsymbol{e}_x$. The polarization vectors for *s*-waves are all the same, $\boldsymbol{e}_{s,i} = \boldsymbol{e}_y$. Since for normal incidence, there is no distinction between *s*-polarization and *p*-polarization, the corresponding Fresnel coefficients must obey

$$P_p = P_s \ , \tag{30.10}$$

$$R_p = -R_s \ . \tag{30.11}$$

The minus sign on the right-hand side of Eq. (30.11) is a consequence of the sign conventions for the polarization vectors, as follows most easily from Fig. 23. The polarization vectors for the *r*-wave, Eq. (30.5) and the *pc*-wave, Eq. (30.6), then simplify to

$$\boldsymbol{\varepsilon}_r = R_s \, \boldsymbol{\varepsilon} \ , \tag{30.12}$$

$$\boldsymbol{\varepsilon}_{pc} = P_s^* \boldsymbol{\varepsilon}^* \ . \tag{30.13}$$

Then we write $R_s = R_o \exp(i\phi_r)$, $P_s = P_o \exp(i\phi_{pc})$, with $R_o \geq 0$, $P_o \geq 0$, and the phases real. The *r*-wave and the *pc*-wave then become

$$\boldsymbol{E}(\boldsymbol{r},t)_r = E_o \, R_o \, \mathrm{Re}\, \boldsymbol{\varepsilon} \, e^{i(\boldsymbol{k}_r \cdot \boldsymbol{r} - \omega_a t + \phi_r)} \ , \tag{30.14}$$

$$\boldsymbol{E}(\boldsymbol{r},t)_{pc} = E_o \, P_o \mathrm{Re}\, \boldsymbol{\varepsilon}^* \, e^{i(-\boldsymbol{k}_{pc} \cdot \boldsymbol{r} - \omega_a' t - \phi_{pc})} \ . \tag{30.15}$$

For the polarization vector of the incident wave we now take, as an example, the spherical unit vector

$$\boldsymbol{\varepsilon} = -\frac{1}{\sqrt{2}} (\boldsymbol{e}_x + i\boldsymbol{e}_y) \ . \tag{30.16}$$

To see the rotation of the $\boldsymbol{E}$ vector, we set $\boldsymbol{r} = 0$ in Eq. (30.7), which then gives

$$\boldsymbol{E}(0,t)_{inc} = -\frac{1}{\sqrt{2}} E_o \, \{\boldsymbol{e}_x \cos(\omega_a t) + \boldsymbol{e}_y \sin(\omega_a t)\} \ . \tag{30.17}$$

This vector rotates counterclockwise in the *xy*-plane with increasing time. Since the propagation direction is the negative *z*-direction, this vector rotates clockwise when you look into the oncoming beam. Therefore, the *inc*-wave is right-circularly polarized. Similarly, for the *r*-wave we have

$$\boldsymbol{E}(0,t)_r = -\frac{1}{\sqrt{2}} E_o \, R_o \, \{\boldsymbol{e}_x \cos(\omega_a t - \phi_r) + \boldsymbol{e}_y \sin(\omega_a t - \phi_r)\} \ , \tag{30.18}$$

which also rotates counterclockwise in the *xy*-plane. But since the specular wave travels in the positive *z*-direction, the $\boldsymbol{E}$ vector rotates counterclockwise when looking into the oncoming beam, so that the *r*-wave is left- circularly polarized. Then, the *pc*-wave is

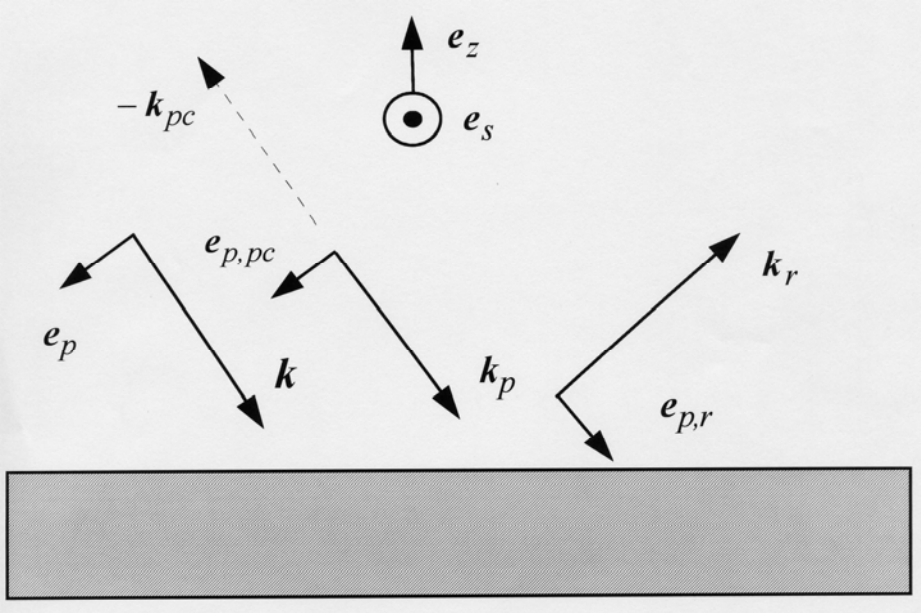

Figure 23: Illustration of the phase conventions for the polarization vectors, as determined by Eqs. (19.1) and (19.2).

$$\boldsymbol{E}(0,t)_{pc} = -\frac{1}{\sqrt{2}} E_o P_o \{\boldsymbol{e}_x \cos(\omega_a' t + \phi_{pc}) - \boldsymbol{e}_y \sin(\omega_a' t + \phi_{pc})\} \ , \tag{30.19}$$

which rotates clockwise. The propagation direction is the positive z-direction, so when looking into the beam, we see a clockwise rotation, and therefore this wave is right-circularly polarized, just as the incident wave. This shows that the helicity is preserved for the phase conjugated wave, unlike for the specular wave. It is interesting to notice that this conclusion is independent of the values of the Fresnel coefficients.

31. SUMMARY AND CONCLUSIONS

We have theoretically studied optical phase conjugation by four-wave mixing in a layer of nonlinear material. The present presentation is a greatly expanded version of an earlier account [111]. No restrictions were imposed on the angle of incidence, the value of the dielectric constant, the third-order susceptibility, the frequency mismatch with the pump beams or the layer thickness. Also included is the possibility that the incident wave is evanescent rather than traveling. Maxwell's equations for the geometry shown in Fig. 1 were solved (almost) exactly, and this proceeded essentially in three steps.

First we worked out the expression for the third-order nonlinear polarization under the assumption that we have two strong counterpropagating and monochromatic laser beams incident on the medium from the left and the right. The field to be conjugated has to be weak compared to the intensity of the pump beams. It then appears that we can derive a set of two

coupled wave equations for the weak field only, which couple a positive- and a negative-frequency component of the Fourier spectral distribution of the radiation. The presence of the pumps enters the equations only parametrically through the third-order polarization, which contains a parameter that is proportional to the third-order susceptibility and the pump intensity.

As the second step we studied the fundamental plane-wave solutions of the coupled wave equations. It appeared that the solutions split into two categories, which could be identified as standard *s*-polarized and *p*-polarized waves. We found that the *s*-waves are transverse, but the *p*-waves are not. We have derived dispersion relations for both the *s*-waves and the *p*-waves, and we found that each has two branches, each corresponding in a particular way to the two waves in the set. Subsequently we evaluated the relative amplitudes of the two coupled waves, and their polarization vectors. The coupling between the waves could be expressed in terms of resonance parameters, like η_1 and η_2 for *s*-waves, which depend in a crucial and sensitive way on the frequency difference between the incident field and the pump beams, and the nonlinear coupling parameter γ.

The third step involves the excitation of plane waves inside the medium by an external field. We assumed an incident plane-wave field, with given amplitude, polarization, frequency and wave vector (which includes the angle of incidence for traveling waves). We have shown that, in general, an incident plane wave does not excite just a single set of two coupled waves in the medium, but that the situation is much more complex. The general picture is summarized in Fig. 6 for traveling and in Fig. 7 for evanescent waves. The wave vectors, and thereby the reflection and refraction angles, follow from the requirement that all wave vectors must have the same parallel components, and that the magnitude of the wave vectors is determined by the dispersion relations. The only unknowns are the relative amplitudes of the various waves, with respect to the amplitude of the incident wave, and these are the Fresnel coefficients. They represent both the intensities and the phases of the various waves. We were able to obtain the sixteen Fresnel coefficients by matching the fields across the two boundaries, according to Maxwell's equations. We have studied the solutions both analytically and numerically, and we have derived simplified expressions for limiting situations.

APPENDIX

The numerical evaluation of the Fresnel coefficients is done by solving the set of four linear equations, Eq. (20.3), both for *s*-polarization and *p*-polarization, by Gauss elimination and pivoting. On the other hand, we can solve this set analytically, as indicated in Sec. 22. The results are rather cumbersome, but of great value for the study of the properties of these coefficients. For reference, we give the full result for the 16 Fresnel coefficients in this Appendix.

The solution of Eq. (20.3) is formally given by

$$\begin{pmatrix} Z_{1\sigma}^{+} \\ Z_{1\sigma}^{-} \\ Z_{2\sigma}^{+} \\ Z_{2\sigma}^{-} \end{pmatrix} = 2\kappa_a \, (F_\sigma)^{-1} \begin{pmatrix} 1 \\ 0 \\ 0 \\ 0 \end{pmatrix} . \tag{A.1}$$

This shows that we only need the first column of the inverse of F_σ. Therefore, the solution can be written as

$$\begin{pmatrix} Z_{1\sigma}^{+} \\ Z_{1\sigma}^{-} \\ Z_{2\sigma}^{+} \\ Z_{2\sigma}^{-} \end{pmatrix} = \frac{2\kappa_a}{\det(F_\sigma)} \begin{pmatrix} f_{\sigma 1} \\ -f_{\sigma 2} \\ f_{\sigma 3} \\ -f_{\sigma 4} \end{pmatrix} , \tag{A.2}$$

with $f_{\sigma i}$ the minor of $(F_\sigma)_{1i}$, that is, the determinant of the 3×3 matrix which remains after row 1 and column i are crossed out in F_σ.

For *s*-waves we find

$$\begin{aligned} f_{s1} = {} & (\kappa_a + \kappa_{\alpha s}) e^{i\phi_{\alpha s}} \left[(\kappa_b + \kappa_{\beta s})^2 e^{-i\phi_{\beta s}} - (\kappa_b - \kappa_{\beta s})^2 e^{i\phi_{\beta s}} \right] \\ & - \gamma_o^2 \eta_1 \eta_2 \Big[2\kappa_{\beta s} (\kappa_a + \kappa_b)(\kappa_b + \kappa_{\alpha s}) \\ & - (\kappa_b - \kappa_{\alpha s}) e^{i\phi_{\alpha s}} \{ (\kappa_a + \kappa_{\beta s})(\kappa_b - \kappa_{\beta s}) e^{i\phi_{\beta s}} \\ & - (\kappa_a - \kappa_{\beta s})(\kappa_b + \kappa_{\beta s}) e^{-i\phi_{\beta s}} \} \Big] , \end{aligned} \tag{A.3}$$

$$\begin{aligned} f_{s2} = {} & (\kappa_a - \kappa_{\alpha s}) e^{-i\phi_{\alpha s}} \left[(\kappa_b + \kappa_{\beta s})^2 e^{-i\phi_{\beta s}} - (\kappa_b - \kappa_{\beta s})^2 e^{i\phi_{\beta s}} \right] \\ & - \gamma_o^2 \eta_1 \eta_2 \Big[2\kappa_{\beta s} (\kappa_a + \kappa_b)(\kappa_b - \kappa_{\alpha s}) \\ & - (\kappa_b + \kappa_{\alpha s}) e^{-i\phi_{\alpha s}} \{ (\kappa_a + \kappa_{\beta s})(\kappa_b - \kappa_{\beta s}) e^{i\phi_{\beta s}} \\ & - (\kappa_a - \kappa_{\beta s})(\kappa_b + \kappa_{\beta s}) e^{-i\phi_{\beta s}} \} \Big] , \end{aligned} \tag{A.4}$$

$$f_{s3} = -\gamma^* \eta_1 \Big[2\kappa_{\alpha s}(\kappa_a + \kappa_b)(\kappa_b + \kappa_{\beta s})$$

$$-(\kappa_b - \kappa_{\beta s}) e^{i\phi_{\beta s}} \{(\kappa_a + \kappa_{\alpha s})(\kappa_b - \kappa_{\alpha s}) e^{i\phi_{\alpha s}}$$

$$-(\kappa_a - \kappa_{\alpha s})(\kappa_b + \kappa_{\alpha s}) e^{-i\phi_{\alpha s}} \}$$

$$+\gamma_o^2 \eta_1 \eta_2 (\kappa_a + \kappa_{\beta s}) e^{i\phi_{\beta s}} \{(\kappa_b - \kappa_{\alpha s})^2 e^{i\phi_{\alpha s}}$$

$$-(\kappa_b + \kappa_{\alpha s})^2 e^{-i\phi_{\alpha s}} \} \Big] , \tag{A.5}$$

$$f_{s4} = -\gamma^* \eta_1 \Big[2\kappa_{\alpha s}(\kappa_a + \kappa_b)(\kappa_b - \kappa_{\beta s})$$

$$-(\kappa_b + \kappa_{\beta s}) e^{-i\phi_{\beta s}} \{(\kappa_a + \kappa_{\alpha s})(\kappa_b - \kappa_{\alpha s}) e^{i\phi_{\alpha s}}$$

$$-(\kappa_a - \kappa_{\alpha s})(\kappa_b + \kappa_{\alpha s}) e^{-i\phi_{\alpha s}} \}$$

$$+\gamma_o^2 \eta_1 \eta_2 (\kappa_a - \kappa_{\beta s}) e^{-i\phi_{\beta s}} \{(\kappa_b - \kappa_{\alpha s})^2 e^{i\phi_{\alpha s}}$$

$$-(\kappa_b + \kappa_{\alpha s})^2 e^{-i\phi_{\alpha s}} \} \Big] , \tag{A.6}$$

in terms of which the determinant of F_s becomes

$$\det(F_s) = \kappa_a (f_{s1} - f_{s2}) + \kappa_{\alpha s} (f_{s1} + f_{s2})$$

$$+ \gamma \eta_2 \{\kappa_a (f_{s3} - f_{s4}) + \kappa_{\beta s} (f_{s3} + f_{s4})\} . \tag{A.7}$$

The Fresnel coefficients for the fields inside the medium are then given by Eq. (A.2), and the Fresnel coefficients for the waves outside the material follow from Eq. (20.4). In terms of the functions $f_{s1},...,f_{s4}$ we find explicitly

$$R_s = -1 + \frac{2\kappa_a}{\det(F_s)} \{f_{s1} - f_{s2} + \gamma \eta_2 (f_{s3} - f_{s4})\} , \tag{A.8}$$

$$P_s = \frac{2\kappa_a}{\det(F_s)}\{\gamma^* \eta_1 (f_{s1} - f_{s2}) + f_{s3} - f_{s4}\} \ , \tag{A.9}$$

$$T_s\, e^{-i\phi_a} = \frac{2\kappa_a}{\det(F_s)}\{e^{-i\phi_{\alpha s}} f_{s1} - e^{i\phi_{\alpha s}} f_{s2} + \gamma \eta_2 (e^{-i\phi_{\beta s}} f_{s3} - e^{i\phi_{\beta s}} f_{s4})\} \ , \tag{A.10}$$

$$N_s\, e^{i\phi_b} = \frac{2\kappa_a}{\det(F_s)}\{\gamma^* \eta_1 (e^{-i\phi_{\alpha s}} f_{s1} - e^{i\phi_{\alpha s}} f_{s2}) + e^{-i\phi_{\beta s}} f_{s3} - e^{i\phi_{\beta s}} f_{s4}\} \ . \tag{A.11}$$

For p-waves the functions $f_{p1},...,f_{p4}$ are

$$\begin{aligned} f_{p1} = {} & (q_3\kappa_a + \bar{q}_3\kappa_{\alpha p}) e^{i\phi_{\alpha p}} \left[(q_6\kappa_b + \bar{q}_6\kappa_{\beta p})^2 e^{-i\phi_{\beta p}} - (q_6\kappa_b - \bar{q}_6\kappa_{\beta p})^2 e^{i\phi_{\beta p}} \right] \\ & - \gamma_o^2 \Big[2\kappa_{\beta p}(q_5\bar{q}_6\kappa_a + \bar{q}_5 q_6 \kappa_b)(q_4\kappa_b + \bar{q}_4\kappa_{\alpha p}) \\ & - (q_4\kappa_b - \bar{q}_4\kappa_{\alpha p}) e^{i\phi_{\alpha p}} \{(q_5\kappa_a + \bar{q}_5\kappa_{\beta p})(q_6\kappa_b - \bar{q}_6\kappa_{\beta p}) e^{i\phi_{\beta p}} \\ & - (q_5\kappa_a - \bar{q}_5\kappa_{\beta p})(q_6\kappa_b + \bar{q}_6\kappa_{\beta p}) e^{-i\phi_{\beta p}}\} \Big] \ , \end{aligned} \tag{A.12}$$

$$\begin{aligned} f_{p2} = {} & (q_3\kappa_a - \bar{q}_3\kappa_{\alpha p}) e^{-i\phi_{\alpha p}} \left[(q_6\kappa_b + \bar{q}_6\kappa_{\beta p})^2 e^{-i\phi_{\beta p}} - (q_6\kappa_b - \bar{q}_6\kappa_{\beta p})^2 e^{i\phi_{\beta p}} \right] \\ & - \gamma_o^2 \Big[2\kappa_{\beta p}(q_5\bar{q}_6\kappa_a + \bar{q}_5 q_6 \kappa_b)(q_4\kappa_b - \bar{q}_{4\kappa_{\alpha p}}) \\ & - (q_4\kappa_b + \bar{q}_4\kappa_{\alpha p}) e^{-i\phi_{\alpha p}} \{(q_5\kappa_a + \bar{q}_5\kappa_{\beta p})(q_6\kappa_b - \bar{q}_6\kappa_{\beta p}) e^{i\phi_{\beta p}} \\ & - (q_5\kappa_a - \bar{q}_5\kappa_{\beta p})(q_6\kappa_b + \bar{q}_6\kappa_{\beta p}) e^{-i\phi_{\beta p}}\} \Big] \ , \end{aligned} \tag{A.13}$$

$$\begin{aligned} f_{p3} = {} & -\gamma^* \Big[2\kappa_{\alpha p}(q_3\bar{q}_4\kappa_a + \bar{q}_3 q_4 \kappa_b)(q_6\kappa_b + \bar{q}_6\kappa_{\beta p}) \\ & - (q_6\kappa_b - \bar{q}_6\kappa_{\beta p}) e^{i\phi_{\beta p}} \{(q_3\kappa_a + \bar{q}_3\kappa_{\alpha p})(q_4\kappa_b - \bar{q}_4\kappa_{\alpha p}) e^{i\phi_{\alpha p}} \end{aligned}$$

$$-(q_3\kappa_a-\overline{q}_3\kappa_{\alpha p})(q_4\kappa_b+\overline{q}_4\kappa_{\alpha p})e^{-i\phi_{\alpha p}}\}$$

$$+\gamma_o^2(q_5\kappa_a+\overline{q}_5\kappa_{\beta p})e^{i\phi_{\beta p}}\{(q_4\kappa_b-\overline{q}_4\kappa_{\alpha p})^2e^{i\phi_{\alpha p}}$$

$$-(q_4\kappa_b+\overline{q}_4\kappa_{\alpha p})^2e^{-i\phi_{\alpha p}}\}\Big]\,, \tag{A.14}$$

$$f_{p4}=-\gamma^*\Big[2\kappa_{\alpha p}(q_3\overline{q}_4\kappa_a+\overline{q}_3q_4\kappa_b)(q_6\kappa_b-\overline{q}_6\kappa_{\beta p})$$

$$-(q_6\kappa_b+\overline{q}_6\kappa_{\beta p})e^{-i\phi_{\beta p}}\{(q_3\kappa_a+\overline{q}_3\kappa_{\alpha p})(q_4\kappa_b-\overline{q}_4\kappa_{\alpha p})e^{i\phi_{\alpha p}}$$

$$-(q_3\kappa_a-\overline{q}_3\kappa_{\alpha p})(q_4\kappa_b+\overline{q}_4\kappa_{\alpha p})e^{-i\phi_{\alpha p}}\}$$

$$+\gamma_o^2(q_5\kappa_a-\overline{q}_5\kappa_{\beta p})e^{-i\phi_{\beta p}}\{(q_4\kappa_b-\overline{q}_4\kappa_{\alpha p})^2e^{i\phi_{\alpha p}}$$

$$-(q_4\kappa_b+\overline{q}_4\kappa_{\alpha p})^2e^{-i\phi_{\alpha p}}\}\Big]\,, \tag{A.15}$$

in terms of which we obtain

$$\det(F_p)=q_3\kappa_a(f_{p1}-f_{p2})+\overline{q}_3\kappa_{\alpha p}(f_{p1}+f_{p2})$$

$$+\gamma\{q_5\kappa_a(f_{p3}-f_{p4})+\overline{q}_5\kappa_{\beta p}(f_{p3}+f_{p4})\}\,, \tag{A.16}$$

and

$$R_p=-1+\frac{2\kappa_a}{\det(F_p)}\{q_3(f_{p1}-f_{p2})+\gamma\,q_5(f_{p3}-f_{p4})\}\,, \tag{A.17}$$

$$P_p=\frac{2\kappa_a}{\det(F_p)}\{\gamma^*q_4(f_{p1}-f_{p2})+q_6(f_{p3}-f_{p4})\}\,, \tag{A.18}$$

$$T_p\,e^{-i\phi_a}=\frac{2\kappa_a}{\det(F_p)}\{q_3(e^{-i\phi_{\alpha p}}f_{p1}-e^{i\phi_{\alpha p}}f_{p2})$$

$$+\gamma\,q_5(e^{-i\phi_{\beta p}}f_{p3}-e^{i\phi_{\beta p}}f_{p4})\}\,, \tag{A.19}$$

$$N_p e^{i\phi_b} = \frac{2\kappa_a}{\det(F_p)}\{\gamma^* q_4(e^{-i\phi_{\alpha p}} f_{p1} - e^{i\phi_{\alpha p}} f_{p2}) + q_6(e^{-i\phi_{\beta p}} f_{p3} - e^{i\phi_{\beta p}} f_{p4})\} \quad . \tag{A.20}$$

REFERENCES

[1] B. Ya. Zel'dovich, V. I. Popovichev, V. V. Ragul'skii and F. S. Faizullov, JETP Lett. **15** (1972) 109.

[2] O. Yu. Nosach, V. I. Popovichev, V. V. Ragul'skii and F. S. Faizullov, JETP Lett.**16** (1972) 435.

[3] B. Ya. Zel'dovich, N. A. Mel'nikov, N. F. Pilipetskii and V. V. Ragul'skii, JETP Lett. **25** (1977) 36.

[4] R. W. Hellwarth, J. Opt. Soc. Am. **67** (1977) 1.

[5] A. Yariv and D. M. Pepper, Opt. Lett. **1** (1977) 16.

[6] D. M. Bloom and G. C. Bjorklund, Appl. Phys. Lett. **31** (1977) 592.

[7] S. M. Jensen and R. W. Hellwarth, Appl. Phys. Lett. **32** (1978) 166.

[8] P. V. Avizonis, F. A. Hopf, W. D. Bomberger, S. F. Jacobs, A. Tomita and K. H.Womack, Appl. Phys. Lett. **31** (1977) 435.

[9] B. Ya. Zel'dovich, N. F. Pilipetskii, A. N. Sudarkin and V. V. Shkunov, Sov. Phys.Dokl. **25** (1980) 377.

[10] O. L. Kulikov, N. F. Pilipetskii, A. N. Sudarkin and V. V. Shkunov, JETP Lett. **31**(1980) 345.

[11] K. Ujihara, J. Opt. Soc. Am. **73** (1983) 610.

[12] N. F. Pilipetskii, A. N. Sudarkin and K. N. Ushakov, Sov. Phys. JETP **66** (1987) 66.

[13] C. V. Heer and N. C. Griffen, Opt. Lett. **4** (1979) 239.

[14] M. Ducloy and D. Bloch, J. Physique **42** (1981) 711.

[15] M. Ducloy and D. Bloch, Phys. Rev. A **30** (1984) 3107.

[16] W. R. Tompkin, M. S. Malcuit, R. W. Boyd and J. E. Sipe, J. Opt. Soc. Am. B **6** (1989) 757.

[17] A. E. Neeves and M. H. Birnboim, J. Opt. Soc. Am. B **5** (1988) 701.

[18] G. Manneberg, J. Opt. Soc. Am. B **4** (1987) 1790.

[19] J. Feinberg, Opt. Lett. **8** (1983) 480.

[20] M. Cronin-Golomb, B. Fisher, J. O. White and A. Yariv, IEEE J. Quantum Electron. **QE-20** (1984) 12.

[21] G. Salamo, M. J. Miller, W. W. Clark III, G. L. Wood and E. J. Sharp, Opt. Commun. **59** (1986) 417.

[22] H. Kong, C. Lin, A. M. Biernacki and M. Cronin-Golomb, Opt. Lett. **13** (1988) 324.

[23] K. Sayano, G. A. Rakuljic and A. Yariv, Opt. Lett. **13** (1988) 143.

[24] P. M. Peterson and P. M. Johansen, Opt. Lett. **13** (1988) 45.

[25] W. Krolikowski and M. R. Belic, Opt. Lett. **13** (1988) 149.
[26] M. D. Ewbank, Opt. Lett. **13** (1988) 47,
[27] A. Bledowski and W. Krolikowski, Opt. Lett. **13** (1988) 146.
[28] M. R. Belic, Phys. Rev. A **37** (1988) 1809.
[29] J. Goltz, C. Denz and T. Tschudi, Opt. Commun. **68** (1988) 453.
[30] J. Feinberg, Opt. Lett. **7** (1982) 486.
[31] M. C. Gower and P. Hribek, J. Opt. Soc. Am. B **5** (1988) 1750.
[32] A. L. Smirl, G. C. Valley, R. A. Mullen, K. Bohnert, C. D. Mire and T. F. Boggess, Opt. Lett. **12** (1987) 501.
[33] E. Wolf, J. Opt. Soc. Am. **70** (1980) 1311.
[34] E. Wolf and W. H. Carter, Opt. Commun. **40** (1982) 397. See also: A. Yariv, Opt. Commun. **40** (1982) 401.
[35] G. S. Agarwal, A. T. Friberg and E. Wolf, Opt. Commun. **43** (1982) 446.
[36] A. T. Friberg, J. Opt. Soc. Am. **73** (1983) 405.
[37] G. S. Agarwal, A. T. Friberg and E. Wolf, J. Opt. Soc. Am. **73** (1983) 529.
[38] R. A. Fisher, B. R. Suydam and B. J. Feldman, Phys. Rev. A **23** (1981) 3071.
[39] B. R. Suydam and R. A. Fisher, Opt. Eng. **21** (1982) 184.
[40] B. R. Suydam, J. Opt. Soc. Am. **73** (1983) 539.
[41] G. P. Djotyan and L. L. Minasyan, J. Phys. B: At. Mol. Opt. Phys. **21** (1988) 713.
[42] G. C. Papen, B. E. A. Saleh and J. A. Tataronis, J. Opt. Soc. Am. B **5** (1988) 1763.
[43] G. C. Papen, B. E. A. Saleh and J. A. Tataronis, Opt. Lett. **14** (1989) 287.
[44] C. Paré, M. Piché and P. A. Bélanger, J. Opt. Soc. Am. B **5** (1988) 679.
[45] R. Yahalom and A. Yariv, J. Opt. Soc. Am. B **5** (1988) 1783.
[46] D. J. Gauthier, P. Narum and R. W. Boyd, Phys. Rev. Lett. **58** (1987) 1640.
[47] M. Nazarathy, A. Hardy and J. Shamir, J. Opt. Soc. Am. B **73** (1983) 576.
[48] M. Nazarathy, J. Shamir and A. Hardy, J. Opt. Soc. Am. B **73** (1983) 587.
[49] M. Nazarathy, Opt. Commun. **45** (1983) 117.
[50] G. Reiner, P. Meystre and E. M. Wright, J. Opt. Soc. Am. B **4** (1987) 675.
[51] E. S. Kim, C. H. Cho, I. E. Young and H. K. Park, IEEE J. Quantum Electron. **QE-23** (1987) 2047.
[52] P. D. Drummond and A. T. Friberg, J. Appl. Phys. **54** (1983) 5618.
[53] A. T. Friberg and P. D. Drummond, J. Opt. Soc. Am. **73** (1983) 1216.
[54] A. T. Friberg, M. Kauranen and R. Salomaa, Opt. Commun. **60** (1986) 191.
[55] I. Linsay and J. C. Dainty, Opt. Commun. **59** (1986) 405.
[56] I. Linsay, J. Opt. Soc. Am. B **4** (1987) 1810.
[57] A. Yariv, IEEE J. Quantum Electron. **QE-14** (1978) 650.
[58] D. M. Pepper, Opt. Eng. **21** (1982) 156.
[59] R. A. Fisher, editor, *Optical Phase Conjugation* (Academic Press, New York, 1983).
[60] B. Ya. Zel'dovich, N. F. Pilipetskii and V. V. Shkunov, *Principles of Phase Conjugation* (Springer, Berlin, 1985).
[61] M. C. Gower, J. Mod. Opt. **35** (1988) 449.
[62] P. N. Butcher and D. Cotter, *The Elements of Nonlinear Optics* (Cambridge, Cambridge, 1990) p. 232.

[63] R. W. Boyd, *Nonlinear Optics* (Academic Press, Boston, 1992) p. 241.
[64] G. S. He and S. H. Liu, *Physics of Nonlinear Optics* (World Scientific, Singapore, 1999) Ch. 9.
[65] H. F. Arnoldus and T. F. George, Phys. Rev. A **43** (1991) 3675.
[66] H. F. Arnoldus and T. F. George, Phys. Rev. A **43** (1991) 6156.
[67] R. J. Cook and P. W. Milonni, IEEE J. Quantum Electron. **24** (1988) 1383.
[68] B. H. W. Hendriks and G. Nienhuis, Phys. Rev. A **40** (1989) 1892.
[69] P. W. Milonni, E. J. Bochove and R. J. Cook, Phys. Rev. A **40** (1989) 4100.
[70] H. F. Arnoldus and T. F. George, J. Quantum Nonlinear Phen. **1** (1992) 95.
[71] G. S. Agarwal, Opt. Commun. **42** (1982) 205.
[72] E. J. Bochove, Phys. Rev. Lett. **59** (1987) 2547.
[73] P. W. Milonni, E. J. Bochove and R. J. Cook, J. Opt. Soc. Am. B **6** (1989) 1932.
[74] A. L. Gaeta and R. W. Boyd, Phys. Rev. Lett. **60** (1988) 2618.
[75] H. F. Arnoldus and T. F. George, Phys. Rev. A **43** (1991) 591.
[76] B. R. Mollow, Phys. Rev. **188** (1969) 1969).
[77] H. F. Arnoldus and T. F. George, J. Phys. B: At. Mol. Opt. Phys. **24** (1991) 2653.
[78] R. W. F. Gross, S. T. Amimoto, L. Garman-DuVall, T. Good and H. F. Arnoldus, Proc. of *Quantum Electronics and Laser Science Conference*, Technical Digest Series **12** (Optical Society of America, Washington, DC, 1993) p. 232.
[79] S. I. Bozhevolnui, O. Keller and I. I. Smolyaninov, Opt. Lett. **19** (1994) 1601.
[80] S. I. Bozhevolnui, O. Keller and I. I. Smolyaninov, Opt. Commun. **115** (1995) 115.
[81] S. I. Bozhevolnui and I. I. Smolyaninov, J. Opt. Soc. Am. B **12** (1995) 1617.
[82] J. D. Jackson, *Classical Electrodynamics* (Wiley, New York, 1962) p. 217.
[83] Y. R. Shen, *The Principles of Nonlinear Optics* (Wiley, New York, 1984) Ch. 1.
[84] M. Schubert and B. Wilhelmi, *Nonlinear Optics and Quantum Electronics* (Wiley, New York, 1986) p. 36.
[85] J. H. Marburger and J. F. Lam, Appl. Phys. Lett. **34** (1979) 389.
[86] S. Trillo and S. Wabnitz, J. Opt. Soc. Am. B **5** (1988) 195.
[87] J. Goltz, C. Denz, H. Klumb, T. Tschudi and J. Albers, Opt. Lett. **13** (1988) 321.
[88] J. Goltz and T. Tschudi, Opt. Lett. **14** (1989) 405.
[89] D. A. Kleinman, Phys. Rev. **126** (1962) 1977.
[90] M. Born and E. Wolf, *Principles of Optics*, 6th edition (Pergamon, New York, 1980) p. 61.
[91] L. Mandel and E. Wolf, *Optical Coherence and Quantum Optics* (Cambridge, Cambridge, 1995) Sec. 3.2.4.
[92] O. Keller, Phys. Rev. B **34** (1986) 3883.
[93] H. F. Arnoldus and J. T. Foley, J. Opt. Soc. Am. A **19** (2002) 1701.
[94] G. C. Sherman, A. J. Devaney and L. Mandel, Opt. Commun. **6** (1972) 115.
[95] J. L. Agudin and A. M. Platzeck, J. Opt. Soc. Am. **70** (1980) 1329.
[96] R. Asby and E. Wolf, J. Opt. Soc. Am. **61** (1971) 52.
[97] C. K. Carniglia and L. Mandel, Phys. Rev. D **3** (1971) 280.
[98] N. Nieto-Vesperinas, Opt. Commun. **67** (1988) 391.
[99] N. Bloembergen and P. S. Pershan, Phys. Rev. **128** (1962) 606.

[100] N. Bloembergen, *Nonlinear Optics* (Benjamin, Reading, Massachusetts, 1965).
[101] Z. Knittl, *Optics of Thin Films* (Wiley, New York, 1976) p. 69.
[102] R. M. A. Azzam and N. M. Bashara, *Ellipsometry and Polarized Light* (North-Holland, Amsterdam, 1987) p. 283.
[103] D. M. Pepper, D. Fekete and A. Yariv, Appl. Phys. Lett. **33** (1978) 41.
[104] D. M. Pepper and R. L. Abrams, Opt. Lett. **3** (1978) 212.
[105] K. R. MacDonald and J. Feinberg, Phys. Rev. Lett. **55** (1985) 821.
[106] W. Krolikowski, M. R. Belic and A. Bledowski, Phys. Rev. A **15** (1988) 2224.
[107] E. Wolf, L. Mandel, R. W. Boyd, T. M. Habashy and M. Nieto-Vesperinas, J. Opt. Soc. Am. B **4** (1987) 1260.
[108] A. A. Jacobs, W. R. Tompkin, R. W. Boyd and E. Wolf, J. Opt. Soc. Am. B **4** (1987) 1266.
[109] P. H. Beckwith, I. McMichael and P. Yeh, Opt. Lett. **12** (1987) 510.
[110] I. McMichael, J. Opt. Soc. Am. B **5** (1988) 863.
[111] H. F. Arnoldus and T. F. George, Phys. Rev. A **51** (1995) 4250.